CHEMICAL REVIEWS

REVIEW

pubs.acs.org/CR

Classical Valence Bond Approach by Modern Methods

Wei Wu,[*,†] Peifeng Su,[†] Sason Shaik,[*,‡] and Philippe C. Hiberty[*,§]

[†]The State Key Laboratory of Physical Chemistry of Solid Surfaces, Fujian Provincial Key Laboratory of Theoretical and Computational Chemistry, and College of Chemistry and Chemical Engineering, Xiamen University, Xiamen, Fujian 361005, China

[‡]Institute of Chemistry and The Lise Meitner-Minerva Center for Computational Quantum Chemistry, The Hebrew University, Jerusalem 91904, Israel

[§]Laboratoire de Chimie Physique, Groupe de Chimie Théorique, CNRS UMR 8000, Université de Paris-Sud, 91405 Orsay Cédex, France

CONTENTS

1. INTRODUCTION

Quantum mechanics has provided chemistry with two general theories of bonding: valence bond (VB) theory and molecular orbital (MO) theory. The two theories were developed at about

Received: July 20, 2010
Published: August 18, 2011

Scheme 1. VB Wave Functions for a Two-Electron Bond between Atoms A and B

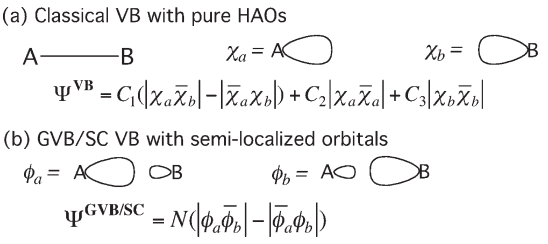

the same time, but quickly diverged into two schools that have competed on charting the mental map of chemistry. Until the mid-1950s, chemistry was dominated by classical VB theory, which expresses the molecular wave function as a combination of explicit covalent and ionic structures based on pure atomic orbitals (AOs) or hybrid atomic orbitals (HAOs), as illustrated in Scheme 1a. However, the computational effort required to perform ab initio calculations in the classical VB framework proved to be overly demanding, and as such, the theory was employed in an oversimplied manner, neglecting ionic structures and using nonoptimized orbitals. At the same time when this early ab initio VB theory was lacking accuracy and did not progress, MO theory was enjoying efficient implementations, which have provided the chemical community with computational software of ever-increasing speeds and capabilities. VB theory was unable to come up with equally popular and useful software, and as such it has gradually fallen into disrepute and was almost completely abandoned. Thus, MO theory took over.

However, from the 1980s onward, VB theory started making a strong comeback and has since enjoyed a renaissance, including the ab initio method development of the theory. A common feature of all modern VB methods is the simultaneous optimization of the orbitals and the coefficients of the VB structures, which thereby lead to an improved accuracy. However, the various modern VB methods differ in the manners by which the VB orbitals are defined.

The modern era began when one of the pioneers of ab initio VB theory, Goddard, and his co-workers developed the generalized VB (GVB) method,[1−5] which employed semilocalized atomic orbitals (having small delocalization tails as in Scheme 1b) used originally by Coulson and Fischer for the H_2 molecule.[6] The GVB theory does not incorporate covalent and ionic structures explicitly, but instead uses formally covalent structures based on semilocalized orbitals, which implicitly incorporate the contributions of ionic structures to bonding (see Scheme 1b). This enables a drastic reduction of the number of VB structures; for example, the π-system of benzene requires a total number of 175 covalent and ionic VB structures based on pure AOs compared with only five formally covalent Kekulé and Dewar structures based on semilocalized orbitals. It is noted that the GVB method as implemented by Goddard is completely equivalent to a strongly orthogonal geminal anzatz with two orbitals per pair. Further progress was made after the initial development of the method, when the GVB wave functions were used as starting points for further configuration interaction (CI)[7,8] or perturbative treatments of electron correlation.[9−12] The method was applied, among others, to the electronic structure of 1,3-dipoles,[13−15] resonance in the allyl radical[16] or cyclobutadiene,[17] dissociation energies,[7] halogen exchange reactions,[18] organometallic complexes,[19−22] and so on.

In a philosophy similar to that of GVB, Gerratt, Raimondi, and Cooper developed their VB method known as the spin-coupled (SC) theory[23−31] and its CI-augmented version, the so-called SCVB.[26,32−35] Like GVB, SC/SCVB theory relies on semilocalized orbitals and includes formally covalent configurations only. The difference between SC and GVB methods is that the former releases the orthogonality and perfect-pairing restrictions, which are usually used in GVB applications. Thus, in SC all orbitals are allowed to be nonorthogonal, and all possible spin couplings between the singly occupied orbitals are included in the wave function. The SC and SCVB methods were applied to aromatic and antiaromatic molecules,[35−41] the allyl radical,[42] Diels−Alder and retro-Diels−Alder reactions,[43,44] sigmatropic rearrangements,[45−47] 1,3-dipolar cycloadditions,[48−50] and so on.

Another VB method that was developed also starting in the 1980s is a semiempirical method based on the Heisenberg Hamiltonian (HH) and AO determinants rather than spin-adapted VB structures. Initially, the method used semiempirical parameters and a zero-differential overlap approximation and was applied to the ground and excited states of hydrocarbons[51−57] and metal clusters.[58] A nonempirical geometry-dependent version was subsequently derived in which the parameters were extracted from accurate ab initio calculations on simple molecules.[59,60] The latter calculations use orthogonalized AOs, which consequently possess significant delocalization tails, but result in computer-time savings. The method has been applied to ground and excited states of conjugated hydrocarbons,[59−61] heteroatomic conjugated systems,[62] polyynes,[63,64] and so on. Eventually this ab initio-parametrized method led to the molecular mechanics/valence bond (MM/VB) method of Robb and Bearpark,[65−73] which was extensively used for demonstrating conical intersections in photochemical reactions.[70,71,74−76]

Since VB theory is well-known for its deep chemical insight, many methods have sprung to extract VB information from MO-based methods. Some of these methods involve mapping of MO- and CI-augmented wave functions into valence bond structures and can be dated to the pioneering studies of Slater and van Vleck and later to Moffitt in his treatment of electronic spectra for large molecules.[77] The first practical implementation of Hartree−Fock (HF) and post-HF wave functions was made by Hiberty and Leforestier,[78] who created such a "VB transcriptor" in 1978 and treated many molecules by showing the VB content of their MO and MO−CI wave functions. Since then, the problem has been explored by others, for example, by Karafiloglou,[79] Bachler,[80,81] Malrieu,[82−84] and so on. Some important developments along these lines were made by Cooper et al.,[85−87] who computed a wave function of the SC type by projecting CASSCF wave functions onto VB structures using maximum overlap criteria. There are also various methods of VB readings of CASSCF wave functions through orbital localization techniques[80,81,83,84,88−92] and through wave function transformation using nonorthogonal orbitals.[89,93]

Concurrently to the developments of all the above methods, the progress that has occurred in computer technology and in computational methodologies has enabled the re-emergence of modern forms of classical VB in which both orbitals and the structural coefficients are simultaneously optimized. The advantage of these modern classical VB methods over other brands of VB theory is two-fold: (i) owing to the strictly local characters of the employed orbitals (either purely atomic or purely localized on fragments as in Scheme 1a above), the VB structures are very clearly interpreted and as close as possible to the intuitive Lewis

Scheme 2. Complete Set of VB Structures for a Hydrogen Abstraction Process

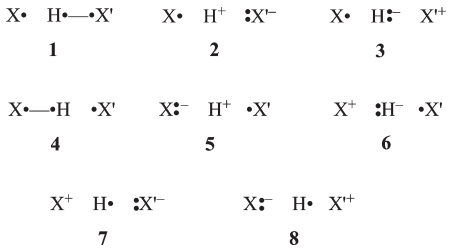

structures that constitute the language of chemists; (ii) because the covalent and ionic structures are explicitly considered, it is possible to meaningfully calculate their weights or their quasi-variational energies. As such, classical VB allows the VB structures to be clearly and accurately defined, which, as will be seen, is important for calculation of resonance energies, for diagrams in chemical reactivity, for in-depth study of the nature of chemical bonds, and so on.

The resurgence of modern classical VB theory involves the development of several methodological advances which allowed new and more accurate applications of the theory.[94−112] Thus, several significant advances have been achieved in overcoming the notorious "*N*! problem", associated with the nonorthogonality in the VB method, and direct algorithms have considerably increased the speed of VB computations, which are nowadays much faster than they used to be in the past. During this effort to speed up VB calculations, there have emerged VB methods that also enable quantitative accuracy to be achieved. Thus, dynamic correlation has been incorporated into VB calculations, so that, at present, sophisticated VB methods are able to achieve the accuracy of high-level post-HF methods. Very recently, classical VB theory was extended to handle species and reactions in solution and is also capable of treating transition-metal complexes.

Indeed the VB culture is broad and involves a variety of techniques and approaches, and a review of all the methods would be vast and too diffuse compared with a more focused review that may benefit the general reader. Thus, since methods that use semilocalized orbitals such as GVB, SCVB, HH, and MM/VB have already been amply reviewed before,[1−4,23−31,53−56,69−71] we shall not review these methods again, and the reader is advised to consult the existing authoritative sources. The present review will focus on those modern VB methods that are based on classical VB theory, which, we recall, deals with purely localized orbitals and explicit consideration of covalent and ionic structures. The combination of the lucid insight of VB into chemistry and the new computational methods is discussed in this review, hopefully establishing a case for the return of VB theory to the classroom and to the laboratory bench in the service of experimental chemists.

1.1. Family of Classical Valence Bond Methods

In all the methods of the classical VB type to be described herein, one uses an active shell, which involves the electrons that participate in the electronic reorganization in a process, which can be bond making/breaking or a reaction such as S_N2, Diels−Alder, and so on. These electrons are then distributed in the valence atomic orbitals or HAOs to generate all the possible covalent and ionic structures. Scheme 2 shows this set of structures for a hydrogen abstraction process; there are two

Scheme 3. Tree of Modern VB Methods That Are Based on Classical VB Theory

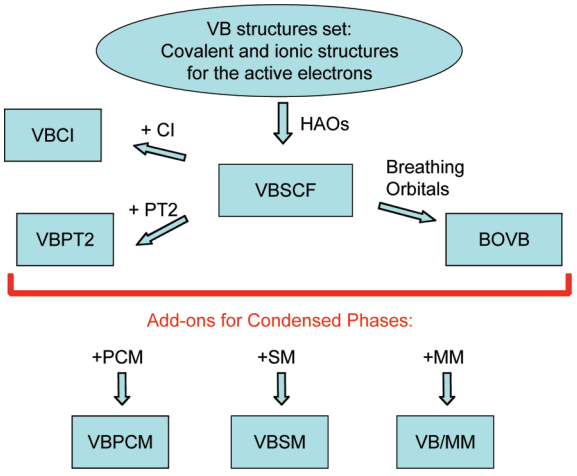

covalent and six ionic structures which distribute the three "active electrons" in the three HAOs of the X---H---X′ system. The wave function is a linear combination of such a structure set and is optimized with respect to both the structural coefficients and the HAOs. The methods differ from each other by the levels in which the dynamic correlation energy is incorporated into the calculations. The relationships among the various methods follow a philosophy similar to the one used in ab initio MO-based theory.

The tree of these VB methods is shown in Scheme 3. The basic method, which was devised by Balint-Kurti and van Lenthe,[94,95] is called the valence bond self-consistent field (VBSCF) method. The method optimizes VB orbitals and structural coefficients simultaneously and uses the same set of HAOs for all the structures. This is analogous to the MO-based CASSCF method, and both methods should be numerically quasi-identical if all structures for a given dimension of the active space are included. However, usually VB methods employ only a few structures that are essential for describing the system of interest and use the strictly localized orbitals. Consequently, the VBSCF results are often less accurate than those of CASSCF. Nevertheless, both of the methods include some degree of static electron correlation, but lack dynamic correlation.

The VBSCF method branches into two sets of methods. The one to the right is the breathing-orbital VB (BOVB) method,[113−115] where one uses the same VBSCF wave function, but with an additional degree of freedom that allows the HAOs to be different for the different structures. Thus, the orbitals adapt themselves to the instantaneous field of each structure, which has the effect of introducing the dynamic correlation that is necessary to provide accurate energies. The two branches to the left in Scheme 3 are two alternative ways of improving VBSCF by introducing dynamic correlation. This is done by means of post-SCF treatments that are analogous to MRCI and MRPT2 in the MO theory. In the valence bond configuration interaction method (VBCI),[116,117] the VBSCF energy and wave function are improved by CI. On the other hand, the valence bond second-order perturbation method (VBPT2)[118] uses perturbation theory, taking the VBSCF wave function as the zeroth-order reference. It is worthwhile to emphasize that, despite the excited VB structures that are

dx.doi.org/10.1021/cr100228r |*Chem. Rev.* 2011, 111, 7557–7593

included in the VBCI or VBPT2 method, the corresponding wave function of the system still retains a compact form by condensing the extensive VBCI/VBPT2 wave function into a minimal set of the fundamental structures that are used in the VBSCF calculation (e.g., in Scheme 2). As such, all VB properties such as weight and resonance energy are still clearly defined in both high-level methods in the same manner as in the VBSCF method. We note that both the BOVB and VBCI come in various internal levels of sophistication, which will be described in the corresponding sections in some detail.

In addition to the above VB methods, there are add-ons that enable one to carry out calculations in solution using the polarizable continuum model (PCM)[119,120] or SMx (x = 1−8) models,[121] hence valence bond polarizable continuum model (VBPCM) and valence bond solvation model (VBSM), or by incorporation of molecular mechanics (MM), hence VB/MM, to carry reactions inside protein cavities.[122] As such, with this arsenal of methods, VB theory is coming of age and starting to be useful for the treatment of some real chemical problems, as this review will show.

In addition to the strict VB methods displayed in Scheme 3, the review will also describe MO-based methods that generate VB-type information which can be used for some specific VB applications. The block-localized wave function (BLW) method[123−127] is a type of VB method that utilizes an HF wave function with block-localized orbitals. By partitioning the molecular orbitals to the subgroups of a molecule, a BLW can describe a specific VB structure at the HF level. Thus, the BLW is capable of computing delocalization/resonance energies and charge transfer effects among molecules. The BLW approach is related to the early Kollmar method,[128] wherein the subgroup orbitals were input and the energy for this so-generated "localized" reference was computed at zero iteration, without optimization of the orbitals. Both methods belong to a general class of MO- and density functional theory (DFT)-based energy decomposition analysis (EDA) approaches[129−133] which use as a reference either a fragment-localized wave function or a density and thereby estimate the various interactions between the fragments, thus providing VB-related information from MO or DFT calculations. For space economy, we shall limit our coverage to the BLW method since this method performs the energy decomposition closer to the VB spirit compared to other EDA methods.

The molecular orbital valence bond method (MOVB)[125] is an extension of the BLW method, which uses a multireference wave function, thus allowing calculation of the electronic coupling energy resulting from the mixing of two or more block-localized structures.

The structure of the review follows the above ordering of VB methods, which are detailed in section 2. This methodology section, which will certainly interest the computation-oriented reader, is followed by applications which demonstrate the capability of VB theory to lead to lucid physical insight into a variety of problems, now approaching "real size". Then section 4 describes algorithms and techniques which make modern VB theory faster and more efficient. Lastly, section 5 illustrates the current capabilities of modern VB methods by displaying ab initio VB calculations for a sizable molecular system, $(CO)_4Fe(C_2H_4)$. The review is written in such a way that the application-oriented reader who is less interested in the methodological details can skip parts of section 2 and then proceed to the applications in sections 3 and 5.

Scheme 4. Five Rumer Structures for the Benzene Molecule

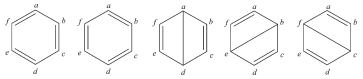

2. AB INITIO VALENCE BOND METHODS

2.1. Theoretical Background

In VB theory, a many-electron wave function is expressed in terms of VB functions:

$$\Psi = \sum_K C_K \Phi_K \tag{1}$$

where the VB function Φ_K corresponds to a classical VB structure. In quantum chemistry, any state function Φ_K should be a spin eigenfunction that is antisymmetric with respect to permutations of electron indices. In general, a VB function is of the form

$$\Phi_K = \hat{A}\Omega_0\Theta_K \tag{2}$$

where $\hat{A}$ is an antisymmetrizer, Ω_0 is a direct product of orbitals $\{\phi_i\}$ as

$$\Omega_0 = \phi_1(1)\,\phi_2(2)\,\ldots\,\phi_N(N) \tag{3}$$

and Θ_K is a spin-paired spin eigenfunction,[134] defined as

$$\Theta_K = 2^{-1/2}[\alpha(k_1)\,\beta(k_2) - \beta(k_1)\,\alpha(k_2)] \times 2^{-1/2}[\alpha(k_3)\,\beta(k_4) - \beta(k_3)\,\alpha(k_4)]\,\ldots\,\alpha(k_p)\,\ldots\,\alpha(k_N) \tag{4}$$

In eq 4, the scheme of spin pairing (k_1, k_2), (k_3, k_4), etc., corresponds to the bond pairs that describe the structure K. Linearly independent electron pairing schemes may be selected by using the Rumer diagrams.[135] In a Rumer diagram, we set down the electron indices, 1, 2, ..., N, in a ring, representing each factor $2^{-1/2}[\alpha(k_i)\,\beta(k_j) - \beta(k_i)\,\alpha(k_j)]$ in eq 4 by an arrow from i to j. On the basis of the Rumer rule, the independent Rumer structure set is obtained by drawing all possible Rumer diagrams in which there are no crossed arrows. Scheme 4 shows the five Rumer structures for the benzene molecule, where, as is well-known, the first two are Kekulé structures and the last three are Dewar structures.

Rumer's rule is applicable for singlet states with spin quantum number S = 0. To extend to the general spin S, extended Rumer diagrams[136] should be applied, where a pole is added in the diagram. A VB function with a Rumer spin function is called a Heitler−London−Slater−Pauling (HLSP) function.

An alternative way of writing the wave function is by use of a Slater determinant form, which will be used in this review. For example, the (k_1, k_2) bond-paired wave function will be given by

$$\Phi_K = |\ldots(\phi_{k_1}\bar{\phi}_{k_2} - \bar{\phi}_{k_1}\phi_{k_2})\ldots| \tag{5}$$

where the bar over the orbital denotes a β spin while lack of it denotes spin α. In turn, Φ_K will be written as a product of the Slater determinant forms for all the bond pairs.

The coefficients C_K in eq 1 can conveniently be determined by solving the secular equation $\mathbf{HC} = E\mathbf{MC}$, where Hamiltonian and overlap matrices are defined as follows:

$$H_{KL} = \langle\Phi_K|H|\Phi_L\rangle \tag{6}$$

dx.doi.org/10.1021/cr100228r |Chem. Rev. 2011, 111, 7557–7593

and

$$M_{KL} = \langle \Phi_K | \Phi_L \rangle \tag{7}$$

VB structural weights can be evaluated by the Coulson–Chirgwin formula,[137] which is an equivalent of the Mulliken population analysis:

$$W_K = \sum_L C_K M_{KL} C_L \tag{8}$$

Apart from the Coulson-Chirgwin formula, other definitions for structural weights have also been proposed, such as Löwdin's symmetrical weights[138] and Gallup's inverse weights.[139] VB structural weights are typically used to compare the relative importance of individual VB structures and can be helpful in the understanding of the correlation between molecular structure and reactivity.

2.2. VB Methods of the HLSP Type

2.2.1. VBSCF Method. In the old classical VB method, VB functions were built upon AOs, taken from the atom calculations, and the coefficients of structures were optimized to minimize the total energy of the system. Obviously, the computational results were extremely poor due to the use of frozen atomic orbitals. The VBSCF method was the first modern VB approach that also optimized orbitals. It was devised by Balint-Kurti and van Lenthe[94,95] and was further modified and efficiently implemented by van Lenthe and Verbeek.[140,141] In the VBSCF method, the wave function is expressed in terms of VB functions as

$$\Psi^{\mathrm{VBSCF}} = \sum_K C_K^{\mathrm{SCF}} \Phi_K^0 \tag{9}$$

where both of the structure coefficients (C_K^{SCF}) and VB functions (Φ_K^0) are simultaneously optimized to minimize the total energy. The VB functions are optimized through their occupied orbitals, which are usually expanded as linear combinations of basis functions:

$$\phi_i = \sum_\mu T_{\mu i} \chi_\mu \tag{10}$$

Basically, whenever VBSCF takes all independent VB structures and uses delocalized orbitals, e.g., overlap-enhanced orbitals (OEOs), it will be equivalent to CASSCF with the same active electrons and orbitals. However, usually the VBSCF method employs only a few structures that are essential to describe the system of interest, whereas CASSCF uses the complete set of configurations within the active-space window. One of the advantages of VBSCF, associated with purely localized HAOs, is having a compact wave function with a limited number of VB structures. Indeed, using pure HAOs to define the VB structures makes the neutral covalent structures largely predominant, as is well-known in the two-electron two-orbital case (Scheme 1a). Following this principle, the selection of VB structures can be done by chemical background in the polyatomic case. Thus, in using VBSCF, it is usually advisable to remove the multi-ionic structures, which are generally of very high energy compared with covalent and monoionic structures. Furthermore, symmetry considerations are often helpful for removing additional structures which have no symmetry match to mix with the low-lying covalent and monoionic structures. For example, in the study of C_2, using 92 VB structures in the VBSCF gives almost the same result as the full set of 1764 structures, both numerically and qualitatively.[142] A discussion of the strategy of selecting only the important VB structures was given in the recent study of the various states of O_2.[143]

The VBSCF method permits complete flexibility in the definition of the orbitals used for constructing VB structures. The orbitals can be allowed to delocalize freely during the orbital optimization (resulting in OEOs), and then it will resemble the GVB and SC methods. The orbitals can be defined also by pairs that are allowed to delocalize over the two bonded centers (bond-distorted orbitals, BDOs[144]), or they can be defined as strictly localized on a single center or fragment (resulting in HAOs).

2.2.2. BOVB Method. The BOVB method[113−115] was devised with the aim of computing diabatic or adiabatic states with wave functions that combine the properties of compactness, unambiguous interpretability in terms of structural formulas, and accuracy of the calculated energies. The following features have to be fulfilled to retain interpretability and achieve reasonably good accuracy for the BOVB method: (i) the VB structures are constructed with HAOs, which means that covalent and ionic forms are explicitly considered; (ii) all the VB structures that are relevant to the electronic system being computed are generated; (iii) the coefficients and orbitals of the VB structures are optimized simultaneously. An important specificity of the BOVB method is that the orbitals are variationally optimized with the freedom to be different for different VB structures. Thus, *the different VB structures are not optimized separately but in the presence of each other*, so that the orbital optimization not only lowers the energies of each individual VB structure but also maximizes the resonance energy resulting from their mixing.

Since the BOVB wave function takes a classical VB form, its implementation is less practical for large electronic systems, because a large number of VB structures would have to be generated in such a case. As such, the usual way of using BOVB is to apply it only on those orbitals and electrons that undergo significant changes during the process, such as bond breaking and/or formation; the remaining orbitals are treated as doubly occupied MOs. However, even though the "spectator electrons" reside in doubly occupied MOs, these orbitals too are allowed to optimize freely, but are otherwise left uncorrelated.

The difference between the BOVB and VBSCF wave functions can be illustrated on the simple example of the description of the A–B bond, where A and B are two polyelectronic fragments. Including the two HAOs that are involved in the bond in the active space, and the adjacent orbitals and electrons in the spectator space, the VBSCF wave function reads

$$\begin{aligned}\Psi^{\mathrm{VBSCF}} = {} & C_1(|\psi\bar{\psi}\phi_a\bar{\phi}_b| - |\psi\bar{\psi}\bar{\phi}_a\phi_b|) \\ & + C_2|\psi\bar{\psi}\phi_a\bar{\phi}_a| + C_3|\psi\bar{\psi}\phi_b\bar{\phi}_b|\end{aligned} \tag{11}$$

where ϕ_a and ϕ_b are the active orbitals, common to all the structures, and ψ is a generic term that represents the product of spectator orbitals, also common to all structures. On the other hand, the BOVB wave function takes the following form:

$$\begin{aligned}\Psi^{\mathrm{BOVB}} = {} & B_1(|\psi\bar{\psi}\phi_a\bar{\phi}_b| - |\psi\bar{\psi}\bar{\phi}_a\phi_b|) \\ & + B_2|\psi'\bar{\psi}'\phi_a'\bar{\phi}_a'| + B_3|\psi''\bar{\psi}''\phi_b''\bar{\phi}_b''|\end{aligned} \tag{12}$$

Physically, one expects the ϕ_a' and ϕ_b'' orbitals to be more diffuse than ϕ_a and ϕ_b since the former are doubly occupied while the latter are only singly occupied. Similarly, the spectator orbitals in the different structures should have different sizes and shapes depending on whether they reside on cationic,

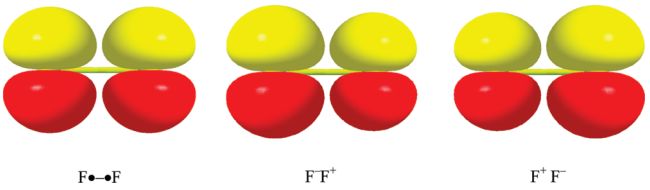

Figure 1. L-BOVB-computed π_y orbitals of F_2. Note the size difference in the left-hand vs right-hand side orbitals of the ionic forms. The two F atoms lie on the horizontal z-axis.

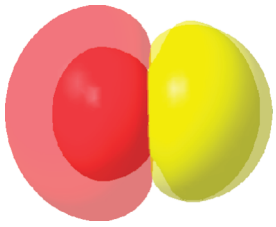

Figure 2. SL-BOVB split p_{1z} orbital of the F^- fragment in the F^-F^+ ionic structure in F_2. The p_{1z} orbital is split into two singly occupied orbitals, one diffuse (faint color) and one more compact (strong color). Red and yellow correspond to different signs of the lobes.

neutral, or ionic fragments. These differences are significant enough to be apparent with the naked eye, as shown in Figure 1, which displays some optimized π-orbitals for the three VB structures of difluorine, obtained by a BOVB calculation using the 6-31+G** basis set.

Thus, both the active and spectator orbitals can be viewed as instantaneously following the charge fluctuation by rearranging in size and shape, hence the name "breathing orbital". The physical meaning of this "breathing-orbital effect" can be grasped by remembering that the CASSCF and VBSCF levels only bring nondynamic electron correlation and that the missing dynamic correlation is obtained by further CI involving single, double, etc., excitations to outer valence orbitals. Now, as CI involving single excitations is physically equivalent to an orbital optimization (to first order), it becomes clear that BOVB brings dynamic correlation and is comparable to VBSCF + singles-CI, with the further advantage that it keeps the wave function as compact as the VBSCF wave function. More specifically, BOVB confers only that part of the dynamic correlation that varies along a reaction coordinate or throughout a potential surface. Therefore, it would be more exact to say that BOVB brings *differential* dynamic correlation. As such, BOVB brings about better accuracy relative to the VBSCF, GVB, SC, and CASSCF levels, as shown in benchmark calculations of bond dissociation energies and reaction barriers.[113−115,145] The relationship between the effect of breathing orbitals and dynamic correlation is particularly well illustrated in three-electron bonds, where all the electron correlation is of dynamic nature.[146]

The BOVB method has several lxevels of accuracy. At the most basic level, referred to as L-BOVB, all orbitals are strictly localized on their respective fragments. One way of improving the energetics is to increase the number of degrees of freedom by permitting the inactive orbitals to be delocalized. This option, which does not alter the interpretability of the wave function, accounts better for the nonbonding interactions between the fragments and is referred to as D-BOVB. Another improvement can be achieved by incorporating radial electron correlation in the active orbitals of the ionic structures by allowing the doubly occupied orbitals to split into two singly occupied orbitals that are spin-paired. This option carries the label "S" (for split), leading to the SL-BOVB and SD-BOVB levels of calculation, the latter being the most accurate one. In this manner, the two electrons are relocated into different regions of the space, as clearly seen in Figure 2, which shows the two split and spin-paired p_z orbitals of F^- in difluorine.

2.2.3. VBCI Method. An alternative way of introducing dynamic correlation into the VB calculation is the VBCI method[116,117], which uses the configuration interaction technique to incorporate the correlation. In MO-based theory, configuration interaction provides a conceptually simple tool for describing dynamic correlation via single-reference methods such as CISD and multi-reference-based methods such as MRCI. Similar ideas have also been applied to VB theory.[7,25,116,117,147−153] The CI technique usually requires a huge number of excited configurations; however, the aim of the VBCI method is to retain the conceptual clarity of the VBSCF method while improving the energetic aspect by introducing further electron correlation.

The VBCI method is a post-VBSCF approach, where the initially calculated VBSCF wave function is used as a reference. The VBCI wave function augments the VBSCF wave function with excited VB structures, which are generated from the reference wave function by replacing occupied (optimized VBSCF) orbitals with virtual orbitals. Different from MO-based methods, where virtual orbitals can be obtained from an SCF procedure, the virtual orbitals in VB theory are not available in the VBSCF calculation and should be defined for the VBCI method. To generate physically meaningful excited structures, the virtual orbitals should also be strictly localized, like the occupied VB orbitals. In the original VBCI method, the virtual orbitals were defined by using a projector:

$$\mathbf{P}_A = \mathbf{T}_A(\mathbf{T}_A{}^+\mathbf{M}_A\mathbf{T}_A)^{-1}\mathbf{T}_A{}^+\mathbf{S}_A \tag{13}$$

where $\mathbf{T}_A$ is the vector of orbital coefficients and the $\mathbf{M}_A$ and $\mathbf{S}_A$ are, respectively, the overlap matrices of the occupied VB orbitals and the basis functions, respectively, while the index A indicates that all matrices are associated with fragment A. It can be shown that the eigenvalues of the projector $\mathbf{P}_A$ are 1 and 0. The eigenvectors associated with eigenvalue 1 are the occupied VB orbitals, while the eigenvectors associated with eigenvalue 0 are used as the virtual VB orbitals of fragment A. By diagonalizing the projectors for all blocks, we can have all the virtual VB orbitals. A simpler way, which was implemented in the current versions of the VBCI and VBPT2 methods, uses Schmidt orthogonalization that is imposed on each fragment.[118]

With localized occupied and virtual orbitals, one can generate excited VB structures by replacing occupied orbitals with virtual orbitals. To create chemically meaningful excited structures, the excitation should involve the replacement of an occupied VB orbital only by those virtual orbitals that belong to the same fragment as the occupied orbital. As such, the excited VB structure Φ_K^i retains the same electronic pairing pattern and charge distribution as Φ_K^0. In other words, both Φ_K^i and Φ_K^0 describe the same "classical" VB structure. A VBCI function Φ_K^{CI} is defined by adding all excited VB structures Φ_K^i to the fundamental structure Φ_K^0:

$$\Phi_K^{CI} = \sum_i C_K^i \Phi_K^i \tag{14}$$

dx.doi.org/10.1021/cr100228r |*Chem. Rev.* 2011, 111, 7557–7593

where summation includes the fundamental structure. Therefore, a many-electron VBCI wave function is written as a linear combination of VBCI functions:

$$\Psi^{\mathrm{VBCI}} = \sum_K C_K^{\mathrm{CI}} \Phi_K^{\mathrm{CI}} = \sum_K \sum_i C_{Ki} \Phi_K^i \qquad C_{Ki} = C_K^{\mathrm{CI}} C_K^i \tag{15}$$

where the coefficients C_{K_i} are determined by solving the secular equation. The total energy of the system is

$$E^{\mathrm{VBCI}} = \frac{\sum_{K,L} \sum_{i,j} C_{Ki} C_{Lj} \langle \Phi_K^i | H | \Phi_L^j \rangle}{\sum_{K,L} \sum_{i,j} C_{Ki} C_{Lj} \langle \Phi_K^i | \Phi_L^j \rangle} \tag{16}$$

The compact forms of the Hamiltonian and overlap matrices may be respectively given by

$$H_{KL}^{\mathrm{CI}} = \sum_{i,j} C_{Ki} C_{Lj} \langle \Phi_K^i | H | \Phi_L^j \rangle \tag{17}$$

and

$$M_{KL}^{\mathrm{CI}} = \sum_{i,j} C_{Ki} C_{Lj} \langle \Phi_K^i | \Phi_L^j \rangle \tag{18}$$

A compact definition of the structure weights is

$$W_K = \sum_i W_{Ki} = \sum_{L,i,j} C_{Ki} M_{KL}^{ij} C_{Lj} \qquad M_{KL}^{ij} = \langle \Phi_K^i | \Phi_L^j \rangle \tag{19}$$

In this manner, the extensive VBCI wave function is condensed to a minimal set of fundamental structures, thus ensuring that the VBCI method keeps the VB advantage of compactness.

The CI space can be truncated following the usual CI methodology. The levels of CI are fashioned as in the corresponding MO−CI approach. Thus, VBCIS involves only single excitations, while VBCISD involves singles and doubles, and so on. VBCI applications[145] show that VBCIS gives results that are on par with those of D-BOVB, while the VBCISD method is somewhat better, and its results match those of the MO-based CCSD method. Furthermore, the VBCI method applies perturbation theory to truncate less important excited structures and estimates their contribution by an approximated perturbation formula, resulting in a VBCIPT level.

2.2.4. VBPT2 Method. The accuracy of VBCI applications is always satisfactory,[143,145,154,155] but the method is computationally demanding. The stumbling blocks in a VBCI calculation are (i) the construction of the Hamiltonian matrix with nonorthogonal AOs and (ii) the solution of the general secular equation, where the overlap matrix is nonunity. Perturbation theory is known to be an economical assessment of electronic correlation and is widely applied not only in MO-based methods, but also in the VB framework, such as in the GVB[11,156−159] and SCVB methods.[152]

The VBPT2 method[118] uses perturbation theory to incorporate dynamic correlation for the VB method, much like CASPT2 (e.g., VBPT2 suffers the same defect as CASPT2, e.g., intruder states). In the VBPT2 method, the wave function is written as the sum of the zeroth- and the first-order wave functions

$$|\Psi^{\mathrm{VBPT2}}\rangle = |\Psi^{(0)}\rangle + |\Psi^{(1)}\rangle \tag{20}$$

where the VBSCF wave function is taken as the zeroth-order wave function

$$|\Psi^{(0)}\rangle = |\Psi^{\mathrm{SCF}}\rangle = \sum_K C_K^{\mathrm{SCF}} |\Phi_K^0\rangle \tag{21}$$

Since higher order excitations do not contribute to the first-order interacting space, the first-order wave function is written as a linear combination of the singly and doubly excited structures, Φ_R:

$$\Psi^{(1)} = \sum_{R \in V^{\mathrm{SD}}} C_R^{(1)} |\Phi_R\rangle \tag{22}$$

The excited VB structures may be generated by replacing occupied orbitals with virtual ones, as in the VBCI method. However, to enhance the efficiency of VBPT2, the VB orbitals are defined in a different way and are partitioned into three groups: inactive, active, and virtual orbitals. The inactive orbitals are always doubly occupied in the VBSCF wave function, the active orbitals are occupied orbitals, with variable occupancies, and the virtual orbitals are always unoccupied in the VBSCF reference. These three groups maintain the following orthogonality properties: (i) The inactive and virtual orbitals are orthogonal within their own groups. (ii) The active orbitals are kept in the VB spirit as mutually nonorthogonal, but are orthogonal to the inactive and virtual orbitals by a Schmidt orthogonalization, which is done in the following order:

(1) The Löwdin orthogonalization is performed for the inactive orbitals.
(2) The Schmidt orthogonalization procedure is carried out between groups (inactive and active orbital groups), rather than each basis, where the order is inactive orbitals first and then active orbitals.
(3) The virtual orbitals are obtained by a two-step procedure: (3.1) group (Schmidt) orthogonalization between occupied orbitals and basis functions (occupied orbitals first and then basis functions); (3.2) removal of linearly independent vectors in the basis functions after step 3.1.

Such a definition of the orbitals keeps the VBSCF energy invariant, while the orthogonalization between orbital groups ensures the efficiency of the VBPT2 method.

In a fashion similar to that of MO-based multireference perturbation theory, a one-electron Fock operator is defined as

$$\hat{f}(i) = \hat{h}(i) + \sum_{m,n} D_{mn}^{\mathrm{SCF}} \left(\hat{J}_{mn}(i) - \frac{1}{2} \hat{K}_{mn}(i) \right) \tag{23}$$

where $\hat{J}_{mn}$ and $\hat{K}_{mn}$ are Coulomb and exchange operators, respectively, D_{mn}^{SCF} is the VBSCF density matrix element, and m and n denote the valence bond orbitals. Using the Fock operator defined in eq 23, the zeroth-order Hamiltonian is defined as

$$\hat{H}_0 = \hat{P}_0 \hat{F} \hat{P}_0 + \hat{P}_K \hat{F} \hat{P}_K + \hat{P}_{\mathrm{SD}} \hat{F} \hat{P}_{\mathrm{SD}} + \ldots \tag{24}$$

where $\hat{F} = \sum_i \hat{f}(i)$, $\hat{P}_0 = |0\rangle\langle 0|$ is a projector onto the VBSCF space, $\hat{P}_K$ is a projector onto the space complementary to that of the VBSCF wave function, and $\hat{P}_{\mathrm{SD}}$ is a projector associated with singly and doubly excited structures from the reference wave function.

On the basis of the Rayleigh−Schrödinger perturbation theory, the expansion coefficients of the first-order wave function and the second-order energy are written respectively as

$$\mathbf{C}^{(1)} = (\mathbf{H}_0^{11} - E^{(0)} \mathbf{M}^{11})^{-1} \mathbf{H}^{10} \mathbf{C}^{(0)} \tag{25}$$

dx.doi.org/10.1021/cr100228r |Chem. Rev. 2011, 111, 7557–7593

$$E^{(2)} = \mathbf{C}^{(0)+}\mathbf{H}^{01}(\mathbf{H}_0^{11} - E^{(0)}\mathbf{M}^{11})^{-1}\mathbf{H}^{10}\mathbf{C}^{(0)} \quad (26)$$

where $\mathbf{C}^{(0)}$ and $\mathbf{C}^{(1)}$ are the coefficient column matrices of the VBSCF, eq 21, and the first-order wave functions, eq 22, respectively, $E^{(0)}$ is the zeroth-order energy, and matrices $\mathbf{H}_0^{11}$, $\mathbf{H}^{01}$, $\mathbf{H}^{10}$, and $\mathbf{M}^{11}$ are respectively defined as

$$(\mathbf{H}_0^{11})_{RS} = \langle\Phi_R|\hat{H}_0|\Phi_S\rangle \quad (27)$$

$$(\mathbf{H}^{01})_{KR} = \langle\Phi_K|\hat{H}|\Phi_R\rangle \qquad (\mathbf{H}^{10})_{RK} = \langle\Phi_R|\hat{H}|\Phi_K\rangle \quad (28)$$

$$(\mathbf{M}^{11})_{RS} = \langle\Phi_R|\Phi_S\rangle \quad (29)$$

In the above equations, index K and indices R and S are respectively for the fundamental and the excited structures. $\hat{H}$ is the total system Hamiltonian.

It is obvious that the largest matrix is $\mathbf{H}_0^{11}$, which is block-diagonal, owing to the orthogonality constraints that are applied to the different orbital sets. Therefore, the VBPT2 method is computationally efficient, compared to VBCI. No Hamiltonian matrix elements with nonorthogonal orbitals are required past the VBSCF step. Owing to the orthogonality between different orbital groups, all matrix elements involved in the perturbation correction procedure of VBPT2 may be easily computed by using the Condon−Slater rules.

Though the VBPT2 wave function involves a large number of excited structures, the wave function is ultimately expressed in terms of a minimal number of fundamental structures, as in the VBSCF, by partitioning the first-order wave function into the fundamental structures.

VBPT2 applications show that the method gives computational results that are on par with those of the VBCISD method and match those of the MO-based MRCI and CASPT2 methods (at the same basis sets). The total VBPT2 energies match those of CASPT2 if one uses a properly designed VB wave function as a reference. Figure 3 shows the computational errors of bond dissociation energies relactive to FCI with various methods, where 3 structures, 1 covalent and 2 ionic, are involved for H_2 and F_2, and 12 and 17 structures are used for O_2 and N_2.

2.3. Add-Ons: VB Methods for the Solution Phase

2.3.1. VBPCM Method. Solvation plays an important role in the molecular energy, structure, and properties. Theoretical treatments of solute−solvent interactions have been the subject of many studies in computational chemistry. In this sense, the continuum solvation model is one of the most economical tools for describing the solvation problem. A typical and commonly used continuum solvation model developed by Tomasi et al.[119,120] is the PCM, wherein the solvent is represented as a homogeneous medium, characterized by a dielectric constant and polarized by the charge distribution of the solute. The interaction between the solute charges and the polarized electric field of the solvent is taken into account through an interaction potential that is embedded in the Hamiltonian and determined by a self-consistent reaction field (SCRF) procedure.

With its lucid insight into the understanding of chemical reaction, VB theory is very well suited for elucidating solvent effects in solution-phase reactions. Coupling the VB method with the PCM[119,120,160−167] generates the VBPCM method,[168] which was developed for exploring the solute−solvent interactions at

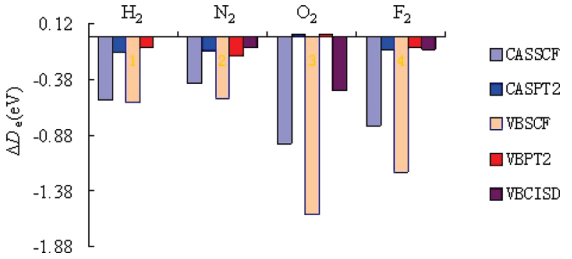

Figure 3. Computational errors of bond dissociation energies relative to the FCI method. Aug-cc-pVTZ basis set for H_2, DZP for N_2 and O_2, and cc-pVTZ for F_2.

the ab initio VB level. VBPCM uses the IEF version of the PCM model,[165−167] which is widely implemented in standard quantum chemical programs. To incorporate solvent effects into a VB scheme, the state wave function is expressed in the usual terms as a linear combination of VB structures, but now these VB structures interact with one another in the presence of the polarizing field of the solvent. The Schrödinger equation for the VBPCM can be expressed as

$$(H^0 + V_R)\Psi^{\mathrm{VBPCM}} = E\Psi^{\mathrm{VBPCM}} \quad (30)$$

where H^0 is the gas-phase Hamiltonian and the interaction potential V_R for the ith iteration is given as a function of the electronic density of the $(i-1)$th iteration and is expressed in the form of one-electron matrix elements that are computed by a standard PCM procedure. The detailed procedures are as follows:

(1) A VBSCF procedure in a vacuum is performed, and the electron density is computed.
(2) Given the electron density from step 1, effective one-electron integrals are obtained by a standard PCM subroutine.
(3) A standard VBSCF calculation is carried out with the effective one-electron integrals obtained from step 2. The electron density is computed with the new optimized VB wave function.
(4) Repeat steps 2 and 3 until the energy difference between the two iterations reaches a given threshold.

Having the optimized wave function, the final energy of a system in solution is evaluated by

$$E = \langle\Psi^{\mathrm{VBPCM}}|H^0 + \frac{1}{2}V_R|\Psi^{\mathrm{VBPCM}}\rangle \quad (31)$$

By performing the above procedure, the solvent effect is taken into account at the VBSCF level, whereby the orbitals and structural coefficients are optimized until self-consistency is achieved. The VBPCM method enables one to study the energy curve of the full VB state as well as that of individual VB structures throughout the path of a chemical reaction and then reveal the solvent effect on the different VB structures as well as on the total VB wave function. The method has been applied to the studies of S_N2 reactions in aqueous solution,[168,169] which will be reviewed in section 3, and to the heterolytic bond dissociation of C_4H_9Cl and C_3H_9SiCl in aqueous solution.[170] Figure 4 shows the potential energy curves of C_4H_9Cl in the gas phase and in the solvated phase, which illustrate intuitively different dissociation behaviors in the two different media, dissociating to radicals in the gas phase and to free ions in water.

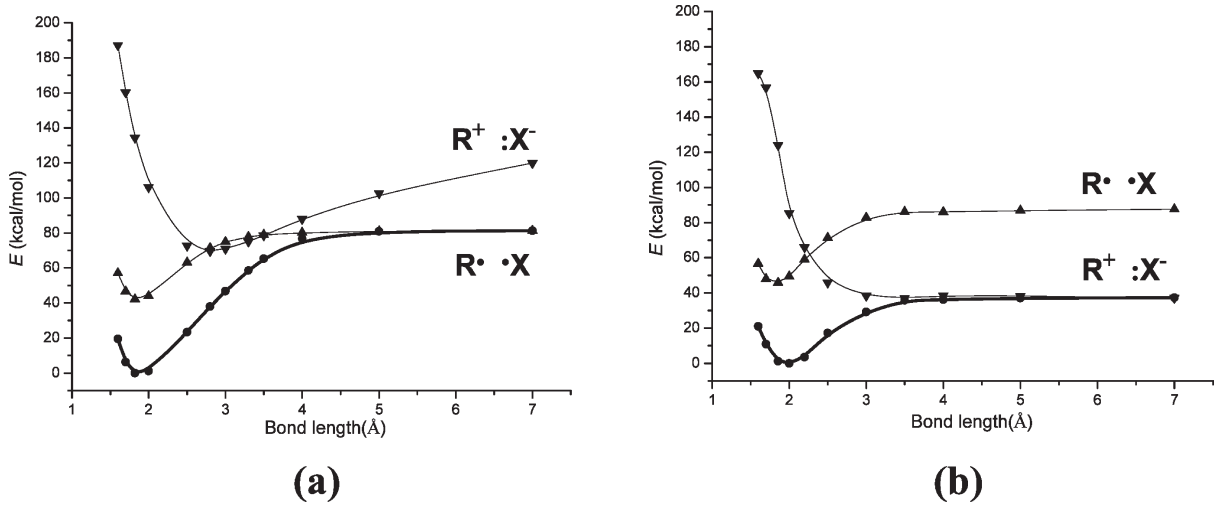

Figure 4. Dissociation curves of RX (R = $(CH_3)_3C$) (a) in the gas phase and (b) in the solvated phase.

2.3.2. VBSM Method. The VBPCM method incorporates PCM into the VB method, while the VBSM method applies the SMx (x = 1−8)[121,171,172] solvation model. SMx (x = 1−8), developed by Truhlar and co-workers, treats the electrostatics due to bulk solvent by the generalized Born approximation with self-consistent partial atomic charges.[121] In the SMx (x = 1−8) model,[121,171,172] the electrostatic free energy of solvation is augmented by terms proportional to the solvent-accessible surface areas of the solute's atoms times empirical geometry-dependent atomic surface tensions, accounting for cavitation, dispersion, and solvent structure effects, where the solvent structure effects include short-range deviations of the electrostatics from the bulk electrostatic model. The solvation free energy of SMx (x = 1−8) can be expressed as

$$\Delta G_S = \Delta E_E + G_P + G_{CDS} \quad (32)$$

where G_P is the negative electric polarization term, ΔE_E is the positive electronic energy term, and G_{CDS} is the term accounting for cavitation, dispersion, and solvent structure. The sum of G_P and ΔE_E is called ΔG_{EP}.

In the VBSM method,[173] electronic density is computed by using a VB wave function, which is used for computing the partial atomic charges, while all other parameters are taken from the normal SM6 solvation model.[171] As such, the VBSM method is able to produce all VB properties and thus provide intuitive insights into studied chemical problems in solution as the VBSCF method does in the gas phase.

To perform a VBSM calculation with orbital optimization, the following steps are involved in the current version of XMVB:

(1) Calculate (i) the Coulomb integrals $\gamma_{kk'}(R)$ that enter the generalized Born calculation, where k and k' label atoms, (ii) the solvent-accessible surface areas $A_k(R)$, and (iii) the geometry-dependent factors that enter the G_{CDS} calculation. R denotes the current geometry of the solute molecule.

(2) Perform a standard VBSCF calculation and then obtain the gas-phase VB wave function.

(3) Using the current VB density, we calculate the current partial atomic charges $q_k(R)$ by Mulliken (M) or Löwdin (L) population analysis, eqs 33 and 34

$$q_k^M(R) = Z_k - \sum_{\alpha \in k} (\mathbf{P}\cdot\mathbf{S})_{\alpha\alpha} \quad (33)$$

$$q_k^L(R) = Z_k - \sum_{\alpha \in k} (\mathbf{S}^{1/2}\cdot\mathbf{P}\cdot\mathbf{S}^{1/2})_{\alpha\alpha} \quad (34)$$

respectively, where Z_k is the nuclear charge of atom k, α is a basis function on atom k, and **P** and **S** are the one-electron density and overlap matrices, respectively. Then the generalized Born polarization energy[121,171,172] is calculated by

$$G_P = -\frac{1}{2}\left(1-\frac{1}{\varepsilon}\right)\sum_k\sum_{k'} q_k(R)\, q_{k'}(R)\, \gamma_{kk'}(R) \quad (35)$$

where ε is the bulk dielectric constant of the liquid solvent. Then ΔG_{EP} is obtained.

(4) Set ΔG_{EP} into a new VBSCF procedure and solve a new secular equation including SM6 terms. After the iterations have converged, the total solvation energy at the ab initio VB level is obtained.

Test calculations for a few systems show that the liquid-phase partial atomic charges obtained by VBSM are in good agreement with liquid-phase charges obtained by the charge model CM4.[171] Free energies of solvation are calculated for two prototype test cases, namely, for the degenerate S_N2 reaction of Cl^- with CH_3Cl in water and for a Menshutkin reaction in water. These calculations show that the VBSM method provides a practical alternative to single-configuration self-consistent field theory for solvent effects in molecules and chemical reactions.

2.3.3. Combined VB/MM Method. The VB/MM method, introduced by Shurki et al.,[122] presents a new kind of combined QM/MM method that combines the ab initio valence bond method with MM by importing the ideas from the empirical valence bond (EVB) approach.[174,175] It utilizes the ab initio VB approach for the reactive fragments and MM for the environment and thus extends VB applications to large biological systems. In the VB/MM method, the Hamiltonian of the whole system is expressed as

$$H^{VB/MM} = H^I(VB) + H^O(MM) + H^{I,O}(VB/MM) \quad (36)$$

where I and O stand for the inner (quantum) and the outer (classical) regions. $H^I(VB)$ is the VB Hamiltonian of an isolated

dx.doi.org/10.1021/cr100228r |Chem. Rev. 2011, 111, 7557–7593

quantum region (the gas-phase Hamiltonian) of all the atoms in the inner region, $H^{O}(MM)$ is the energy of all the atoms in the outer region determined by use of an empirical force field, and $H^{I,O}(VB/MM)$ is the Hamiltonian that accounts for all the interactions between the quantum and the classical atoms.

The diagonal matrix elements of the Hamiltonian, which include all the nonbonded interactions, are calculated by

$$H_{KK} = E_{KK} = E^{0}_{KK}(VB) + E^{int}_{KK} \quad (37)$$

where E^{0}_{KK} (VB) is the Kth diagonal matrix element of the VB structure energy in an isolated quantum region and E^{int}_{KK} describes the interactions of the ab initio VB active subsystem with the MM part involving all the nonbonded interactions, such as electrostatic, van der Waals, bulk, etc.

Following the idea underlying the EVB methodology,[174,175] the off-diagonal matrix elements of the Hamiltonian can be approximated as

$$H_{KL} = H^{0}_{KL}(VB) + (W_K E^{int}_{KK} + W_L E^{int}_{LL}) M^{0}_{KL} \quad (38)$$

where H^{0}_{KL} (VB) and M^{0}_{KL} are the off-diagonal elements of the Hamiltonian and overlap matrices between the Kth and Lth diabatic states (VB structures) in a vacuum, respectively. W_K and W_L are the respective weights of VB structures K and L given by eq 8.

The VB/MM method combines molecular mechanics for the diagonal elements with ab initio VB calculations for the off-diagonal elements, hence avoiding parametrizations as well as interpolations. The method maintains the advantages of the EVB methodology and provides an ab initio VB wave function. Recently, a new version of VB/MM, called density-embedding VB/MM (DE-VB/MM), was developed.[176] The improvement of the DE-VB/MM method is that the electrostatic interaction between the VB active subsystem and the MM environment is involved during the optimization of the VB wave function for the QM fragment, which is implemented by adding effective one-electron integrals to the ab initio VB Hamiltonian, hence taking into account the wave function polarization of the QM fragment due to the environment. A somewhat related method is the MOVB/MM approach of Mo and Gao.[177]

2.4. Molecular Orbital Methods That Provide Valence-Bond-Type Information

2.4.1. BLW Method. The BLW method is a simple bridge between MO and VB methods which provides VB-type information (e.g., resonance energies). As such, it is considered herein as a variant of the ab initio valence bond method which can be used for some specific applications, with the advantage of retaining the efficiency of molecular orbital methods.[123−127] The basic principle consists of partitioning the full basis set of orbitals into subsets each centered on a given fragment. The molecular orbitals are then optimized in a Hartree−Fock way, with the restriction that each orbital is expanded only on its own fragment. The MOs of a given fragment are orthogonal among themselves, but the orbitals of different fragments have finite overlaps.

The applications of the BLW method are designed primarily to evaluate the electronic delocalization and charge transfer effects between fragments/molecules. Thus, the block-localized wave function represents a reference for evaluating delocalization energies relative to the fully delocalized wave function.

A typical application of the BLW method is the energy calculation of a specific resonance structure in the context of resonance theory. As a resonance structure is composed, by definition, of local bonds plus core and lone pairs, a bond between atoms A and B will be represented as a bonding MO strictly localized on the A and B centers, a lone pair will be an atomic orbital localized on a single center, etc. With these restrictions on orbital extension, the self-consistent field solution can be decomposed to coupled Roothaan-like equation sets, each corresponding to a block. The final block-localized wave function is optimized at the constrained Hartree−Fock level and is expressed by a Slater determinant. Consequently, the energy difference between the Hartree−Fock wave function, where all electrons are free to delocalize in the whole system, and the block-localized wave function, where electrons are confined to specific zones of the system, is defined as the electron delocalization energy. Recently, the BLW method has been extended to DFT[178] by replacing the Hartree−Fock exchange potential by a DFT exchange-correlation (XC) potential in the Roothaan SCF procedure. This improved BLW method, referred to as BLW-DFT, has the advantages over the original method to bring electron correlation to both the individual structure and the final adiabatic states.

2.4.2. MOVB Method. The MOVB[125] method is an extension of BLW, which allows calculation of the electronic coupling energy resulting from the mixing of two or more diabatic states, i.e., states corresponding to single-resonance structures. The diabatic states are first calculated by the BLW method, and then a nonorthogonal configuration interaction Hamiltonian is constructed using these diabatic states as the basis functions. Thus, MOVB is a mixed molecular orbital and valence bond method, since it makes use of a Hartree−Fock or DFT description for the covalent bonds, while being able to calculate diabatic states. Importantly, solvent effects can be incorporated into the MOVB method. Thus, the MOVB method has been used to model the proton transfer between ammonium ion and ammonia in water,[125] as well as a solvated S_N2 reaction,[177] using Monte Carlo simulations.

One concern of the MOVB method is that the adiabatic state wave function is simply a mixture of two diabatic states without further reoptimization of the orbitals. To remedy this defect, an alternative BLW-based two-state model has been devised[179] that is applicable to cases where a ground state Ψ_0 can be approximately described in terms of a resonance between two diabatic structures, Φ_A and Φ_B:

$$\Psi_0 = C_A\Phi_A + C_B\Phi_B \quad (39)$$

Differently than in MOVB, here both the ground state and diabatic states are independently optimized at the same Hartree−Fock or DFT level, yielding the ground-state energy ε_0 and the diabatic energies ε_A and ε_B. The method assumes that, on one hand, the diabatic states are orthogonal to each other

$$S_{AB} = \langle\Phi_A|\Phi_B\rangle = 0 \quad (40)$$

but, on the other hand, the nonorthogonality effects are absorbed by the effective off-diagonal Hamiltonian $\langle\Phi_A|H|\Phi_B\rangle$, whose value is not directly computed but determined via a "reverse configuration interaction" procedure from the known values of ε_0, ε_A, and ε_B.

The orthogonality constraint further allows the construction of the first excited state as

$$\Psi_1 = C_B\Phi_A - C_A\Phi_B \quad (41)$$

dx.doi.org/10.1021/cr100228r |Chem. Rev. 2011, 111, 7557–7593

Table 1. Bond Dissociation Energies Calculated with Valence Bond Methods[180]

		D_e (kcal/mol)			
bond	basis set	BOVB	VBCISD[a]	CCSD(T)	exptl
F−F	6-31G*	36.2	32.3	32.8	
	cc-pVTZ	37.9	36.1	34.8	38.3
Cl−Cl	6-31G*	40.0	41.6	40.5	
	cc-pVTZ	50.0	56.1	52.1	58.0
Br−Br	6-31G*	41.3	44.1	41.2	
	cc-pVTZ	44.0	50.0	48.0	45.9
F−Cl	6-31G*	47.9	49.3	50.2	
	cc-pVTZ	53.6	58.8	55.0	60.2
H−H	6-31G**	105.4	105.4	105.9	109.6
Li−Li	6-31G*	20.9	21.2	21.1	24.4
H_3C-H	6-31G**	105.7	113.6	109.9	112.3
H_3C-CH_3	6-31G*	94.7	90.0	95.6	96.7
HO−OH	6-31G*	50.8	49.8	48.1	53.9
H_2N-NH_2	6-31G*	68.5	70.5	66.5	75.4 ± 3
H_3Si-H	6-31G**	93.6	90.2	91.8	97.6 ± 3
H_3Si-F	6-31G*	140.4[b]	151.1	142.6	160 ± 7
H_3Si-Cl	6-31G*	102.1	101.2	98.1	113.7 ± 4

[a] With Davidson correction.[116] [b] Two-structure calculations ($H_3Si^-F^+$ is omitted).

Thus, on the basis of the energies of the two diabatic states and the adiabatic state at the same level, one can derive the structural weights of the diabatic states in the ground state, the coupling energy between the two diabatic states, and the transition energy to the first excited state without introducing any empirical parameter.

Alongside the VB/MM method due to Shurki et al., MOVB/MM[177] is another kind of combined VB-type QM/MM method which is based on the BLW method discussed above.

3. APPLICATIONS

This section covers a variety of applications of the VB methods described above. It begins with a short survey of the accuracy of the methods and then discusses a panoramic set of applications.

3.1. Accuracy of Modern VB Methods

Any computational method dealing with reactivity must describe as accurately as possible the elementary events of a reaction, i.e., bond breakage or bond formation. This feature has been tested for various VB methods,[113−118,145,180] and the emerging conclusion is that the methods which account for dynamic correlation, e.g., BOVB, VBCI, and VBPT2, are reasonably accurate. On the other hand, the VB methods that involve only nondynamical correlation, e.g., GVB and VBSCF, generally provide good qualitative trends, but poor quantitative accuracy.

Table 1 shows bonding energies for a sample of homopolar and heteropolar bonds calculated by various methods with basis sets ranging from 6-31G* to cc-pVTZ.[180] It is seen that BOVB and VBCI give results on par with those of CCSD(T) calculations performed with the same basis sets. Furthermore, with a large enough basis set, all these methods give results close to experimental values.

Another important feature of modern VB methods is their ability to calculate reaction barriers with reasonable accuracy.

Table 2. Barriers for the Hydrogen Exchange Reactions $X^\bullet + HX \rightarrow XH + X'^\bullet$ ($X = CH_3$, SiH_3, GeH_3, SnH_3, PbH_3, and H)[a]

molecule	HF	CCSD	VBSCF	BOVB	VBCISD	VBCIPT
CH_3[b]	35.1	26.5	33.0	23.1	25.8	25.5
SiH_3[b]	25.2	19.3	25.5	19.1	19.7	19.0
GeH_3[b]	22.0	16.6	25.5	18.0	18.1	17.0
SnH_3[b]	18.5	13.5	20.5	14.9	15.3	14.1
PbH_3[b]	15.2	13.0	17.3	12.3	12.5	11.5
H[c]		9.8[d]	20.6	10.2	10.0	

[a] Energies in kilocalories per mole. [b] 6-31G* basis set: columns 2−5, ref 117; columns 6 and 7, ref 116. [c] Aug-cc-pVTZ basis set.[145] [d] CCSD(T) calculation.

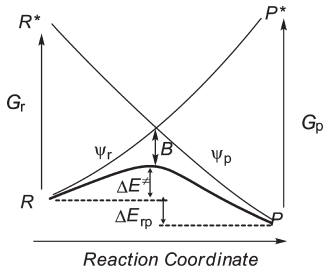

Figure 5. VBSCD for a general reaction $R \rightarrow P$. R and P are the ground states of the reactants and products, and R^* and P^* are the promoted excited states.

This is illustrated in Table 2, where some barriers for hydrogen abstraction reactions are calculated with various methods using the 6-31G* basis set (entries 1−5). It is seen that the BOVB, VBCISD, and VBCIPT methods provide barriers that are on par with CCSD results using the same basis set. Moreover, for the $H^\bullet + H-H' \rightarrow H-H + H'^\bullet$ reaction (last entry), BOVB and VBCISD also provide a barrier value very close to the exact barrier and comparable to the experimental value of 9.8 ± 0.2 kcal/mol. On the other hand, the less elaborate VBSCF method, which lacks dynamic correlation, generates barriers that are way too high in all cases.

The ab initio VB method has also been applied to the excited states of several diatomic molecules, such as O_2, NF, B_2, and LiB^+.[143,155,181] All the VB studies provide satisfactory numerical results with intuitive insights for the bonding of excited states.

Further examples, where VB-calculated barriers are on par with benchmark values and close to experimental estimates, are shown in the following sections.

3.2. Chemical Reactivity

There are two fundamental questions that any model of chemical reactivity would have to answer: What are the origins of the barriers? What are the factors that determine the reaction mechanisms? Since chemical reactivity involves bond breaking and making, VB theory, with its focus on the bond as the key constituent of the wave function, is able to provide a lucid model that answers these two questions in a unified manner. The centerpiece of the VB model is the VB state correlation diagram (VBSCD), which traces the energy of the VB configurations along the reaction coordinate and provides a mechanism for the barrier formation and generation of a transition state in an elementary reaction (Figure 5).[182]

dx.doi.org/10.1021/cr100228r |Chem. Rev. 2011, 111, 7557–7593

This diagram applies to elementary reactions wherein the barrier can be described as the interplay of two major VB states, that of the reactants and that of the products. It displays the ground-state energy profile for the reacting system (bold curve), as well as the energy profiles for individual VB states (thinner curves); these latter curves are also called "diabatic" curves, while the full state energy curve (in bold) is called "adiabatic". Thus, starting from the reactant geometry on the left, the VB structure Ψ_r that represents the reactant's electronic state, *R*, has the lowest energy and merges with the ground state. Then, as one deforms the reacting molecules toward the product geometry, Ψ_r gradually rises and finally reaches an excited state *P** that *represents the VB structure of the reactants in the product geometry*. A similar diabatic curve can be traced from *P*, the VB structure of the products in its optimal geometry, to *R**, the same VB structure but in the reactant geometry. Consequently, the two curves cross somewhere in the middle of the diagram. The crossing is of course avoided in the adiabatic ground state, owing to the mixing of the two VB structures, which stabilizes the resulting transition state by a resonance energy term, labeled *B*. The barrier is thus interpreted as arising from avoided crossing between two diabatic curves which represent the energy profiles of the VB state curves of the reactants and products.

The nature of the *R** and *P** promoted states depends on the reaction type and will be explained below using specific examples. In all cases, the promoted state *R** is the electronic image of *P* in the geometry of *R*, while *P** is the image of *R* at the geometry of *P*. The *G* terms are the corresponding promotion energy gaps, *B* is the resonance energy of the transition state, $\Delta E^{\ddagger}$ is the energy barrier, and ΔE_{rp} is the reaction energy. The simplest expression for the barrier is given by

$$\Delta E^{\ddagger} = fG_r - B \tag{42}$$

Here, the term fG_r is the height of the crossing point, expressed as some fraction (f) of the promotion gap at the reactant side (G_r).

A more explicit expression is

$$\Delta E^{\ddagger} \approx f_0 G_0 + (G_p/2G_0)\Delta E_{rp} + (1/2G_0)\Delta E_{rp}{}^2 - B$$

$$G_0 = 0.5(G_r + G_p) \qquad f_0 = f_r + f_p \tag{43}$$

which considers the two promotion gaps and *f* factors through their average quantities, G_0 and f_0. Equation can be further simplified by neglecting the quadratic term and taking $G_p/2G_0$ as ~1/2, thus leading to

$$\Delta E^{\ddagger} = f_0 G_0 + 0.5\Delta E_{rp} - B \tag{44}$$

Equation 44 expresses the barrier as a balance of the contributions of an intrinsic term, $f_0G_0 - B$, and a "driving force" term, $0.5\Delta E_{rp}$. The model is general and has been described in detail before[183−187] and applied to a large number of reactions of different types. Here we will briefly summarize some VB computational applications on hydrogen abstraction reactions and various S_N2 reactions.

3.2.1. Hydrogen Abstraction Reactions. Consider a general hydrogen abstraction reaction that involves cleavage of a bond H−Y by a radical $X^{\bullet\uparrow}$ (X, Y = a univalent atom or a molecular fragment):

$$X^{\bullet\uparrow} + H{-}Y \rightarrow X{-}H + Y^{\bullet\uparrow} \tag{45}$$

Practically, Ψ_r is a linear combination of covalent and ionic forms that contribute to the Lewis structure "$X^{\bullet\uparrow}$ + H−Y", as shown in the following:

$$\Psi_r = C_1(X^{\bullet\uparrow} + H^{\bullet}{-}{}^{\bullet}Y) + C_2(X^{\bullet\uparrow} + H^{+}{:}Y^{-}) + C_3(X^{\bullet\uparrow} + H{:}^{-}Y^{+}) \tag{46}$$

This combination is maintained in Ψ_r from *R* to *P** throughout the reaction coordinate, while the coefficients of the contributing structures change and adapt themselves to the geometric change (e.g., at infinite H---Y distance, C_1 = 1). The curve Ψ_p, which stretches between *P* and *R** is defined in an analogous manner. Two definitions are possible for the diabatic state curves Ψ_r and Ψ_p. In the variational diabatic configuration (VDC) method, the energies of the diabatic states are variationally minimized, as is done in the applications described below unless otherwise noted. In this way, each diabatic state has the best possible combination of coefficients and orbitals for this specific state. Alternatively, in the consistent diabatic configuration (CDC) method,[188] the diabatic states are simply extracted from the ground-state wave function by projection. As explained before,[183] the inconvenience of the CDC technique is that the so-constructed diabatic states involve orbitals and VB coefficients of the ground state and are therefore not optimal for the diabatic states. By comparison, the VDC technique gives quasi-variational quantities for all the parameters in the diagram (f, G, B).

Since the promoted state *R** is the VB structure of *P* in the geometry of R, its electronic state is illustrated by

$$R^{*} = (X^{\bullet\uparrow} + H^{\bullet})\text{--------}{}^{\bullet}Y \tag{47}$$

where the H−Y bond is infinitely long, while the $X^{\bullet\uparrow}$ radical (spin-up) experiences some Pauli repulsion with the electron of H, which is 50% spin-up and 50% spin-down. As such, the R* state is 75% a triplet state, and hence, the G_r gap is $(3/4)\Delta E_{ST}$, ΔE_{ST} being the singlet−triplet excitation of the X−H bond that undergoes activation.

In the study of identity reactions (X = Y), it has been shown that, indeed, the promotion energy G_r required to go from *R* to *R** is proportional to the singlet−triplet gap of the X−H bond[186,189] or to the X−H bonding energy D(X−H). Actually, systematic VB ab initio calculations by the VBCI method have shown that, to a good approximation, G_r can be expressed as follows:[189]

$$G_r \approx 2D(X{-}H) \tag{48}$$

Moreover, a semiempirical derivation showed[189] that the resonance energy *B* is also proportional to D(X−H) by the following expression:

$$B \approx 0.5D(X{-}H) \tag{49}$$

From the semiempirical expression for the height of the crossing point, it was possible to derive the value of the *f* factor for a series of identity H abstraction reactions. As the *f* factor appears to be relatively constant and close to 1/3, eqs 42 and 49 can be turned into the very simple eq 50, where it is seen that the barrier for identity H abstraction reactions depends on a single parameter of the reactants, D(X−H).

$$\Delta E^{\ddagger} \approx (2f - 0.5)D(X{-}H) \qquad f = 1/3 \tag{50}$$

The so-calculated barriers were shown to correspond quite well to the corresponding CCSD(T) barriers for a series of

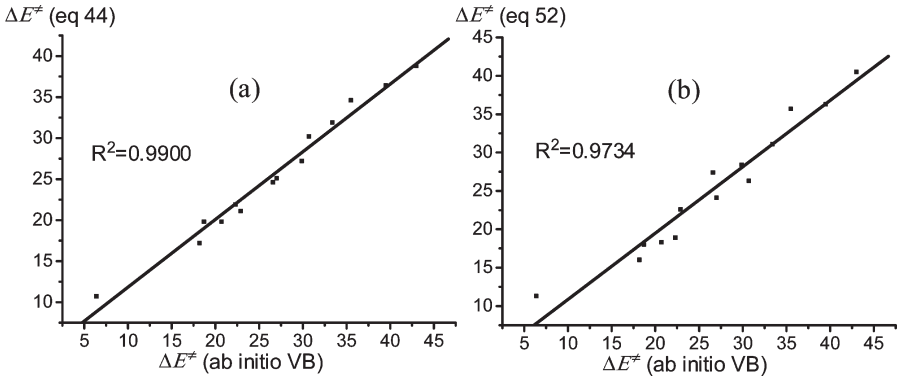

Figure 6. VBSCD-derived barriers plotted against ab initio VB-calculated barriers (kcal/mol).

identity abstraction reactions (X = Y = H, CH_3, SiH_3, GeH_3, SnH_3, PbH_3).[189] While the limitations of this expression have been discussed in detail, e.g., in the case where the transition state is not colinear for which B is larger than its value in eq 49 due to mixing of additional structures,[183] still eq 50 yields good orders of magnitude and correctly reproduces the trends in the series.

For nonidentity reactions (X ≠ Y), eq 44, which accounts explicitly for all the reactivity factors, was applied[190] to estimate the barriers for a series of 14 H abstraction reactions. The plot in Figure 6a shows good agreement with VBCISD-computed barriers.

Albeit being apparently more difficult to treat than identity reactions, if one assumes that the transition state coincides with the geometry of the lowest crossing point in the VBSCD, one can treat nonidentity reactions using semiempirical approximations that enable estimation of barriers from easily available quantities. Since the A−X and A−Y bonds are of different strengths, one being the weakest and the other the strongest, they have respective bonding energies D_W and D_S. VB calculations for the 14 reactions showed that B is approximately half of the weakest bonding energy, D_W, or, in other words, of the bond energy of the bond that is broken in the reactants of the exothermic direction of the reaction, while G_0 is close to the sum of both bonding energies:[190]

$$B = 0.5D_W \qquad G_0 = D_W + D_S \tag{51}$$

Thus, by taking $f_0 \approx 1/3$ as in identity reactions (accurate VB calculations yield $f_0 = 0.32-0.36$),[190] one gets the following very simple equation:

$$\Delta E^{\ddagger} = K(D_S - 0.5D_W) + 0.5\Delta E_{rp} \qquad K \approx 1/3 \tag{52}$$

Figure 6b displays a good correlation of the barriers calculated through eq 52 for the same 14 reactions as in Figure 6a plotted against the VBCISD calculations. Thus, it appears that the VBSCD model is able to express semiquantitative barriers for H abstraction reactions in terms of the bonding energies of reactants and products. Recent applications of eq 52 to the reactivity of cytochrome P450 in alkane hydroxylation shows that a good correlation with DFT-computed barriers is achieved with eq 52 using $f = 0.3$ and a constant B value, which is very close to $0.5D_W$.[191,192]

The MOVB method (see section 2.4.2) has also been applied by Mo and Gao to describe the diabatic and adiabatic potential energy curves in a model proton abstraction reaction:[125]

$$H_3N: + H{-}NH_3^+ \rightarrow H_3N^+{-}H + :NH_3 \tag{53}$$

At each point of the reaction coordinate, the three diabatic VB structures, respectively those of the reactants and products, complemented by an ionic structure $[H_3N{:}\,H^+{:}NH_3]$, were calculated by the BLW method, and the adiabatic ground state was calculated by configuration interaction between these VB structures, without further optimization of the orbitals. The MOVB results were found to be in good accord with the corresponding ab initio Hartree−Fock calculations for the proton transfer process. The authors also incorporated solvent effects into the MOVB Hamiltonian like in QM/MM calculations and have modeled the proton transfer between ammonium ion and ammonia in water using statistical Monte Carlo simulations in a cubic cell involving 510 water molecules with periodic boundary conditions.[125] By comparison to previous semiempirical treatments,[174,175] both diagonal and off-diagonal matrix elements in the MOVB Hamiltonian explicitly include solvent effects in the calculation. The reaction coordinate in solution is chosen as the energy difference between the diabatic reactant and product VB states, which ensures that the solvent degrees of freedom are adequately defined because the change in solute−solvent interaction energy reflects the collective motions of the solvent molecules as the reaction.[125] As a result, solvent effects were found to increase the barrier by 2.2 kcal/mol relative to that of the gas-phase process.

3.2.2. S_N2 Reactions in the Gas Phase. A generic S_N2 reaction is shown in eq 54 where the nucleophile, $X{:}^-$, shifts an electron to the A−Y electrophile and forms a new X−A bond while the leaving group Y departs with the negative charge.

$$X{:}^- + A{-}Y \rightarrow X{-}A + :Y^- \tag{54}$$

Let us derive now an expression for G_r by simply examining the nature of the excited state R^* relative to the corresponding ground state.[183−187] In R^*, A and Y are geometrically close to each other (as in the ground state, R) and separated from X by a long distance. The X fragment, which is neutral in the product P, must remain neutral in R^* and therefore carries a single active electron. As a consequence, the negative charge is located on the A---Y complex, so that the R^* state is the result of a charge transfer from the nucleophile ($X{:}^-$) to the electrophile (A−Y), as depicted by

$$R^* = X^{\bullet} \;//\; (A{\therefore}Y)^- \tag{55}$$

It follows that the promotion from R to R^* has two parts: an electron detachment from the nucleophile, $X{:}^-$, and an electron attachment to the electrophile, A−Y. The promotion energy G_r is therefore the difference between the vertical ionization

dx.doi.org/10.1021/cr100228r |Chem. Rev. 2011, 111, 7557–7593

potential of the nucleophile, $I^*_{X:}$, and the vertical electron affinity of the electrophile, A^*_{A-Y}, given by

$$G = I^*_{X:} - A^*_{A-Y} \quad (56)$$

where the asterisk denotes vertical quantities. Thus, the mechanism of a nucleophilic substitution may be viewed as an electron transfer from the nucleophile to the electrophile and a coupling of the supplementary electron of the electrophile to the remaining electron of the nucleophile. In fact, the description is general for any electrophile−nucleophile combination.

Ab initio BOVB calculations have been performed by Song et al.[193] for the following identity reaction using the XMVB program:[108,109]

$$X:^- + H_3C{-}X \rightarrow X{-}CH_3 + X:^- \ (X = F, Cl, Br, I) \quad (57)$$

In the gas phase, the barriers from the reactant complex $[X^- (H_3C{-}X)]$ to the transition state, as calculated at the BOVB/6-31G* level, were found to be within less than 3 kcal/mol of the CCSD(T) values in the same basis set (see Table 3). The BOVB method was also used to derive the barrier-controlling factors for the VBSCD model using eq 42. It was found that the f parameter is quasi-constant, 0.197, 0.181, and 0.197 for X = F, Cl, and Br, respectively, and somewhat larger, 0.234, for X = I (Table 3). This indicates that f is relatively independent of the nature of X, at least within the series of halide exchange reactions. On the other hand, as expected from previous treatments,[186] the value of B should be sensitive to the charge on the central methyl group. This expectation was indeed realized in the BOVB calculations, which showed that B is not constant and obeys the following semiempirical expression:

$$B(S_N2) = (1 - Q)0.5D \quad (58)$$

where D is the bonding energy of the $X{-}CH_3$ bond and Q is the weight of the $X^- [CH_3]^+ X^-$ VB structure in the transition state or, more simply, the net charge of the CH_3 fragment in the transition state. Importantly, the Q parameter is close to 0.5 in the X = F, Cl, Br series, varying between 0.53 and 0.41 (see Table 3). Therefore, the barrier can be estimated through eq 42 from a property of the reactants, G_r, a quasi-constant parameter, f, and an easily quantifiable parameter, B.

It is tempting to consider the f and Q parameters for the identity reactions as being universal within a given row of the periodic table and to use them unchanged to predict barriers in nonidentity S_N2 reactions. This has been done with a *very* unsymmetrical reaction,[169] the Menshutkin reaction (eq 59

$$H_3N: + H_3C{-}Cl \rightarrow H_3N^+{-}CH_3 + X:^- \quad (59)$$

and Figure 7), which is very endothermic in the gas phase and at the same time proceeds with neutral reactants while the products are ionic. As the backward reaction is not a simple nucleophilic attack but also involves the breaking of an ion pair in the gas phase (IP in Figure 7), we will only consider the forward process and eq 42, discarding eqs 43 and 44, which would be meaningless in this case. As the nucleophile is NH_3, it is legitimate to take the same f factor as in the identity reaction with chlorine (Table 3), i.e., f = 0.181, since N and Cl have the same electronegativity (3.0).

For the B factor, we can use a formula derived from eq 58, remembering that for a nonidentity reaction one uses the bonding energy of the bond that is broken in the reactants of the exothermic reaction, here $H_3N^+{-}Cl$ (see Figure 7):

$$B(S_N2) = (1 - Q)0.5D_W \qquad D_W = D(H_3N^+{-}Cl) \quad (60)$$

Using a standard (MP2-calculated) value of 122.6 kcal/mol for $D(H_3N^+{-}Cl)$ and an average value of 0.5 for Q in eq 60 yields a value of 30.7 kcal/mol for B, in excellent agreement with the BOVB/6-31G*-calculated value of 30.2 kcal/mol (Table 4). The so-estimated f and B parameters can now be used in eq 42, together with an estimation of G_r, to get a semiempirical barrier for the Menshutkin reaction in the gas phase. G_r can be calculated in the MO or VB framework or directly taken as an experimental quantity when available.[194] Here, the BOVB-calculated promotion energies led to a G_r value of 372 kcal/mol. Now, applying eq 42 leads to a semiempirical barrier estimate of 36.7 kcal/mol for the gas-phase Menshutkin reaction, in excellent agreement with the BOVB-calculated value, 35.1 kcal/mol (Table 4).

As was done in a hydrogen abstraction reaction (section 3.2.1),[125] the MOVB approach was applied to S_N2 reactions to reduce the multiconfigurational Hamiltonian, here into an effective two-state model,[188,195] and compared to the VBSCF approach. In the VBSCF calculation, the diabatic states Ψ_r and Ψ_p are defined as in the following equations, where the coefficients are optimized at each point of the reaction coordinate:

$$\Psi_r = C_1(X:^- A\bullet{-}\bullet Y) + C_2(X:^- A:^+ Y^+) + C_3(X:^- A^+ Y:^-) \quad (61)$$

$$\Psi_p = C_4(X\bullet{-}\bullet A:Y^-) + C_5(X^+:A^-:Y^-) + C_6(X:^- A^+:Y^-) \quad (62)$$

where it is seen that Ψ_r and Ψ_p share a common ionic VB structure, $(X:^- A^+:Y^-)$, so that the VBSCF calculation is actually a five-structure one.

In the MOVB model, both Ψ_r and Ψ_p are defined as BLW wave functions, referred to as Ψ_r^{MOVB} and Ψ_p^{MOVB}, i.e.,

Table 3. VBSCD Parameters and Reaction Barriers for the Identity Reaction $X:^- + H_3C{-}X \rightarrow X{-}CH_3 + X:^-$ (X = F, Cl, Br, I)[a]

VBSCD quantity	F	Cl	Br	I
		Gas Phase		
B	29.2	21.2	21.1	20.2
G	218.9	194.6	164.6	129.0
f	0.197	0.181	0.197	0.237
$\Delta E^{\ddagger}$(BOVB)	14.0	14.0	11.4	10.4
$\Delta E^{\ddagger}$(CCSD(T))	11.3	13.7	10.5	9.1
		Aqueous Phase		
B	25.1	16.9	17.8	16.3
G^b	343.8	281.2	246.0	200.0
f	0.166	0.155	0.169	0.194
$\Delta E^{\ddagger}$(BOVB)	32.0	26.8	23.8	22.6
$\Delta E^{\ddagger}$(exptl)	31.8	26.5	23.7	23.2

[a] Energies in kilocalories per mole. [b] Calculated from the gas-phase value through eq 67.

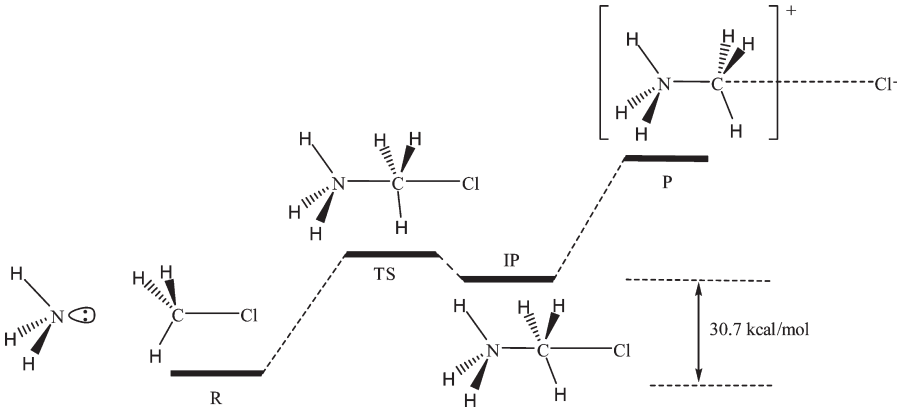

Figure 7. Schematic energy levels and geometries for the Menshutkin reaction in the gas phase.

Table 4. VBSCD Parameters and Reaction Barriers for the Menshutkin Reaction[a]

	G_r	G_p	G_0	B(BOVB)	semiempirical B	$\Delta E^{\ddagger}$(BOVB)	$\Delta E^{\ddagger}$(CCSD(T))	semiempirical[b] $\Delta E^{\ddagger}$
gas phase	372.5			30.2	30.7[c]	35.1	36.8	36.4
water	308.3	314.6	311.2	21.4	20.9[d]	14.2	15.2	13.5

[a] Energies in kilocalories per mole. [b] Semiempirical reaction barriers calculated with f values taken from the identity S_N2 reaction $Cl:^- + H_3C{-}Cl \rightarrow Cl{-}CH_3 + Cl:^-$ and B values calculated through eqs 60 (gas phase) and 69 (water). [c] Equation 60. [d] Equation 69.

represented by a single determinant (see section 2.4.1), and the ground state is represented as a combination of the two diabatic functions:

$$\Phi^{\mathrm{MOVB}} = C_r\Psi_r^{\mathrm{MOVB}} + C_p\Psi_p^{\mathrm{MOVB}} \tag{63}$$

The MOVB model has been applied and compared to VBSCF calculations with both the CDC and VDC definitions of the diabatic states (vide supra) on the S_N2 reaction shown in the following equation using the XMVB program:[108,109]

$$H_3N: + H_3C{-}NH_3^+ \rightarrow H_3N^+{-}CH_3 + :NH_3 \tag{64}$$

It was shown that the CDC diabatic states from VBSCF and from MOVB are in remarkable agreement, and the same agreement was found for the adiabatic ground-state curve.[188]

However, one shortcoming of both the five-structure VBSCF and MOVB approaches is that they do not include the long-bond VB structure that is further needed to fully describe the four-electron three-orbital system of the S_N2 reaction, namely, the $(X^{\bullet}\,A:^{-}\,{}^{\bullet}Y)$ structure. As a result, the reaction barrier in the adiabatic groun- state curve is always found too large relative to accurate calculations. To remedy this defect, the effective-Hamiltonian MOVB (EH-MOVB) model was proposed,[195] in which a diabatic coupling scaling factor is introduced to match the calculated barrier with a target value.

In this model, the diabatic states are calculated in a CDC fashion; i.e., the coefficients C_r and C_p and the orbitals of Ψ_r^{MOVB} and Ψ_p^{MOVB} in eq 63 are variationally optimized to minimize the energy of the adiabatic ground state on each point of the reaction coordinate. Then the adiabatic ground-state curve is recalculated by 2×2 configuration interaction among the diabatic states, but with a scaled off-diagonal effective Hamiltonian matrix element H_{12}^{EH}, as in the following equation:

$$H_{12}^{\mathrm{EH}} = \beta\langle\Psi_r^{\mathrm{MOVB}}|H|\Psi_p^{\mathrm{MOVB}}\rangle \tag{65}$$

where β is a diabatic scaling coupling constant that is kept invariant for all points of the reaction coordinate and is chosen so it reproduces exactly the barrier height of a target potential, derived either from experiment or from high-level ab initio calculations. In addition, if the energy of the reaction is not in good agreement with experiment, the EH-MOVB results can be further adjusted to match experiment by shifting the energy of the product diabatic state Ψ_p^{MOVB}. The EH-MOVB model has been applied to the S_N2 reaction (eq 66),[195] with a scaled diabatic coupling (β in eq 65) calibrated to reproduce the reaction barrier of a six-structure VBSCF calculation, involving the full set of VB structures necessary to describe the reaction.

$$HS:^- + H_3C{-}Cl \rightarrow HS{-}CH_3 + Cl:^- \tag{66}$$

The shapes of the potential surfaces, diabatic as well as adiabatic, were found to display good agreement between the EH-MOVB and VBSCF levels.[195] On the other hand, the diabatic coupling maps were found to be qualitatively different for the two methods.

3.2.3. S_N2 Reactions in the Aqueous Phase from an Implicit Solvent Model. The computational approaches for the inclusion of solvation effects can roughly be divided into two categories, one implicit and the other explicit. The PCM model[119,120] belongs to the first category and is one of the most widely used methods in the framework of dielectric continuum models. The recently developed VBPCM method incorporates PCM into modern VB calculations.[168] The VBPCM method has an important conceptual bonus since it enables us to compute energy profiles for the full state as well as for the individual VB structures. In so doing, the VB calculations reveal the effect of solvent on the constituents of the wave function, thereby providing a useful insight into the reaction in solution.

The VBPCM method, with the BOVB option, has been used to study the identity reaction $X:^- + H_3C{-}X \rightarrow XCH_3 + X^-$

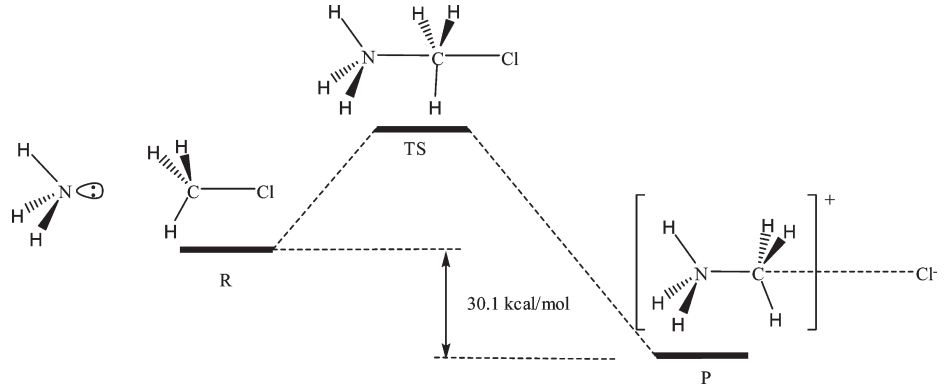

Figure 8. Schematic energy levels and geometries for the Menshutkin reaction in the aqueous phase.

(X = F, Cl, Br, I) in aqueous solution,[193] as was done for the gas-phase reaction (vide supra). As shown in Table 3, the BOVB-calculated barriers in the solvated phase are in excellent agreement with the experimental values, within 1 kcal/mol or less. The calculations also provide the key parameters of the VBSCD model, such as the resonance energy B at the transition-state geometry (see Figure 5) and the height of the crossing point of the diabatic curves relative to the reactants. On the other hand, the promotion gap G_r cannot be directly calculated by the VBPCM method because the two species that form the R^* promoted state, i.e., $X^\bullet$ and $[H_3C\therefore X]^-$, should be solvated with the same solvent configurations as for the ground state; that is, they are in a state of nonequilibrium solvation, whereas the PCM model deals only with equilibrium solvation. As such, the promotion gap in a solvent would be underestimated if calculated by any method coupled with a continuum solvation model. However, the problem can be circumvented by using a semiempirical nonequilibrium solvent model developed previously.[196−198] In the present case, this model takes the following simple form[196−198], which estimates the promotion gap in the solvent, G_s, from the promotion gap in the gas phase (G_g).

$$G_s \approx G_g + 2\rho S_{X^-} \tag{67}$$

where S_{X^-} is the desolvation energy of $X:^-$ and ρ is the solvent reorganization factor, which can be quantified from the static and optical dielectric constants of the solvent by

$$\rho = (\varepsilon - \varepsilon_{opt})/[\varepsilon_{opt}(\varepsilon - 1)] \tag{68}$$

where $\varepsilon_{opt} = n^2$ and n is the refractive index of the solvent.

With water as the solvent, the value of ρ is 0.56. The reorganization factor takes into consideration the fact that the species in the excited state are not solvated in their equilibrium solvent configurations, but in the same ones as the ground-state species beneath them, and hence, their solvation energy is downsized. The so-calculated promotion gaps in solvent are displayed in Table 3 and are seen to be significantly larger than their gas-phase analogues, G_s, as expected. The f parameters in solvent are deduced from the calculated G_g, $\Delta E^{\ddagger}$, and B values. As for the gas-phase reactions, the f parameters for the solvated reactions are found to be somewhat constant in the series X = F, Cl, Br, slightly larger for X = I, and in all cases larger than the corresponding values in the gas phase (Table 3).[193]

Once again, one may tentatively use the parameters of the identity reactions, this time in the aqueous phase, to make semiempirical predictions on the barriers of solvated nonidentity reactions. This has been done for the aqueous solution Menshutkin reaction,[169] which displays thermochemistry and a barrier extremely different from those of the gas-phase reaction owing to the neutral nature of the reactants and the ionic nature of the products. As illustrated in Figure 8, the Menshutkin reaction, which was endothermic from the reactants to the ion pair in the gas phase by 30.7 kcal/mol,[169] is *exothermic* by 30.1 kcal/mol in the aqueous phase, and the two ionic products are independently solvated.

Since there is no stable ion pair in the products in the solvated phase, both forward and backward processes are "normal" S_N2 reactions and the general eq 44 is appropriate. The promotion energies are first estimated from their gas-phase values using the semiempirical nonequilibrium solvation model,[196,197] leading to the G_0 value (Table 4). Then, to estimate B semiempirically, one must use eq 58 in which D is the bonding energy of the bond that is broken in the reactants of the exothermic reaction. This is now the H_3C-Cl bond, since the exothermic reaction is now the forward one, in contrast to the gas-phase reaction:

$$B(S_N2) = (1 - Q)0.5D_W \qquad D_W = D(H_3C-Cl) \tag{69}$$

With an MP2/6-31G* value of 83.4 kcal/mol for the C−Cl bond energy in H_3C-Cl,[169] and the mean value of 0.5 for Q, one gets a semiempirical value of 20.9 kcal/mol for B, to be compared with the accurately calculated value of 21.4 kcal/mol (Table 4). Finally, taking f_0 = 0.155 as in the identity S_N2 reaction of chloride (Table 4), application of eq 44 leads to a semiempirical barrier of 36.4 kcal/mol, in excellent agreement with the BOVB-calculated value of 35.1 kcal/mol.[169]

The very recent VBSM valence-bond-based solvation model (see section 2.3.2) has also been applied to the identity exchange reaction (eq 57) and to the Menshutkin reaction (eq 59) for the sake of comparison with the VBPCM model (section 2.3.1) and with the SM6 model,[171] the latter being used in the DFT framework (hence DFT/SM6).[171] For the identity reactions (eq 57), both SM6/DFT and VBPCM/BOVB models perform well, providing free energies of activation of 25.8 and 26.1 kcal/mol, respectively, to be compared with an experimental value of 26.5 kcal/mol. On the other hand, all the VBSM free energies of activation for the identity reactions were found to be too large in the VBSM model, even at the VBSM/BOVB level, where the value was still 10 kcal/mol higher than the experimental value. By contrast, for the Menshutkin reaction the VBSM and VBPCM methods were in excellent agreement. In both frameworks, the VBSCF level was found to be inaccurate, for lack of dynamic correlation, but

dx.doi.org/10.1021/cr100228r |*Chem. Rev.* 2011, 111, 7557–7593

at the BOVB level, both VBPCM and VBSM methods gave free energies of activation in excellent agreement with the SM6 calculation.

3.2.4. S_N2 Reactions in the Aqueous Phase from Molecular Dynamics with Explicit Solvent Molecules. The identity S_N2 reaction $Cl^- + CH_3Cl$ (eq 57) in water has been studied by Sharir-Ivry and Shurki[199] using their VB/MM model, which employs explicit solvent molecules (see section 2.3.3). This approach has the advantage of directly addressing nonequilibrium solvation for the calculation of the *G* promotion energy in the VBSCD model in solution. Recall that since *G* is defined as the vertical excitation energy between the reactant state *R* and the promoted state *R** in the reactant's geometry, the orientation of the solvent molecules in the promoted state should retain the original orientation as in the reactant state. While the VBPCM model cannot compute nonequilibrium solvation, and requires a semiempirical approximation (e.g., eq 67), the VB/MM approach provides a direct solution by keeping the same solvent configuration in both *R* and *R**. The simulation system was divided into four regions: Region I included the reacting fragments methyl halide and the halide anion ($CH_3X + X^-$), region II included the water molecules up to a radius of 18 Å, and region III included water molecules that were subjected to distance and polarization constraints according to the surface-constrained all-atom solvent boundary condition.[199] The rest of the system was presented by a bulk region with a dielectric constant of 80.

The VB calculations were performed at the BOVB level and resulted in calculated aqueous solution barriers in very good agreement with experimental values. The parameters of the VBSCD model were also calculated and compared to those calculated in the VBPCM solvation model. Expectedly, the *G* promotion energies in solvent were found to be much larger than the same quantities in the gas phase due to the aforementioned effect of the nonequilibrium solvation that destabilizes R*. Moreover, the BOVB/MM-calculated *G* values, respectively 392, 324, 270, and 217 kcal/mol (for X = F, Cl, Br, I), were in reasonably good agreement with the values estimated through the semiempirical eq 67 in the VBPCM model: 344, 281, 246, and 200 kcal/mol (Table 4). The tendencies in the *G* values are the same, and the ratio of VBPCM to VB/MM values is fairly constant, ca. 1.09−1.15. This nice agreement between the semiempirical model and the rigorous molecular dynamics with explicit solvent molecules confirms that the former can be meaningfully applied to the study of chemical reactions in solution.

The same identity S_N2 reaction (eq 57) in water was also studied by Mo and Gao[177] using a combined VBSCF/MM and MOVB/MM approach with explicit solvent molecules in the same spirit as their study of a hydrogen abstraction reaction (eq 53, section 3.2.1). The aim of the study was to test the validity of the MOVB/MM approach and find a simple way of incorporating the solvent reaction coordinate for chemical reactions in solution. The problem that had to be faced is that the barrier height for simple reactions in water can be significantly altered if the reaction coordinate excludes solvent degrees of freedom, owing to nonequilibrium solvation effects.[200] As in the study of the hydrogen abstraction reaction,[125] the adopted strategy consisted of defining the reaction coordinate as the difference between the energies of the reactant and product diabatic states in water.

The same three resonance structures were used in both the VBSCF and MOVB calculations, including the reactant and product configurations, plus the zwitterionic state, $Cl:^{-}\ ^{+}CH_3:Cl^-$. In the MOVB calculations, these structures are described as usual in the BLW fashion (see section 2.4.1), i.e., as single Slater determinants which are optimized independently, and the final adiabatic ground state is calculated by a 3×3 CI calculation that only optimizes configurational coefficients. On the other hand, in VBSCF, the VB configurations are optimized within the full multiconfigurational adiabatic wave function. The gas-phase barrier and the binding energy for the ion−dipole complex were found in good agreement with experiment at the VBSCF level, while MOVB slightly overestimated the barrier.[177]

Statistical mechanical Monte Carlo simulations were performed in a box containing 740 water molecules with periodic boundary conditions. At the HF/MM level, the computed free energy of activation was found to be in excellent agreement with experiment, with an error of only 0.6 kcal/mol, thus confirming the validity of the chosen solvent reaction coordinate. On the other hand, the MOVB/MM barrier was found too large by 10 kcal/mol, attributed partly to the gas-phase difference and partly to solvent effects. It was concluded that it is important to optimize each VB state in the presence of all other states in a full SCF calculation.[177]

Scheme 5. Spectrum of the Rumer Structures for (a) Polyenes and (b) Polyenyl Radicals

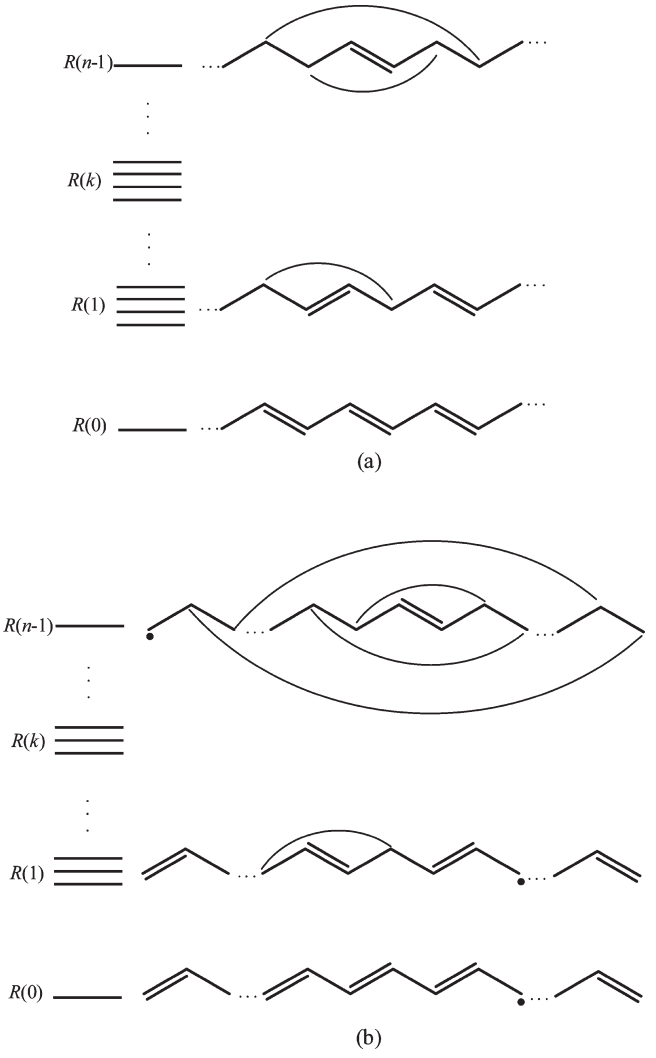

3.3. Excited States of Polyenes and Polyenyl Radicals

VB theory provides a powerfully intuitive tool for understanding the chemical bonding not only for the ground states but also for the excited states.[183] Ab initio VB theory was applied to the ground states and the covalent states of polyenes $C_{2n}H_{2n+2}$ (n = 2−8) and polyenyl radicals $C_{2n-1}H_{2n+1}$ (n = 2−8)[154] using Rumer structures. These structures are shown in Scheme 5 and are classified by the number of short bonds, which are π-bonds between two neighboring atoms, and where parts a and b are for polyenes and polyenyl radicals, respectively. Two levels, VBSCF and VBCI, were applied to calculate excitation energies, which are from 1^1A_g to 2^1A_g for polyenes and from $^2B_1$ to $^2A_2$ or from $^2A_2$ to $^2B_1$ (depending on the number of carbon atoms) for polyenyl radicals. Two types of truncations were employed in the calculation; one truncates the Rumer space of VBSCF level, e.g., VBSCF(S,D), while the other truncates the excitation space of the VBCI level, e.g., VBCI(S,D).

The computed VB vertical excitation energies, Table 5, are in good agreement with the MO-based method MRCI at the same basis set. For the polyenes, the deviations of VBCISD from the MRCI results are in the range of 0.03−0.08 eV. Compared to the semiempirical VBDFT(s), which is a semiempirical VB method that incorporates the DFT energy of the nonbonded reference state,[201−204] the ab initio VB values are slightly higher by 0.3−0.4 eV. For the polyenyl radicals, all the results of the three ab initio levels, VBSCF, VBCIS, and VBCISD, are in very good mutual agreement. At the same time, all the ab initio VB results are in very good agreement with the corresponding VBDFT(s) data, though the latter is just a Hückel-type VB method. The match between ab initio VB results with MRCI is also good. The differences between VBCISD and the MRCI methods are in the range of 0.03−0.06 eV.

It was found that the variation of the VBSCF excitation energy as a function of the number of carbons in the polyene chain follows an exponential fit:

$$\Delta E = 2.63 + 7.848e^{-0.189(2n)}$$
$$R^2 = 0.99987 \qquad n = 2, 3, 4, \ldots \tag{70}$$

The intercept value of 2.63 eV at $n \rightarrow \infty$ means that long polyenes will have a residual energy gap, presumably due to bond alternation. For the radical series, the VBSCF data fit as a cosine function, which at $n \rightarrow \infty$ converges to zero, having no residual gap:

$$\Delta E = 5.037 \cos\frac{n-1}{2n}\pi \qquad R^2 = 0.86629 \qquad n = 2, 3, 4, \ldots \tag{71}$$

The study of the polyenes and polyenyl radicals shows that the ab initio VB theory is able to provide numerical accuracy for the physical properties of excited states. Additionally, the VB wave function, which is made up of Rumer structures, enables lucid understanding of excited-state properties, such as the makeup of the various states and their energies and geometries, the opposite bond alternation properties of the ground and excited states, isomerization patterns, soliton characteristics, etc.[183]

3.4. Quantitative Evaluation of Common Chemical Paradigms

3.4.1. BLW Examination of the Role of Conjugation in the Rotational Barrier of Amides. The amide functional group plays a fundamental role in biology as a basic building block of proteins and enzymes. It is characterized by specific properties such as coplanarity of the groups attached to the nitrogen atom, a substantial rotational barrier, and kinetic stability toward nucleophilic attack or hydrolysis. All these properties are readily rationalized on the basis of the most popular concept of amide resonance by which the nitrogen atom is able to delocalize its lone pair over the whole C, N, O π-system to gain stabilization. This delocalization of the π-electrons implies that the planar amide group has to be represented by a set of three resonance structures (Scheme 6, **1**−**3**).

In the resonance model, the delocalization also implies the planarity of the nitrogen group. This delocalization is disrupted when the C−N bond is twisted as in **4**, leading to a net destabilization that accounts for the significant rotational barrier. Other properties of the amide group, such as the shortened C−N distance, reduced C═O stretching frequency, and reduced nitrogen basicity, are also satisfactorily explained by the resonance model, which implies contribution of structure **2** to the ground state of the planar form.

However successful, the simple resonance picture has been challenged by several authors,[205−209] mostly on the basis of electron population analyses, and alternative models were suggested. Thus, the rotational barriers of amides have been proposed to arise from carbonyl polarization,[205,206] stabilizations/destabilizations related to hybridization changes,[209] and so on. The challenge of the resonance model and the suggestion of alternative models stirred up a significant controversy involving theoreticians and experimentalists.[210−212]

Table 5. VB- and MRCI-Computed Vertical Excitation Energies (eV) for Polyenes $C_{2n}H_{2n+2}$ (n = 2−8) and Polyenyl Radicals $C_{2n-1}H_{2n+1}$ (n = 2−8) with the D95V Basis Set

n	no. of Rumer structures	VBSCF	VBCIS	VBCISD	VBDFT(s)	MRCI
2	2	6.47	6.47	6.56	6.28	6.53
3	5	5.29	5.28	5.36	5.02	5.42
4	14	4.49	4.49	4.55	4.19	4.60
5	42	3.95	3.94	4.00	3.63	4.07
6	132	3.56	3.55	3.60[a]	3.32	3.68
7	429	3.27	3.26[b]		2.93	
8	225[a]	3.06[a]			2.70	
2	2	3.21	3.21	3.26	3.26	3.29
3	5	2.54	2.53	2.57	2.49	2.62
4	14	2.07	2.07	2.10	2.01	2.16
5	42	1.76	1.75	1.78	1.68	1.84
6	132	1.53	1.53	1.58	1.45	1.61
7	429	1.40	1.41[b]	1.44[b]	1.29	
8	120[b]	1.27[b]	1.19[b]		1.16	

[a] VB(S,D) type. [b] VB(S) type.

Scheme 6. VB Resonance Structures for Planar Amide (1−3) and Rotated Amide (4)

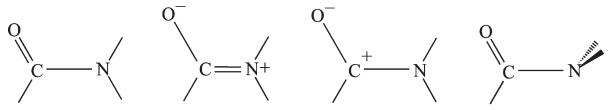

1 **2** **3** **4**

We note that all the arguments that have been invoked either in favor of or in opposition to the resonance model are somewhat indirect, since they deal with probes such as charge distributions, Fermi correlation, or bond length changes upon C−N rotation. At the same time, the crucial quantity that is needed to test the resonance model is the delocalization energy (DE), which presumably accounts for the disputed origins of the rotational barrier. In fact, the validity of the resonance model can be directly tested by means of VB methods. Thus, the stabilization brought by the delocalization of the nitrogen lone pair in planar amide is estimated by comparing the energy of the fully delocalized ground state to that of a localized state in which the lone pair is constrained to remain on the nitrogen atom. The BLW method (vide supra) offers quick and reliable DE values. At the Hartree−Fock level, these two states are designated as Φ^{RHF} and Φ^{BLW}_{loc}, respectively. Thus, DE is given by

$$DE = E(\Phi^{BLW}_{loc}) - E(\Phi^{RHF}) \quad (72)$$

Here DE provides the vertical delocalization energy if both calculations are performed in the geometry of the delocalized ground state Φ^{RHF}. Note that all orbitals in Φ^{BLW}_{loc}, except for the nitrogen lone pair, are free to delocalize over the entire molecule. In this manner, the DE takes into account the inductive effects and the polarities of the various bonds, including the C−O π-bond.

The BLW-HF method was used by Lauvergnat et al. to calculate delocalization energies in formamide and thioformamide[213] with the aim of providing a quantitative answer to the following questions: (i) How much does the delocalization of the nitrogen's lone pair over the carbonyl or thiocarbonyl group stabilize the planar forms of amides relative to the twisted forms? (ii) Does the resonance model fully account for the rotational barrier of amides? (iii) Why is the rotational barrier of thioformamide larger than that of formamide? Using the 6-311G** basis set, Lauvergnat et al. found vertical delocalization energies of 27.3 and 37.6 kcal/mol, respectively, for formamide and thioformamide, indicative of a strong delocalization of the lone nitrogen pair in both molecules. These values were subsequently confirmed by Mo et al. in a similar study extended to selenoformamide, $SeCHNH_2$, and the planar forms of formamidine, $NHCHNH_2$, and vinylamine, CH_2CHNH_2, yielding vertical delocalization energies of 37.6, 25.5, and 19.1 kcal/mol, respectively, for these three compounds.[214] Using the BLW method in conjunction with DFT, thus dynamic correlation taken into account, increases the vertical delocalization energies of formamide and thioformamide by ca. 4 and 2 kcal/mol, respectively.[179] Of course, the large vertical delocalization energies cannot be directly compared to the rotational barriers around the C−N bond because (i) the nitrogen lone pair also delocalizes in the rotated geometry **4** and (ii) the rotated form is stabilized by pyramidalization at nitrogen and more generally by geometry relaxation. Using the BLW-HF technique, the vertical delocalization energy of the rotated forms was estimated to be 12.4 and 10.2 kcal/mol, respectively, for formamide and thioamide.[213] These values, which correspond to hyperconjugation, are clearly smaller than in the planar form but not negligible.

The contribution of nitrogen lone pair delocalization to the rotational barriers is best elucidated by considering adiabatic delocalization energies, calculated through eq 72 using optimized geometries for both Φ^{BLW}_{loc} and Φ^{RHF}. Comparison of the adiabatic DEs for the unrotated and rotated forms shows that the delocalization of the nitrogen lone pair stabilizes the unrotated conformation more than the rotated one by 7.3 kcal/mol for formamide vs 13.7 kcal/mol for thioformamide. Thus, the resonance stabilization of the planar conformers is responsible for about half of the rotational barrier of formamide and two-thirds of that of thioformamide. The larger rotational barrier of thioformamide is therefore due to a greater importance of conjugation effects relative to those of formamide.

These results demonstrate that conjugation of the π-electrons is an important feature of the electronic structure of amides and thioamides and that the nitrogen lone pair is significantly delocalized over the (thio)carbonyl group. All in all, the BLW calculations support the qualitative resonance model and show that even if resonance stabilization is not the sole factor responsible for the rotational barriers, it is still a significant one.

Scheme 7. 1,3-Dehydrobenzene[a]

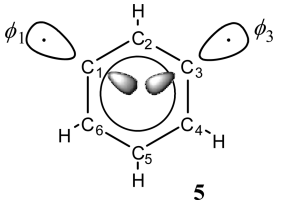

5

[a] ϕ_1 and ϕ_3 are pure in-plane atomic orbitals.

3.4.2. VBSCF Application to Through-Bond versus Through-Space Coupling in 1,3-Dehydrobenzene. 1,3-Dehydrobenzene (*m*-benzyne, **5** in Scheme 7) is a singlet diradical that owes its stability relative to the triplet state to a weak bonding between the carbons C_1 and C_3. Although it was generally assumed that most of the bonding between these two carbons is due to direct, through-space (TS) interactions, the possibility of an additional contribution from through-bond (TB) interactions was raised by Hoffmann.[215] More recently, Winkler and Sander also concluded, on the basis of topological and NBO analyses, that the C_2−H, C_1−C_2, and C_2−C_3 bonds mediate the interactions between C_1 and C_3.[216]

To distinguish and quantify the respective contributions of TB and TS to the singlet−triplet gap, Borden et al. carried out VB-type calculations on **5**.[217] For the singlet state, the calculations are of the VBSCF/BDO type; i.e., a single formally covalent VB structure is written to describe the C_1−C_3 bonds, but the orbitals are allowed to delocalize over only the C_1 and C_3 centers. As is well-known,[1−3,183,218,219] VB wave functions of this type implicitly take into account the ionic component of the bond, owing to the partial delocalization of the orbitals. The pure TS interaction is described as a singlet coupling between two BDOs, φ_1 and φ_3, as in $^1\Psi^{VB}_{bdo}$:

$$^1\Psi^{VB}_{bdo} = |\varphi_1\bar{\varphi}_3 - \bar{\varphi}_1\varphi_3| \qquad \varphi_1 = \phi_1 + \varepsilon\phi_3$$
$$\varphi_3 = \phi_3 + \varepsilon\phi_1 \quad (73)$$

where ϕ_1 and ϕ_3 are the pure AOs of C_1 and C_3 involved in the TS interaction (see Scheme 7) and φ_1 and φ_3 are allowed to delocalize on C_1 and C_3 but not on the other atoms. In this manner, $^1\Psi^{VB}_{bdo}$ does not contain any contribution from any atoms other than C_1 or C_3, and it is therefore devoid of any TB interaction. On the other hand, $^1\Psi^{GVB}_{full}$ allows full delocalization of the GVB pair (φ_1, φ_3) over the entire molecule, as in the standard GVB method that uses OEOs:

$$^1\Psi_{full}^{GVB} = |\varphi_1\bar{\varphi}_3 - \bar{\varphi}_1\varphi_3|$$

$$\varphi_1 = \phi_1 + \varepsilon\phi_3 + \varepsilon'\phi_i + \ldots$$
$$\varphi_3 = \phi_3 + \varepsilon\phi_1 + \varepsilon'\phi_i + \ldots \quad (74)$$

Thus, $^1\Psi_{full}^{GVB}$ now contains both TS and TB interactions.

An analogous use of partially delocalized "atomic" orbitals and OEOs allows calculation of triplet states with or without inclusion of TB interactions. Thus, it was possible to calculate adiabatic singlet−triplet gaps by taking only TS interactions into account or by including both TS and TB interactions, leading to ΔE_{S-T}(TS) and ΔE_{S-T}(TS+TB), respectively.

In the CCSD(T)/cc-pVTZ-optimized geometry, a value of 4.7 kcal/mol was found for ΔE_{S-T}(TS), as compared to a total singlet−triplet gap ΔE_{S-T}(TS+TB) of 9.9 kcal/mol. Thus, it was concluded that the stabilization provided by TB interactions contributes 10% more than the stabilization provided by the TS interactions to the adiabatic singlet−triplet energy difference, at least at this level of VB calculation, which only takes nondynamic correlation into account. However, it was found that dynamic correlation is rather important, as it increases the adiabatic singlet−triplet gap by 11 kcal/mol relative to the previous calculation,[217] so that the question of the precise contributions of TS vs TB interactions remains somewhat open. BOVB calculations that take dynamic correlation into account may resolve this issue.

3.5. Direct Estimate of Hyperconjugation Energies by VBSCF and BLW Methods

3.5.1. Magnitude of Hyperconjugation in Ethane. The hindered rotation about the carbon−carbon bonds in organic compounds is a common phenomenon in conformational analysis. Taking ethane as a prototypical example, the barrier to rotation has been traditionally attributed to Pauli exchange repulsions, or steric hindrance, between the vicinal C−H bonds. However, this simple picture has been questioned in a number of theoretical studies, on the basis of natural bond orbital (NBO) analyses. It was suggested that, contrary to intuition, electrostatic and Pauli repulsions actually favor the eclipsed conformation, while the preferred staggered conformation is due to hyperconjugative interactions between the methyl groups.[220−222] This proposal stirred a controversy[223−225] and led Bickelhaupt and Baerends to evaluate the Pauli and electrostatic interactions explicitly using the aforementioned EDA method, with a zeroth-order wave function constructed from fragment orbitals of the methyl groups. They concluded that although hyperconjugation favors the staggered conformer, Pauli exchange repulsions are the dominant force responsible for the rotational barrier in ethane.[223] Another quantitative estimate was proposed by Mo et al.[224,226,227] using VB theory which directly evaluates the stabilizing effect of hyperconjugation (Scheme 8).

In VB theory, hyperconjugation in ethane is expressed as a resonance between the main VB structure, involving one C−C and six C−H single bonds, and a group of 18 VB structures displaying a C═C double bond and one proton in one methyl group and a hydride in the other (see Scheme 8). Removing these 18 VB structures from the VB calculation defines a reference state Φ_{loc}^{VB} which is devoid of hyperconjugation. Accordingly, the hyperconjugative stabilization energy E_{hc}^{VB} is defined as the energy difference between Φ_{loc}^{VB} and the ground state Φ_{GS}^{VB}, which includes all the VB structures:

$$E_{hc}^{VB} = E(\Phi_{loc}^{VB}) - E(\Phi_{GS}^{VB}) \quad (75)$$

Scheme 8. Resonance Structures Which Contribute to Hyperconjugation in Ethane

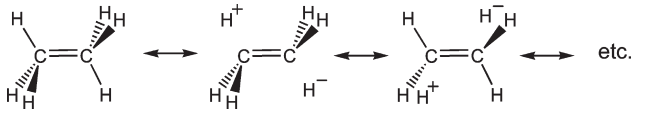

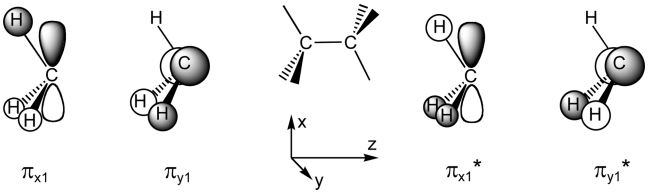

Figure 9. Some of the e-symmetric CH_3 group orbitals of ethane.

The VB calculations have been performed at the VBSCF level.[226] With the best basis set, the calculated hyperconjugative stabilizations amount to 13.1 kcal/mol for the staggered form and 12.1 kcal/mol for the eclipsed one, thus favoring the staggered conformation by 1.0 kcal/mol. It should be noted that these estimates are much smaller than the hyperconjugative stabilizations calculated by the NBO methods, respectively 27.7 and 23.0 kcal/mol for the staggered and eclipsed forms.[221] This large difference between the BLW and NBO estimations has been interpreted by Mo and Gao.[226] In the NBO analysis, the antibonding methyl orbitals are deleted but the remaining orbitals, which form the localized state, are not reoptimized after this deletion. This tends to exaggerate the energy difference between the localized and delocalized states, thus overestimating the hyperconjugation stabilizations. By contrast, the orbitals of the reference state are reoptimized in the VBSCF calculation, which therefore leads to smaller values.

The contribution of hyperconjugation to the rotational barrier of ethane has also been investigated by the BLW method. Thus, to quantitatively estimate the stabilization energy of hyperconjugation effects, it is necessary to know the energy of the hypothetical ethane reference that has no hyperconjugative interactions. Such a reference system is BLW-computed by preventing electron delocalization between vicinal methyl groups. Using symmetry-adapted group orbitals, only the e-symmetric orbitals of the methyl groups are relevant to the barrier since the other orbitals, of a-symmetry, are invariant to rotation. The e-symmetric bonding orbitals of the left carbon are represented in Figure 9, labeled as π_{x1} and π_{y1}, together with their antibonding counterparts, π_{x1}^* and π_{y1}^*.

Of course, identical orbitals (not shown in Figure 9) exist on the right carbon, labeled as π_{x2}, π_{y2}, π_{x2}^*, and π_{y2}^*. During the BLW procedure, the occupied orbitals of the methyl groups are optimized but kept fully localized on their specific methyl groups, leading to the wave function Φ_{loc}^{BLW} in which hyperconjugation is "turned off":

$$\Phi_{loc}^{BLW} = (\ldots)(\pi_{x1})^2(\pi_{y1})^2(\pi_{x2})^2(\pi_{y2})^2 \quad (76)$$

On the other hand, using the standard RHF method allows delocalization to take place during the orbital optimization and leads to e-symmetric bonding and antibonding delocalized molecular orbitals, labeled as e_x, e_y, e_x^*, and e_y^*, which are the

components of the RHF wave function Φ^{RHF}:

$$\Phi^{RHF} = (...)(e_x)^2(e_y)^2(e_x*)^2(e_y*)^2 \quad (77)$$

Since vicinal hyperconjugation is fully at work in Φ^{RHF} and absent in Φ^{BLW}_{loc}, the stabilization resulting from hyperconjugation is defined as

$$E^{BLW}_{hc} = E(\Phi^{BLW}_{loc}) - E(\Phi^{RHF}) \quad (78)$$

The BLW and RHF calculations were performed using the same basis sets as for VBSCF and proved little basis-set dependency.[224,226] As a result, hyperconjugation was found to favor the staggered conformation by 0.76−0.84 kcal/mol, depending on the basis set, at the BLW-RHF level (eq 78) and by 0.90−0.98 kcal/mol at the VBSCF level (eq 75). By comparison, the total preference of ethane for the staggered conformation relative to the eclipsed one, all effects included, amounts to 3.0 kcal/mol, as calculated at the RHF level. Thus, both VBSCF and BLW methods converge to the same conclusion that hyperconjugation accounts for about 25−33% of the total rotational barrier in ethane. The rest can be entirely attributed to steric hindrance, which represents the collective contributions from the Pauli exchange repulsion and electrostatic interactions between the vicinal methyl groups. This conclusion, which is based on a direct estimation of hyperconjugative effects, is in agreement with the deduction of Bickelhaupt and Baerends,[223] based on an estimation of Pauli and electrostatic interactions, and brings quantitative support to the traditional view about the rotational barrier in ethane.

3.5.2. Physical Origin of the Saytzeff Rule. Alkene formation during elimination reactions is known to proceed by the preferential removal of the β-hydrogen from the carbon that has the smallest number of hydrogens. This statement, known as Saytzeff's rule,[228] is illustrated in Scheme 9 using two different alcohols.[229,230]

The Saytzeff rule is generally confirmed by experiment, but different textbooks give different interpretations for the physical reason behind the observed selectivities and/or alkene stabilities. A common interpretation[231] rests on the hyperconjugation between the highest occupied orbital of the alkyl fragment and the π- and π^*-MOs of the C−C double bond, which thereby stabilizes the more substituted double bond. On the other hand, an alternative explanation is based on the hybridization effect on the strengths of the C−C bonds.[232] Thus, an sp^2-sp^3 C−C bond is stronger than an sp^3-sp^3 C−C bond, and the more the alkene is substituted, the higher the ratio of sp^2-sp^3 C−C bonds to sp^3-sp^3 C−C bonds. Note that this explanation does not take into account the effect of hybridization on the C−H bonds, which acts in the opposite direction, as will be discussed below. Finally, inductive effects and steric repulsions must also be considered.

Since hyperconjugation and hybridization effects are the most frequently invoked explanations, Braida et al.[233] quantified them independently by use of the BLW and VBSCF methods, which allow hyperconjugation to be turned "on" or "off". The ab initio calculations deal with the products of reactions in Scheme 9 to understand the origin of their different relative stabilities.

Let us discuss in detail the reasons why the most substituted isomers are more stable than the less substituted ones. When going from $CH_3CH{=}CRCH_3$ to $CH_2{=}CREt$, the following stabilizing/destabilizing effects are taking place:

(i) Loss of hyperconjugation, $\Delta E > 0$.

Scheme 9. Product Distributions for Some Acid-Catalyzed E1 Eliminations of H_2O from Secondary (Eq 79) and Tertiary (Eq 80) Alcohols

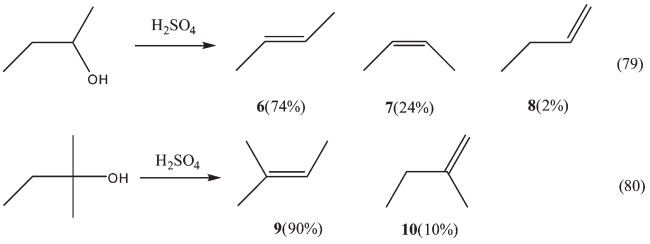

(ii) $C_{sp^3}-H \rightarrow C_{sp^2}-H$, $\Delta E < 0$.

(iii) $C_{sp^2}-CH_3 \rightarrow C_{sp^3}-CH_3$, $\Delta E > 0$.

(iv) π-Polarization in $CH_2{=}CREt$, $\Delta E < 0$.

(v) Other effects (strain, σ-inductive effects, etc.)

Hyperconjugation was first estimated by BLW calculations. The state with delocalization on is simply the RHF wave function of the alkene, Φ^{RHF}. The state with π-delocalization off is Φ^{BLW}_{loc}. In accord, the hyperconjugation energy, E^{BLW}_{hc}, can be estimated by eq 78 as in the preceding section.

The BLW results[233] show that localizing the orbitals of one methyl group raises the energy by 6.0 ± 0.1 kcal/mol, no matter which methyl group is chosen. Furthermore, hyperconjugation effects of the various methyl groups are nearly additive and independent of each other. The hyperconjugative stabilization energy of an ethyl group, for both **8** and **10**, is estimated to be close, ca. 6.4 kcal/mol. It follows that, for both C_4H_8 and C_5H_{10}, hyperconjugation effects stabilize the most substituted product by about 6 kcal/mol, which is significantly more than the actual thermodynamic preference expressed by Saytzeff's rule, respectively 2.6 and 1.1 kcal/mol for eqs 79 and 80 in Scheme 9 at the RHF level at 0 K (experimentally 2.4 and 1.5 kcal/mol at 298 K). It is therefore concluded that the other effects, listed above, neatly operate in the anti-Saytzeff direction.

The effects of C−C and C−H hybridization changes (items ii and iii above) were estimated from calculated or experimentally measured dissociation energies of simple reactions, i.e., extrusion of hydrogen from methane and from ethane and extrusion of methyl from ethane and from propene (removing the hyperconjugative effect in the latter case). At the G3 (0 K) computational level, the following results were obtained:

$$C_{sp^3}-H \rightarrow C_{sp^2}-H \qquad \Delta E = -5.9 \text{ kcal/mol} \quad (81)$$

$$C_{sp^2}-CH_3 \rightarrow C_{sp^3}-CH_3 \qquad \Delta E = 4.8 \text{ kcal/mol} \quad (82)$$

As both hybridization changes take place as one shifts from the most substituted alkene to the less substituted one, it follows that hybridization effects *destabilize* the former isomer by 1.1 kcal/mol. Experimental measurements at 298 K yield a destabilization of the same order of magnitude, 0.7 kcal/mol.[233] Thus, the hybridization effects do not account for the Saytzeff rule, but contribute an anti-Saytzeff effect that slightly lowers the hyperconjugative effects.

Another effect that may possibly play a role in the relative stabilities of isomers is the polarization of the π-bond by the π-donor substituents. The π-polarization can be turned on and off using VBSCF with BDOs. In this brand of VB theory, the bond

dx.doi.org/10.1021/cr100228r |Chem. Rev. 2011, 111, 7557–7593

under study (here the π-bond) is described as a singlet-coupled interaction between two BDOs, φ_1 and φ_2, that form a bond pair. Thus, the ground state with π-polarization on is represented by the wave function Ψ_{pol}^{on}:

$$\Psi_{pol}^{on} = |... \psi\bar{\psi} \ ... (\varphi_1\overline{\varphi_2} - \overline{\varphi_1}\varphi_2)| \quad (83)$$

in which the orbitals φ_1 and φ_2 are not equivalent, owing to polarization. It is therefore straightforward to turn the polarization off by averaging φ_1 and φ_2 as in the wave function Ψ_{pol}^{off}:

$$\Psi_{pol}^{off} = | \ ... \psi\bar{\psi} \ ... (\varphi_1^{av}\overline{\varphi_2^{av}} - \overline{\varphi_1^{av}}\varphi_2^{av})| \quad (84)$$

where φ_1^{av} and φ_2^{av} are mirror images of each other and are obtained by averaging the expressions of φ_1 and φ_2. Accordingly, the stabilization energy due to π-polarization is simply the energy difference between Ψ_{pol}^{off} and Ψ_{pol}^{on}. As a result, it turns out that π-polarization is a weakly stabilizing factor, accounting for 0.3 kcal/mol stabilization of **8** relative to **6** and 0.4 kcal/mol stabilization of **10** relative to **9**. Thus, this effect too slightly favors the anti-Saytzeff products.

Summing up the calculated effects of hyperconjugation, hybridization changes, and π-polarization, these cumulated effects favor **8** over **6** by 4.45 kcal/mol and **10** over **9** by 4.55 kcal/mol, which are more than the actual stability differences as calculated at the G3 (0 K) level, respectively 2.42 and 1.20 kcal/mol (see Table 6). This means that the remaining effects, σ-polarization and steric effects, amount to 2−3 kcal/mol and act in the anti-Saytzeff direction.

In summary, it appears that the Saytzeff rule is entirely governed by hyperconjugation between the π-bond and the π-donating substituents, whereas all other factors have a smaller opposite effect.

3.5.3. Tetrahedranyltetrahedrane. The shortest C−C single bond ever in a noncyclic saturated hydrocarbon was experimentally characterized by Tanaka and Sekiguchi[234] in 2005 in tetrahedranyltetrahedrane, a dimer of tetrahedranyl radicals (Scheme 10). The bond length of 1.436 Å is 0.091 Å shorter than the C−C bond in ethane at the RHF/6-311+G** level. Knowing that the greater the s character in hybrid atomic orbitals, the shorter the bond between such hybrids, Tanaka and Sekiguchi ascribed the very short bond length to the high s character of the exocyclic bond, as could be deduced from the CCC angles in this highly strained molecule. However, an alternative explanation is the partial double bond character in this C−C bond due to the hyperconjugative interactions between the two tetrahedranyl groups.

As in the case of ethane, the study of hyperconjugative interactions in tetrahedranyltetrahedrane was carried out by Mo[235] using the BLW-RHF method, which deactivates hyperconjugation by confining the electrons in localized orbitals of one tetrahedranyl group or the other. Only e-symmetric orbitals were localized in the BLW wave function, Φ_{loc}^{BLW}, since these are the only orbitals capable of hyperconjugation. As there are eight e-symmetric group orbitals on each group, labeled $1e_1-8e_1$ and $1e_2-8e_2$, respectively, for the left and right groups, the block-localized wave function, which is devoid of hyperconjugation, reads as in the following equation:

$$\Phi_{loc}^{BLW} = (...)(1e_1-8e_1)(1e_2-8e_2) \quad (85)$$

On the other hand, the RHF wave function that describes the ground state involves the fully delocalized e-symmetric orbitals, labeled 1e−16e, as in the following equation:

$$\Phi^{RHF} = (...)(1e-16e) \quad (86)$$

Table 6. Summary of the Various Effects That Contribute to the Thermodynamic Difference between the Saytzeff Products (6, 9) and the Anti-Saytzeff Products (8, 10) in Scheme 9

	6 → 8	9 → 10
hyperconjugation	5.8	6.1
hybridization changes	−1.1	−1.1
π-polarization	−0.3	−0.4[a]
other effects[a]	−2.0	−3.4
total[b]	2.4	1.2

[a] These include π-polarization and steric effects. [b] Calculated at the G3 (0 K) level.

Scheme 10. Tetrahedranyltetrahedrane Molecule

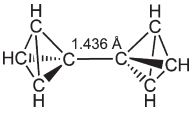

At the optimized geometry of the molecule, the difference between Φ_{loc}^{BLW} and Φ^{RHF} is 15.2 kcal/mol for the staggered conformer vs 14.1 kcal/mol for the eclipsed one in the 6-311+G** basis set. This difference of 1.1 kcal/mol is notably smaller than the rotational barrier of 3.0 kcal/mol, leading to the conclusion that hyperconjugation differences contribute only slightly to the rotational barrier of tetrahedranyltetrahedrane.

To probe the influence of hyperconjugation on the central C−C bond length, the geometry of the molecule was optimized for the Φ_{loc}^{BLW} pseudostate in which hyperconjugation is turned off. The C−C distance was found to be 1.491 Å at the BLW/6-311+G** level, in comparison with the actual distance of 1.436 Å in the molecule calculated at the RHF/6-311+G** level. Thus, Mo concluded that the stabilizing hyperconjugation effect shortens the central C−C bond in tetrahedranyltetrahedrane by 0.055 Å. However, the same author performed analogous calculations on ethane and found that hyperconjugation effects also shorten the C−C bond in ethane by 0.040 Å, which suggests that hypercoordination in tetrahedranyltetrahedrane is not outstanding relative to that of other saturated hydrocarbons and explains only partly the short central C−C bond length. Thus, the rest of the C−C bond length difference compared with ethane, 0.076 Å, was ascribed to the much larger s character that is found in the exocyclic hybrid orbitals of the tetrahedranyl groups as compared to the methyl groups in ethane. It is interesting to point out that the very same conclusion has been made on the basis of MO-based energy decomposition analysis.[236] It is gratifying to see that MO and VB methods come to the same conclusion when it comes to the interpretation of unusual bonding situations.

3.6. VBSCF and BLW Applications to Aromaticity

Aromaticity is a central issue in chemistry. VB theory defines the stability associated with this property in terms of the resonance energy (RE), which measures the magnitude of contributions from resonance structures other than the principal Lewis structure to the ground state of a conjugated molecule.[237] SC VB calculations were used to estimate the REs for benzene,[38,238−242] cyclobutadiene,[239,240] distorted benzene,[243] pyrene derivatives,[244,245]

the H_6 cluster,[246] and so on. Similarly, classical VB calculations, including all VB covalent and ionic structures, were also employed for the same purpose.[247−249] A disadvantage of the SC method is that a given formally covalent structure implicitly contains some minor components from other structures, due to the semidelocalized nature of the AOs that are employed, so that the definition of a reference structure for the calculation of RE is ambiguous. Here we will describe a few applications of the VBSCF and BLW methods, which have been shown to provide comparable values for the REs.[242]

3.6.1. Energetic Measure of Aromaticity and Antiaromaticity. The first easy-to-apply method to estimate the RE in the classical VB spirit is due to Kollmar[128] and consists of constructing the reference nonconjugated VB structure by replacing its π-MOs by a set of strictly two-center-localized ethylenic MOs, each taken from an RHF calculation of ethylene having the appropriate C−C bond length.[128] Calculations of REs using this simple technique were reviewed in 2001, along with VBSCF-computed and Kollmar's computed values.[249]

The BLW method[123−127] (see section 2.4.1) improves on Kollmar's method by optimizing the orbitals of the nonconjugated VB structure. At this point it is useful to define[249] the various quantities that are associated with resonance and aromaticity and that are sometimes mixed up in the literature. The "vertical resonance energy" (VRE) stands for the Pauling−Wheland RE of a conjugated molecule, calculated by taking both the ground state and the most stable VB structure in the ground-state geometry. On the other hand, the "adiabatic resonance energy" (ARE) is calculated by taking these two states each in their own optimal geometry. Finally, the "extra cyclic resonance energy" (ECRE) measures the extra stabilization of conjugated rings with respect to an appropriate acyclic conjugated system which is taken as the nonaromatic reference. The ECRE is known also as the thermochemical resonance energy.[249] Thus, ECRE is expected to be positive for aromatic systems and negative for antiaromatic ones. All these quantities can be readily estimated by means of valence bond calculations.

Mo and Schleyer found a VRE for benzene of 91.6 kcal/mol at the BLW-RHF level,[250] in the 6-311+G** basis set, a value which is comparable to 86 kcal/mol calculated with the Kollmar method[249] using the 6-31G basis set. On the other hand, a much smaller value was found for the VRE of rectangular cyclobutadiene, as expected, only 10.9 kcal/mol,[250] compared with 22 kcal//mol for square cyclobutadiene with VBSCF.[249]

Mo and Schleyer also used the BLW-RHF method to calculate AREs.[250] For benzene, the geometry-optimized nonconjugated VB structure, the so-called "1,3,5-cyclohexatriene", was found to display alternated bond lengths of 1.319 and 1.522 Å, to be compared with the regular bond lengths of 1.386 Å for benzene at the RHF level. AREs of 57.5 and 10.3 kcal/mol were calculated for benzene and cyclobutadiene, respectively. Thus, the very different values of the AREs for benzene and cyclobutadiene reflect their fundamental difference in terms of aromaticity/antiaromaticity. More quantitatively, the stabilization/destabilization energies associated with these concepts are best estimated by the ECRE, defined as

$$\mathrm{ECRE(CM)} = \mathrm{ARE(CM)} - \mathrm{ARE(Ref)} \qquad (87)$$

where CM is the cyclic conjugated molecule under study and Ref is an acyclic conjugated molecule taken as a reference nonaromatic system. This reference molecule is a linear polyene that can be chosen as having the same number of double bonds as the cyclic molecule (i.e., *trans*-1,3,5-hexatriene for benzene)[249] or the same number of diene conjugations (i.e., *trans*-1,3,5,7-octatetraene for benzene). The first model is referred to as ECRE1, while the second model, generally considered as more meaningful than the former for neutral systems,[251] is referred to as ECRE2. Note that the ECRE2 model defines a reference molecule that has two more atoms than in the cyclic molecule. Whatever the nonaromatic reference that is chosen, the ECRE is similar in spirit to the well-known "aromatic stabilization energy" (ASE), an experimental quantity that is taken as a measurement of the extra stabilization of a cyclic molecule in excess of the RE of analogous acyclic conjugated systems. For benzene, the experimental endothermicity of reaction 88 has been proposed[252] to estimate the ASE, which amounts to 28.8 kcal/mol.

(88)

On the side of VB calculations, the ECRE1 and ECRE2 values for benzene, as calculated at the BLW-RHF/6-311+G** level,[250] amount to 36.7 and 25.7 kcal/mol, respectively, suggesting that ECRE2 is indeed more relevant than ECRE1. For cyclobutadiene, ECRE1 is close to zero at the BLW-RHF level, while ECRE2 is definitely negative, −10.5 kcal/mol, thus reflecting very well the antiaromaticity of cyclobutadiene and further establishing ECRE2 as the best energetic criterion for aromaticity of neutral molecules. For ionic systems the ECRE1 model works better, since ECRE2 has the inconvenience of defining an acyclic reference that has more atoms than in the cyclic molecule. This feature, which is of no concern in the neutral system, introduces a bias in ionic systems owing to greater stabilization in the acyclic reference due to better charge delocalization.

The BLW-RHF method was further used to calculate the various resonance energies (VRE, ARE, and ECRE) of a series of twelve five-membered rings C_4H_4X (X = AlH, BH, CH^+, CH_2, NH, O, PH, S, SiH^+, SiH^-, SiH_2).[250] The ECRE values were systematically compared to the magnetic criterion for aromaticity, the "nucleus-independent chemical shift" (NICS), which is known to be negative for aromatic systems and positive for antiaromatic ones. As a result, ECRE2 values were found to better correlate than ECRE1 with NICS values, with a correlation coefficient of 0.95. This and the above results for benzene tend to demonstrate that acyclic references with the same kind and numbers of single bonds between the π-units measure aromaticity better than references having the same number of π-electrons. In particular, negative (positive) NICS values correlate with positive (negative) ECRE2 values in all cases. Accordingly, the ECRE2 values for cyclopentadiene cation and anion are −35.4 and 19.1 kcal/mol, with 46.9 and −13.7 ppm NICS values, respectively.

Thus, it is seen that VB calculations can complement the often-used magnetic criterion for aromaticity with an energetic criterion, which has the advantage of providing stabilization energies of direct chemical interest.

3.6.2. Cyclopropane: Theoretical Study of σ-Aromaticity. The concept of σ-aromaticity was first proposed by Dewar[253] in 1979 to explain the surprisingly small conventional strain energy of cyclopropane, only 27.5 kcal/mol, practically the same as the strain energy of cyclobutane despite the larger CCC angles in the latter. Extending the Hückel rule originally

proposed for π-systems, Dewar suggested that rings with $4n + 2$ skeletal electrons, such as cyclopropane, are stabilized by σ-aromaticity while those with $4n$ electrons are σ-antiaromatic and destabilized. Since then, the concept of σ-aromaticity has been extended to many other systems and is now well established, but the question remains of whether cyclopropane indeed follows this paradigm. In fact, there is a large discrepancy in estimates of the σ-aromatic stabilization energy of cyclopropane, ranging from 55.1 kcal/mol[254] to 5.0 kcal/mol,[255,256] and even in the conclusion that "There is no need to invoke σ-aromaticity to explain the thermochemistry of cyclopropane."[257] However, as all these estimations were indirect, Wu, Schleyer, and Mo (WSM) recently used the ab initio VBSCF method to get direct estimations of the stabilization due to σ-aromaticity in cyclopropane.[258]

As in other applications (vide supra), the method utilized by WSM takes advantage of the ability of the VB method to turn electronic delocalization off or on. Note that there are two kinds of delocalization modes in cyclopropane: (i) in-plane delocalization of the σ-orbitals of the CH_2 groups and (ii) out-of-plane delocalization among the set of π-like CH_2 group orbitals. The stabilization energies arising from these two types of delocalization are referred to as RE^{σ} and RE^{π}, respectively.

A semilocalized wave function of the VBSCF type in which σ-delocalization is turned off is defined as in the following equation, dropping the spin function:

$$\Phi^{\sigma}_{\mathrm{loc}} = \hat{A}(\Omega_{\mathrm{C}}\Omega^{\sigma}_{\mathrm{loc}}\Omega^{\pi}_{\mathrm{del}}) \tag{89}$$

where Ω_{C} refers to the core orbitals, $\Omega^{\sigma}_{\mathrm{loc}}$ is a direct product of BDOs that are constrained to be localized on a given CH_2 group, and $\Omega^{\pi}_{\mathrm{del}}$ is a product of π-BDOs that are allowed to delocalize freely over the molecule.

A similar definition is used for a semilocalized wave function where π-delocalization is turned off:

$$\Phi^{\pi}_{\mathrm{loc}} = \hat{A}(\Omega_{\mathrm{C}}\Omega^{\sigma}_{\mathrm{del}}\Omega^{\pi}_{\mathrm{loc}}) \tag{90}$$

Finally, $\Phi^{\sigma+\pi}_{\mathrm{loc}}$ is a fully localized wave function in which both σ- and π-delocalizations are turned off. With these definitions, the delocalization energies RE^{σ} and RE^{π} are defined as in eqs 91 and 92,

$$RE^{\sigma} = \Phi^{\sigma}_{\mathrm{loc}} - \Phi^{\sigma+\pi}_{\mathrm{loc}} \tag{91}$$

$$RE^{\pi} = \Phi^{\pi}_{\mathrm{loc}} - \Phi^{\sigma+\pi}_{\mathrm{loc}} \tag{92}$$

respectively. The VBSCF/cc-pVDZ-calculated values for RE^{σ} and RE^{π} are 12.5 and 10.2 kcal/mol, respectively. While these values might appear significant, it must be kept in mind that similar delocalization energies due to hyperconjugative interactions exist even in acyclic alkanes such as ethane[224,226] (see section 3.5.1). Consequently, the ECRE, defined as the RE difference between the cyclic aromatic compound and its appropriate acyclic reference, is more suitable for evaluating the σ-aromaticity. The selection of the acyclic reference can be based either on having the same number of carbons (i.e., propane, giving ECRE1) or on having the same number of C−C bonds (i.e., butane, giving ECRE2). In both cases, the extra cyclic delocalization energy of propane is found to be quite small, with ECRE1 values of 3.5 and 1.8 kcal/mol, respectively, for σ- and π-delocalization, and even slightly negative ECRE2 values, −0.7 and −2.7 kcal/mol.[258]

It is concluded that the extra σ-stabilization energy (at most 3.5 kcal/mol) is far too small to explain the small difference in strain energy between cyclopropane (27.5 kcal/mol) and cyclobutane (26.5 kcal/mol) by σ-aromaticity. Thus, there is no need to invoke σ-aromaticity for cyclopropane energetically.

3.7. Electronic Structure of Conjugated Molecules

The weights of the various resonance structures in a conjugated molecule can be reliably assessed using ab initio VB theory by applying Chirgwin−Coulson's formula (eq 8 in section 2.1) or the alternative Löwdin definition.[138] As the various VB structures are nonorthogonal within the classical VB scheme, both these definitions contain some overlap terms (M_{KL} in eq 8) that must be partitioned between the various VB structures, hence the difference in weights between the various formulas when the overlap is large. To get rid of this defect, some authors have proposed to perform the VB analysis in terms of VB structures defined with orthogonalized atomic orbitals.[83,259] These orbitals, called "nearly atomic molecular orbitals" (NAMOs)[83] or "orthogonalized atomic orbitals" (OAOs),[260] are each mainly centered on a single atom but have tails, which ensure orthogonality, on other atoms. The advantages and disadvantages of the orthogonal VB approach have been discussed by Angeli et al. in a recent paper.[260] As an advantage, the ambiguity attached to the partitioning of overlap terms is avoided since the VB structures are mutually orthogonal. Furthermore, this method makes the orthogonal VB reading of a CASSCF wave function very easy and cost-efficient.[83] On the other hand, one disadvantage is that the covalent VB structures defined with orthogonal NAMOs are always repulsive,[261] in contrast to classical VB which views covalent interactions as strongly bonding in the majority of cases, in accord with chemical wisdom. Thus, the definition of the VB structures in terms of purely local AOs or HAOs, as is done in classical VB, is closer to the chemists's language. Furthermore, classical VB guarantees a nonambiguous correspondence between the VB wave function and the intuitive Lewis structures, owing to the absence of delocalization tails in the HAOs.

A number of authors have performed such analyses of ab initio classical VB wave functions on molecules such as NNO,[262,263] NO_2,[264,265] ClO_2,[266] N_2O_2,[267] linear N_5^+ cation,[268,269] 1,3-dipoles,[266,270] cyclobutadiyl diradicals,[271] cyclopenta-fused naphthalenes and fluoranthenes,[272] and many others. Here we will describe two applicatory examples in detail.

3.7.1. Ground States of S_2N_2 and S_4^{2+}. S_2N_2 is an intriguing molecule. As a four-membered ring with six electrons in the π-system, it satisfies the generally accepted criteria for aromaticity: electron count following Hückel's $4n + 2$ rule, stability, planarity with uniform bond lengths, and negative nucleus-independent chemical shift due to the π-electrons.[273] However, its aromatic stabilization energy was found to be quite small or altogether absent, in the range of −0.7 to +6.5 kcal/mol, depending on the reactions that are used for such estimations.[273] On the other hand, the closed shell character (in principle associated with aromaticity) of this molecule has been questioned by some authors who interpreted their theoretical results in terms of significant singlet diradical character.[274−276] Thus, Gerratt et al. described S_2N_2 as a unique predominant Lewis structure, **11** (Scheme 11), with the radical sites on the S atoms, which bear a substantial positive charge, while the N atoms bear a complementary negative

Scheme 11. Weights of the VB Structures for S_2N_2 and S_4^{2+} Using a Double-ζ Basis Set[a]

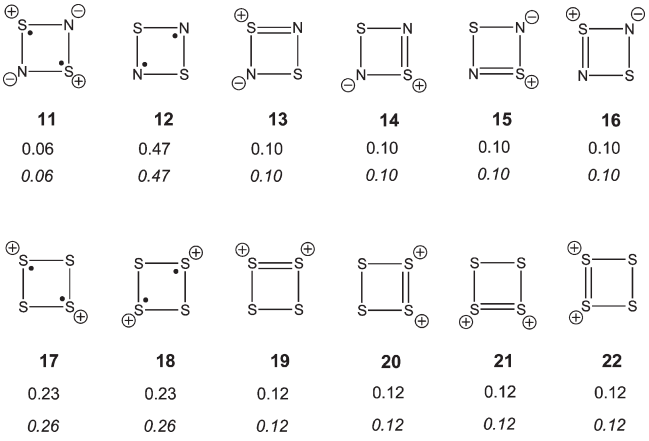

11	12	13	14	15	16
0.06	0.47	0.10	0.10	0.10	0.10
0.06	*0.47*	*0.10*	*0.10*	*0.10*	*0.10*

17	18	19	20	21	22
0.23	0.23	0.12	0.12	0.12	0.12
0.26	*0.26*	*0.12*	*0.12*	*0.12*	*0.12*

[a] Plain characters: Chirgwin-Coulson definition. Italics: Löwdin definition.

charge.[274,275] However, it might be argued that the semidelocalized nature of some of the orbitals involved in the VB wave function preclude the nonambiguous interpretation of the results in terms of weighted VB structures. A different assessment of the radical sites was proposed by Harcourt et al.,[277,278] who computed the weights of the complete set of VB structures, **11**−**16** in Scheme 11, by a nearly classical ab initio VB method using strictly local AOs in the STO-6G basis set. On the basis of these calculations, Harcourt proposed structure **12** to be the major one, with the radical sites on the N atoms, but the calculations, carried out in a minimal basis set, were not really comparable to Gerratt's calculations, which used larger basis sets.

To settle the question, Harcourt and Klapötke[279] repeated the VB calculation in a double-ζ basis set on S_2N_2 and on the isoelectronic S_4^{2+} molecule. These calculations are close to the classical type, i.e., involving all relevant covalent and ionic VB structures, constructed with orbitals defined as primarily one-centered AOs (however not fully localized in this case, as a stricto sensu "classical VB" calculation would imply). For both molecules, the VB description of the six-electron four-orbital π-system requires a set of ten linearly independent VB structures, which have all been included in the calculations. The most important of these structures, **11**−**16** for S_2N_2 and **17**−**22** for S_4^{2+}, are shown in Scheme 11. The remaining ones are practically negligible, with calculated weights smaller than 0.02, and are not shown in Scheme 11.

Only the valence electrons and orbitals of the π-system were treated at the VB level. The σ-electrons and inner-shell π-electrons were accommodated in Hartree−Fock SCF MOs. The VB calculations were performed in Dunning's D95 double-ζ basis set using geometries optimized in the density functional framework at the MPW1PW91/cc-pVTZ level. The weights of the VB structures were calculated by means of the Chirgwin−Coulson[137] and Löwdin[138] formulas, both methods displaying excellent agreement in all cases.

The calculated weights are displayed in Scheme 11. It can be seen that S_2N_2 has a strong diradical character, with a cumulated weight of 0.53 for the diradical structures **11** and **12**. However, structure **12** is clearly the major one, with a weight of 0.47, indicating that the radical sites are on the nitrogen atoms rather than on the sulfur atoms. This result is in agreement with an earlier classical VB calculation in a minimal basis set,[277,278] but is at variance with Gerratt's interpretation based on the spin-coupled method, in which the radical sites are rather viewed on the sulfur atoms. However, since neither Gerratt's nor Harcourt−Klapötke's calculations deal with purely localized AOs, the question may be considered as still open-ended.

Scheme 12. Weights of the Main π-VB Structures for Al_4^{2-} Calculated with the Chirgwin−Coulson Definition in the 6-31G Basis Set**

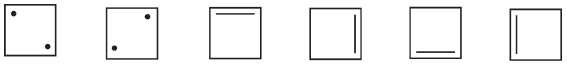

23	24	25	26	27	28
0.243	0.243	0.128	0.128	0.128	0.128

The calculated structure weights for S_4^{2+} (structures **17**−**22** in Scheme 11) bear some resemblance to those of S_2N_2, as the diradical structures (**17**, **18**) are once again predominant, with a cumulated weight of 0.46−0.52 according to the weight definition. By contrast, the structures displaying covalent bonds (**19**−**22**) have smaller weights, 0.12 each. The calculated weights were found to be in close accord with those obtained from single-ζ STO-6G calculations.[280,281] This predominance of diradical structures for both molecules is truly remarkable. In the S_2N_2 case, it can be explained by the fact that **12** is the only VB structure that bears no formal charge. In the S_4^{2+} case, all VB structures have two cationic sites, but the distance between these sites is maximized in the diradical structures **17** and **18**. Thus, it seems that the criteria of atomic neutrality or minimal repulsion between formal charges are more important than the presence or absence of π-bonds to rule the VB content of these two molecules.

For the sake of simplifying the six-structure description of these molecules, Harcourt and Klapötke proposed a two-structure description in terms of so-called "increased valence" structures,[279] aimed at summarizing resonance between the **11**−**16** structures in S_2N_2 or the **17**−**22** structures in S_4^{2+}.

3.7.2. σ- and π-Aromatic Dianion Al_4^{2-}. The Al_4^{2-} dianion has a D_{4h} symmetric structure and possesses two delocalized π-electrons, thus satifying the geometric criterion and $4n + 2$ electron-count rule for aromaticity. As such, its π-system is isoelectronic with that of the aromatic cyclobutadiene dication, $C_4H_4^{2+}$. However, Al_4^{2-} was judged on the basis of its magnetic properties to possess double $(\sigma + \pi)$ aromatic character. This interpretation prompted Havenith and van Lenthe[282] to perform ab initio VB calculations on the ground state of Al_4^{2-} using the 6-31G** basis set. The geometry optimization was performed at the CASSCF(2,4) level, and two definitions of the orbitals were used: semidelocalized, in the SCVB spirit, and strictly atom-centered. Focusing on the latter calculations, we note that the π- and σ-systems were treated separately: in the π-VB calculation, the σ-system is treated as a Hartree−Fock core, and the situation is reversed in the σ-VB calculations.

Like S_2N_2 or S_4^{2+} above, the π-system of Al_4^{2-} involves, with neglect of ionic structures, a set of six covalent VB structures (**23**−**28**) having a covalent bond between adjacent atoms or a long bond along a diagonal and hence a diradicaloid character.

dx.doi.org/10.1021/cr100228r |*Chem. Rev.* 2011, 111, 7557–7593

Scheme 13. Schematic Representation of the Spin-Coupling Mode for the σ-Frame of Al_4^{2-} [a]

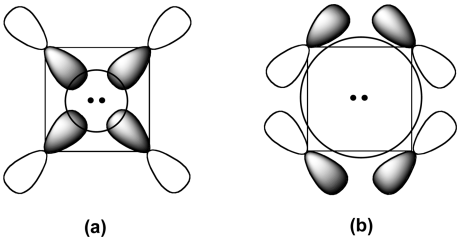

[a] Key: (a) In one of the two-electron four-center systems, two electrons are shared by four radial p-orbitals. (b) In the other two-electron four-center system, two electrons are shared by four tangential p-orbitals.

The VB structures are shown in Scheme 12, along with their weights as calculated by the Chirgwin−Coulson formula, eq 8. Remarkably, one can see an amazing similarity with the structure weights in S_4^{2+}, as calculated by Harcourt and Klapötke, with a clear predominance of the two diradicaloid structures (**23**, **24**), which together account for almost 50% of the ground electronic state.

While the electronic structure of the π-system is in conformity with expectations, that of the σ-frame is truly remarkable. Different spin-coupling schemes were tried to address the plausibility of the different possible bonding modes of the tangential and radial hybrids. The best coupling mode, which combines low energy and simplicity, is illustrated in Scheme 13. It consists of two separate σ-systems each possessing two electrons, one built from the radial p-orbitals (Scheme 13a), the other from the tangential p-orbitals (Scheme 13b), with the remaining eight valence electrons being accommodated in doubly occupied 2s AOs. For each of these two subsystems, six VB structures can be constructed, leading to a total of 36 VB structures for the σ-frame. As the two sets of p-orbitals do not overlap much, the two subsystems can be considered as two independent two-electron delocalized systems, both of them complying with the $4n + 2$ aromaticity rule. Thus, some significant σ-aromatic stabilization is expected. It follows that Al_4^{2-} can be schematically described as a combination of *three* intricate aromatic rings, all of them being of the aromatic two-electron four-center type, thus explaining the stability of this dianion and its magnetic properties showing double ($\sigma + \pi$) aromatic character.

4. ALGORITHM ADVANCES IN AB INITIO VB METHODS

4.1. VB Wave Function and Hamiltonian Matrix

There are two ways of evaluating the Hamiltonian matrix elements and overlaps between VB structures (eqs 6 and 7 in section 2). In the first, by expanding the spin function Θ_K in terms of elementary spin products, attaching the spatial factor Ω_0, and antisymmetrizing, a VB function is expressed in terms of 2^m determinants:

$$\Phi_K = \sum_{\kappa} d_{\kappa}^{K} D_{\kappa} \tag{93}$$

The Hamiltonian matrix elements, eq 6, become sums of contributions from all pairs of determinants, and these may be evaluated by

$$\langle D_\kappa|H|D_\lambda\rangle = \sum_{r,s} h_{rs}^{\kappa\lambda} D(S_{rs}^{\kappa\lambda}) + \sum_{r<u,s<t} (g_{rs,ut}^{\kappa\lambda} - g_{rs,tu}^{\kappa\lambda}) D(S_{rs,ut}^{\kappa\lambda}) \tag{94}$$

where $h_{rs}^{\kappa\lambda}$ and $g_{rs,ut}^{\kappa\lambda}$ are one- and two-electron integrals, respectively, defined as

$$h_{rs}^{\kappa\lambda} = \langle \kappa_r|h|\lambda_s\rangle \quad \text{and} \quad g_{rs,ut}^{\kappa\lambda} = \langle \kappa_r \kappa_s|g|\lambda_u \lambda_t\rangle \tag{95}$$

and $D(S_{rs}^{\kappa\lambda})$ and $D(S_{rs,ut}^{\kappa\lambda})$ are the first- and second-order cofactors of the overlap matrix between the two VB determinants, respectively.

The algorithm of evaluating cofactors for determinants of nonorthogonal orbitals was first obtained by Löwdin[283] and further developed by Prosser and Hagstrom.[284] The Löwdin rules were widely used for VB calculations long ago by Matsen,[285] Simonetta,[286] and Balint-Kurti[287] with their co-workers. This algorithm has been further improved by van Lenthe and co-workers,[140] especially for the singular overlap matrix. Roughly speaking, the computational costs are of order N^3 for the first-order and N^4 for the second-order cofactors. As such, the scaling of computing a Hamiltonian matrix element between determinants is N^4, and thus, it scales as KN^4 for a Hamiltonian matrix element between VB structures, where K is the number of determinant pairs for a VB structure.

The second method is to use symmetric group theory, as the spin function Θ_K forms irreducible representation of the symmetric group S_N. This method may be regarded as another application of the spin-free approach of Matsen[288] and is discussed below.

4.2. Orbital Optimization in the VBSCF Procedure

As mentioned above, the computational cost for the Hamiltonian matrix is $O(KN^4)$ and is not too high when the studied molecules contain only a few covalent bonds. The computation-intensive step in VB calculations is, in fact, the optimization of the orbitals. Apparently, the VBSCF procedure is identical to the minimization of its corresponding expectation energy, which leads to SCF equations. The latter is reminiscent of the much familiar MO-based MCSCF equations, but contains the third-order cofactors of determinants.[289,290] Though the SCF equations may be solved iteratively essentially in the same manner as the MCSCF equations, it is evident that the computational cost runs high due to the six-index third-order cofactors. A more practical approach is to find such a stationary point on the energy surface by direct search methods, instead of attempting to solve the SCF equation. One widely used method is the super-CI method,[141] which is based on the generalized Brillouin theorem.[291] In the super-CI method, the wave function is expressed as a linear combination of the approximate ground-state wave function and all its singlet excitations, and then the new orbital coefficients are updated by the CI coefficients for every new iteration step. An alternative way is to use Newton−Raphson (NR)-type methods, for which energy gradients are critical, where the first-order energy gradients were obtained by evaluating the Hamiltonian matrix elements between the VB wave function and its corresponding single excitations, and the Hessian matrix is obtained approximately.[141]

Since in both methods the energy term is expressed with VB orbitals, computations require two-electron integral transformation from the basis functions to the VB orbitals for each iteration. This raises the demands for both CPU time and storage space. Clearly,

the high-order scaling of computational cost is a hindrance to the further development of ab initio VB theory.

4.3. Spin-Free Form of VB Theory

The conventional determinant method encounters a serious difficulty when the number of covalent bonds of the studied molecule is not small. The length of the expansions and the need for repeated evaluation of determinantal cofactors lead to very heavy computational cost. An alternative approach is to use the spin-free formulation[288] of many-electron problems by using a project operator of symmetric group S_N.

In spin-free quantum chemistry, the Hamiltonian operator is spin-free, and thus, its matrix elements are determined only by the spatial part of the wave function. Using the symmetric group approach, the form of the spatial function may be taken as[98,292,293]

$$\Phi_K = N_K e_{r1}^{[\lambda]} \Omega_K \tag{96}$$

where N_K is a normalization factor, $e_{rs}^{[\lambda]}$ is the standard projection operator of the symmetric group, and Ω_K is the orbital product corresponding to the given K-structure. Φ_K is called bonded tableau (BT) function in the BTUGA.[98,293] It can be seen from eq 96 that a VB function is characterized by the orbital product, i.e., the ordering of occupied orbitals. In convention, in this review, we assume that $\Omega_K = k_1(1)\, k_2(2) \ldots k_N(N)$ and $\Omega_L = l_1(1)\, l_2(2) \ldots l_N(N)$, where $(k_1, k_1, \ldots, k_N)$ and $(l_1, l_1, \ldots, l_N)$ are taken from orbital set $\{\phi_i\}$. With the spin-free form, eq 96, the Hamiltonian and overlap matrix elements, eqs 6 and 7, are written as[98,292,293]

$$H_{KL} = \langle \Phi_K | H | \Phi_L \rangle = \sum_{P \in S_N} D_{11}^{[\lambda]}(P) \langle \Omega_K | HP | \Omega_L \rangle \tag{97}$$

and

$$M_{KL} = \langle \Phi_K | \Phi_L \rangle = \sum_{P \in S_N} D_{11}^{[\lambda]}(P) \langle \Omega_K | P | \Omega_L \rangle \tag{98}$$

where $D_{rs}^{[\lambda]}(P)$ are the irreducible representation matrix elements, which have been well discussed[98,292,293] and are easily determined. It is worthwhile to emphasize that eqs 97 and 98 are the unique formulas of the matrix elements in the spin-free approach if HLSP functions are adopted, even though one can take some other forms of VB functions. For example, it is possible to construct VB functions by the Young operator,[288] but the forms of the matrix elements are identical to eqs 97 and 98.[294]

Different from the above method, in which the first diagonal element of the irreducible representation matrix of the symmetric group is used for constructing HLSP functions, Gallup and co-workers developed another spin-free VB method, called the tableau function approach,[148] by using the last element of the irreducible representation. The method leads to rather efficient computational procedures. However, this tableau function is not equivalent to HLSP functions.

Both eqs 97 and 98 involve $N!$ terms of all permutations of S_N, which is similar to a determinant expansion or a permanent expansion, except for different coefficients. If VB orbitals are orthogonal, only a few terms are nonzero and make contributions to the matrix elements,[293] and consequently, the matrix elements are conveniently obtained. However, the use of nonorthogonal orbitals is one of the most important characteristics of the VB approach, and thus, all $N!$ terms make contributions to the matrix elements. Obviously, it is impracticable to sum over all $N!$ terms by one-by-one permutations. In the next section, we will review an approach, called the paired-permanent-determinant (PPD) method,[295] to discuss how to calculate the Hamiltonian matrix elements as efficiently as possible, which will enable one to implement a spin-free VB program.

4.4. Paired-Permanent-Determinant Approach

The purpose of the PPD approach is to overcome the difficulty of the determinant expansion length in the conventional VB methods by applying the spin-free form of VB theory. To do this, a direct approach is to define a spin-free VB function, eq 96, as a new function, instead of using 2^m determinant expansion.

In the PPD approach, for an $N \times N$ matrix $\mathbf{A} = (a_{ij}, i, j = 1, 2, \ldots N)$, a PPD function is defined as[295]

$$\mathrm{ppd}(\mathbf{A}) = \sum_{P \in S_N} D_{11}^{[\lambda]}(P) a_{1p_1} a_{2p_2} \ldots a_{N-1,p_{N-1}} a_{N,p_N} \tag{99}$$

where the permutation P is

$$P = \begin{pmatrix} 1 & 2 & 3 & 4 & \ldots & N-1 & N \\ p_1 & p_2 & p_3 & p_4 & \ldots & p_{N-1} & p_N \end{pmatrix} \tag{100}$$

It can be seen from eq 99 that the definition of PPD is similar to those of determinants and permanents, all of them containing the same $N!$ terms. The difference is in the expansion coefficients. Instead of ± 1 for determinant or 1 for permanent, it is the first diagonal element of the representation matrix, $D_{11}^{[\lambda]}(P)$, whose value is of the form $(-1)^a(-1/2)^b$, where a and b depend on the permutation.

The evaluation of a PPD may be performed by a recursion formula, which is similar to Laplacian expansion for determinants. A PPD of order N may be expressed in a linear combination of the product of PPDs of order 2 and their corresponding cofactors, which is also a PPD of order $N - 2$. By repeating the Laplacian expansion, an N-order PPD can be gradually reduced to PPDs of order $N - 2$, $N - 4$, etc.

It can be shown that the overlap matrix element between two VB functions, Φ_K and Φ_L, eq 98, is a PPD function, shown as

$$M_{KL} = \mathrm{ppd}(\mathbf{S}) \tag{101}$$

where $\mathbf{S}$ is the VB orbital overlap matrix with elements $s_{ij} = \langle k_i | l_j \rangle$ and thus can be straightforwardly calculated by the Laplacian expansion algorithm for a PPD.

The expansion for the Hamiltonian matrix element is much more complicated.[295] The evaluation of a Hamiltonian matrix element requires the order $N - 2$ and order cofactors of $\mathrm{ppd}(\mathbf{S})$. From the computational point of view, the PPD algorithm does not solve the so-called "$N!$ problem". Fortunately, in the routine of a PPD expansion, there are many redundant sub-PPDs, and thus, a well-designed routine can avoid the repeated evaluation of sub-PPDs. In implementation, all required sub-PPDs may be computed beforehand, and labeled in indices, and a PPD is computed by collecting all sub-PPDs that are involved in the PPD according to the indices.

It is worthwhile to point out that the expansion of PPDs is much more demanding computationally than that of determinants, and thus, in most cases the conventional determinant algorithm for VB methods is more efficient than the PPD algorithm. However, the advantage of the PPD algorithm will

show up with an increasing number of covalent bonds, in which only a few PPDs are involved in the calculation. In contrast, the number of determinants that are involved in VB calculations goes up steeply in the determinant algorithm with an increasing number of covalent bonds.

The PPD approach is based on the representation theory of the symmetric group. A similar algorithm based on the group algebra of the symmetric group was developed by Li and Pauncz.[102] They derived the expansion expressions for the evaluation of VB matrix elements by defining algebrants of VB wave functions. An algebrant can be expanded with subalgebrants of lower orders in a successive way. The algorithm has been implemented in VB2000.[296]

4.5. Direct VBSCF/BOVB Algorithm

In the conventional VBSCF or BOVB calculations, the Hamiltonian matrix elements are expressed explicitly in the form of orbital integrals, and thus, an integral transformation from basis functions to VB orbitals is required for each iteration. Wu et al. presented an algorithm for the VBSCF/BOVB calculations.[297] In the algorithm, the total energy of the system and its gradients are expressed in terms of basis functions, and thus, integral transformation is not required, saving much computational time.

In the algorithm, a transition density matrix $\mathbf{P}^{\kappa\lambda}$ connecting a pair of Slater determinants, D_κ and D_λ, is defined as

$$\mathbf{P}^{\kappa\lambda} = \mathbf{T}^{\kappa}(\tilde{\mathbf{T}}^{\lambda}\mathbf{S}\mathbf{T}^{\kappa})^{-1}\tilde{\mathbf{T}}^{\lambda} \tag{102}$$

where matrices $\mathbf{T}^{\kappa}$ and $\mathbf{T}^{\lambda}$ are orbital coefficients that correspond to D_κ and D_λ, respectively, defined as

$$\kappa_i(j) = \sum_{\mu} T^{\kappa}_{\mu i}\chi_\mu(j) \qquad \text{and} \qquad \lambda_i(j) = \sum_{\mu} T^{\lambda}_{\mu i}\chi_\mu(j) \tag{103}$$

and $\mathbf{S}$ is the overlap matrix of spin−orbital basis functions. The Hamiltonian matrix element between Slater determinants D^{κ} and D^{λ} is written as

$$H_{\kappa\lambda} = M_{\kappa\lambda}\left(\sum_{\mu,\nu} P^{\kappa\lambda}_{\mu\nu}h_{\nu\mu} + \frac{1}{2}\sum_{\mu,\nu,\sigma,\lambda} P^{\kappa\lambda}_{\mu\nu}P^{\kappa\lambda}_{\sigma\lambda}(g_{\nu\lambda,\mu\sigma} - g_{\nu\lambda,\sigma\mu})\right) \tag{104}$$

The overlap matrix element between two Slater determinants, D_κ and D_λ, $M_{\kappa\lambda}$, is the determinant of the orbital overlap matrix $\mathbf{V}^{\kappa\lambda}$:

$$M_{\kappa\lambda} = |\mathbf{V}^{\kappa\lambda}| = |\tilde{\mathbf{T}}^{\kappa}\mathbf{S}\mathbf{T}^{\lambda}| \tag{105}$$

By defining a Fock matrix $\mathbf{F}^{\kappa\lambda}$ as

$$\mathbf{F}^{\kappa\lambda} = \mathbf{h} + \mathbf{G}^{\kappa\lambda} \tag{106}$$

where $\mathbf{h}$ is the one-electron integral matrix and $\mathbf{G}^{\kappa\lambda}$ is a matrix whose elements are defined as

$$G^{\kappa\lambda}_{\mu\nu}(P) = \sum_{\sigma,\lambda} P^{\kappa\lambda}_{\sigma\lambda}(g_{\mu\lambda,\nu\sigma} - g_{\mu\lambda,\sigma\nu}) \tag{107}$$

The matrix element $H_{\kappa\lambda}$ is written as

$$H_{\kappa\lambda} = \frac{1}{2}M_{\kappa\lambda}(tr\ \mathbf{P}^{\kappa\lambda}\mathbf{h} + tr\ \mathbf{P}^{\kappa\lambda}\mathbf{F}^{\kappa\lambda}) \tag{108}$$

and the energy is expressed as

$$E = \frac{\sum_{K,L} C_K C_L H_{KL}}{\sum_{K,L} C_K C_L M_{KL}} = \frac{\sum_{K,L,\kappa,\lambda} C_K C_L d^K_\kappa d^L_\lambda M_{\kappa\lambda}(tr\ \mathbf{P}^{\kappa\lambda}\mathbf{h} + tr\ \mathbf{P}^{\kappa\lambda}\mathbf{F}^{\kappa\lambda})}{2\sum_{K,L,\kappa,\lambda} C_K C_L d^K_\kappa d^L_\lambda M_{\kappa\lambda}} \tag{109}$$

Furthermore, the energy gradients with respect to orbital coefficients $T^{\kappa}_{\mu i}$ associated with determinant D^{κ} are

$$\frac{\partial E}{\partial T^{\kappa}_{\mu i}} = \frac{1}{M^2}\sum_{K,L,\lambda} C_K C_L d^K_\kappa d^L_\lambda [M(\mathbf{Z}^{\kappa}_{\kappa\lambda})_{\mu i} - H(\mathbf{Y}^{\kappa}_{\kappa\lambda})_{\mu i}] \tag{110}$$

where

$$M = \sum_{K,L,\kappa,\lambda} C_K C_L d^K_\kappa d^L_\lambda M_{\kappa\lambda}$$
$$H = \sum_{K,L,\kappa,\lambda} C_K C_L d^K_\kappa d^L_\lambda H_{\kappa\lambda} \tag{111}$$
$$\mathbf{Y}^{\kappa}_{\kappa\lambda} = \mathbf{S}\mathbf{T}^{\lambda}(\mathbf{V}^{\kappa\lambda})^{-1}$$
$$\mathbf{Z}^{\kappa}_{\kappa\lambda} = [H_{\kappa\lambda}S + M_{\kappa\lambda}(1 - \mathbf{S}\tilde{P}^{\kappa\lambda})\tilde{F}^{\kappa\lambda}]\mathbf{T}^{\lambda}(\mathbf{V}^{\kappa\lambda})^{-1}$$

Though the above formulas are derived tediously, the most time-consuming part in applications is the construction of Fock matrices $\mathbf{F}^{\kappa\lambda}$, which need $O(m^4)$ computer operations. Thus, in one iteration the overall scaling for gradients with each pair of determinants is $O(m^4)$, similar to that of one iteration in the HF method. Therefore, if the number of determinant pairs (K) is not large, the algorithm is much more efficient than the conventional VBSCF algorithms. Another advantage is that all derived formulas above are orbital-free and thus may be performed in the integral direct mode easily, without the integral transformation procedure. It is worthwhile to emphasize that the algorithm is especially efficient for the BOVB method. As discussed above, the BOVB wave function allows each structure to have its own orbital set, and thus, the number of occupied orbitals will greatly increase. In the current algorithm, the computational cost mainly depends on the number of basis functions, rather than the number of breathing orbitals. Thus, the cost of a single BOVB iteration is almost the same as that of a VBSCF iteration.

5. CURRENT CAPABILITIES OF AB INITIO VB METHODS

With the advances in VB methods made in the past three decades, ab initio VB theory is now capable not only of accurate calculations of small molecules, by using BOVB and VBCI, but also of reasonable VB calculations of medium-sized molecules, even for transition-metal complexes. In this section, we shall discuss the rotational barrier for the organometallic complex $(CO)_4Fe(CH_2{=}CH_2)$ as an example of the current computational capabilities of full-electron VB calculation.

The rotational barrier of $(CO)_4Fe(C_2H_4)$ was computed by VBSCF, Hartree−Fock, B3LYP, CASSCF, and CCSD methods. Elian and Hoffman[298] analyzed the rotational barrier in terms of fragment orbital (FO) interactions between the FOs of the $Fe(CO)_4$ and C_2H_4 fragments. As discussed before,[183,299] one can actually use such FOs in a VB scheme to do FO-VB calculations.[182] Thus, the $(CO)_4Fe$ fragment possesses in the

dx.doi.org/10.1021/cr100228r |Chem. Rev. 2011, 111, 7557–7593

missing sites of the octahedron two hybrid orbitals (h1 and h2). These two hybrid orbitals can be combined to form two localized symmetry-adapted FOs, one being symmetric (h1 + h2) and the other antisymmetric (h1 − h2) with respect to the horizontal symmetry plane in the complex. These FOs can in turn couple with the π- and π^*-orbitals of ethylene and form two new bond pairs, as shown in Scheme 14, wherein the lines connecting the FOs signify that the corresponding electrons are singlet paired ($\alpha\beta-\beta\alpha$).[299] Note that the FO-VB approach imports the MO advantage of orbital symmetry into the VB wave function.[299]

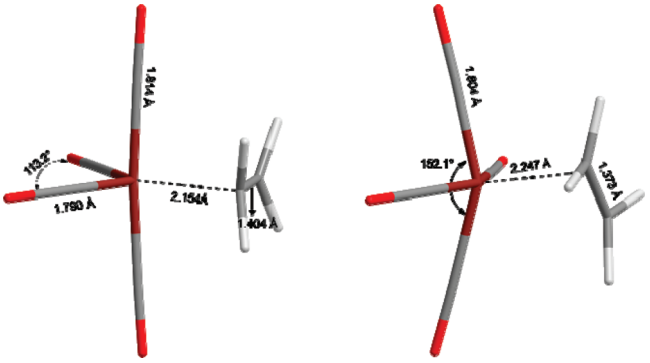

Figure 10. Optimized geometries of the EC and transition state.

Table 7. Calculated Energies (au) of the Equilibrium Conformation (EC) and Transition State and Rotation Barriers ($\Delta E^{\ddagger}$, kcal/mol) by HF, B3LYP, CASSCF, CCSD, and VBSCF.[a]

method	EC	transition state	$\Delta E^{\ddagger}$
HF	−651.392537	−651.368292	15.2
B3LYP	−655.402461	−655.386899	9.8
VBSCF(FO-VB,20st)	−651.427379	−651.393932	21.0
VBSCF(OEO-VB,20st)	−651.498822	−651.476816	13.8
CASSCF(4,4)	−651.498808	−651.476771	13.8
CCSD	−653.238957	−653.215200	14.9

[a] All calculations involve Lanl2dz for Fe and 6-31G* for the other atoms.

Scheme 14. FO-VB Diagram Using Lines To Show Bond Pairing between FOs on $Fe(CO)_4$ and C_2H_4

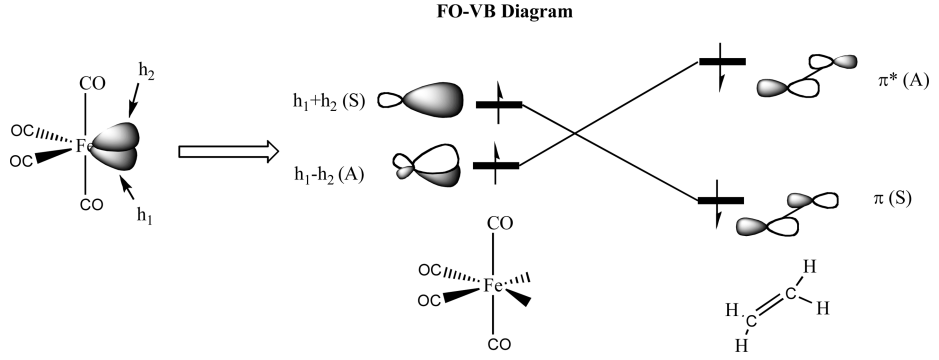

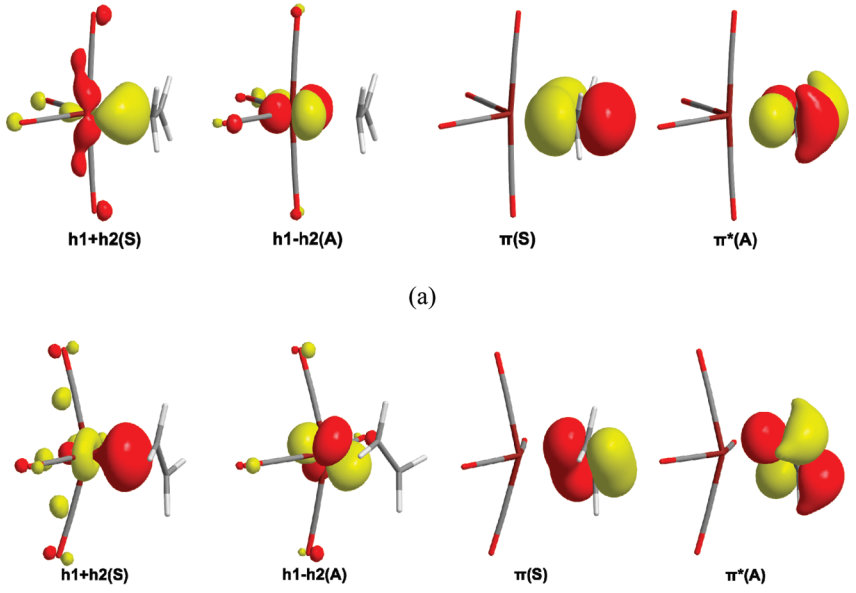

Figure 11. (a) Optimized FOs at the EC (see Scheme 14). (b) Optimized FOs at the transition state.

dx.doi.org/10.1021/cr100228r |*Chem. Rev.* 2011, 111, 7557–7593

Here we present the results of VBSCF calculations using VBSCF(FO-VB) and VBSCF(OEO-VB). The geometries of the equilibrium conformation (EC) and transition state, shown in Figure 10, are optimized at the B3LYP level with the same basis set.

In the VBSCF calculations, all electrons except for the ECP electrons of Fe are included in the VB calculations; thus, there are totally 88 electrons in 46 VB orbitals, among which 42 are doubly occupied, while the active shell involves four electrons in the four FOs, (h1 + h2)(S) and (h1 − h2)(A) on the $Fe(CO)_4$ fragment and π(S) and π^*(A) on ethylene. All 20 VB structures that form a complete Rumer basis for the active shell were included in the calculation.

Table 7 shows the detailed results with various methods, where CASSCF and CCSD methods used the same basis set as in the VBSCF calculation, and the geometries were optimized using the B3LYP method with the same basis set. As can be seen, the rotation barrier calculated by the VBSCF(FO-VB,20st) method is 21.0 kcal/mol, much higher than the MO-based CCSD values. On the other hand, the VBSCF(OEO-VB,20st) barrier is identical to the CASSCF(4,4) barrier, as expected.

Parts a and b of Figure 11 show the optimized FOs at the EC and the transition state. It is seen that, as expected from the FO-VB analysis in Scheme 14,[183,299] the ethylene moiety is bonded by the $(CO)_4Fe$ fragment by a double bond, and this is the root cause of the substantial barrier for rotation.

This combination of reasonable accuracy and insight is already encouraging. Better accuracy can be achieved by higher levels of VB methods, especially VBPT2, which, as reviewed above, is a very cheap post-VBSCF method. The new version of VBPT2 that applies the contraction technique of active space is in progress and will hopefully provide the long sought after powerful tool for VB studies of many problems for medium-sized molecules.

6. CONCLUDING REMARKS

This review provides a snapshot of the current state of classical valence bond theory, in its modern ab initio fashion, and demonstrates that the theory is coming of age. There now exists a family of methods which form a lineage that resembles the family of CASSCF MO theory and its post-CASSCF levels. Thus, starting with the VBSCF theory, which is the equivalent of CASSCF, one can further improve the numerical results by using methods such as BOVB, VBCI, and VBPT2, which incorporate dynamic correlation effects and which have accuracies that converge to CCSD or CASPT2 theories using the same basis sets. In addition, any one of these VB methods can be combined with a solvent model or an MM force field, as in VBPCM, VBSM, and VB/MM, and thereby provide a method that can handle molecules and reactions in solution and in proteins. Thus, from a quantitative point of view, today VB theory enables the calculations of "real" chemical problems for organic molecules, as well as molecules that contain transition metals, and all these can be done in the gas phase or in solution. Especially promising is the VBPT2 method, which emerges as a fast and accurate method that in the future will be able to handle much larger systems than those presented here.

The review describes another family of quantitative methods, which derive from the BLW approach. This method extracts from MO- or DFT-based theories VB-type information such as resonance energies and delocalization energies such as hyperconjugation, etc. Thus, while the many successful applications of these methods show that VB ideas are not chained to VB calculations in a strict sense, they also demonstrate the creative and portable nature of VB theory that enables the two traditionally rival theories to be bridged and get useful insight about structure and reactivity.

Indeed, the other aspect of VB theory that is emphasized in this review is insight. Thus, despite the sophistication and accuracy of the above VB methods, all of them rely on a compact wave function which includes a minimal number of structures in the VB structure set. The insight of this compact wave function is projected by a panoramic set of applications starting from simple bond energies, to reactivity, reactivity in solution, and all the way to the rotational behavior of an organometallic complex, $(CO)_4Fe(C_2H_4)$. Indeed, while well-designed VB software is still challenging, the existing software (see the Appendix) is sufficiently friendly to non-VB experts and offers reasonable efficiency and lucid insight.

Finally, as the example of the rotational barrier of $(CO)_4Fe(C_2H_4)$ shows, there is room for improvement, but there is also a horizon for VB theory. Future improvement that will enable the calculations of bioinorganic species with different spin states will take VB theory to a frontier research area.

APPENDIX: SOME AVAILABLE VB SOFTWARES

Other than the GVB method that is implemented in many packages by now, here are brief descriptions of the main VB softwares we are aware of and with which we have some experience to varying degrees.

XMVB Program. The XMVB software[108,109] is a general program that is designed to perform multistructure VB calculations. It can execute either nonorthogonal CI or nonorthogonal MCSCF calculations with simultaneous optimization of orbitals and coefficients of VB structures. Complete freedom is given to the user to deal with HAOs, BDOs, or OEOs, so that calculations of VBSCF, SCVB, BLW, BOVB, VBCI, and VBPT2 types can be performed. Particularly, the "pure" VB methods, VBSCF, BOVB, VBCI, and VBPT2, described in section 2.2 are implemented as standard methods in the package and can be easily performed by specifying appropriate keywords in the input file. In this sense, XMVB is a fairly user-friendly package applicable to a variety of chemical problems. XMVB is a stand-alone program, but for flexibility, it can be interfaced to most QM software, e.g., GAUSSIAN, GAMESS-US, etc. In addition, it is also feasible to combine XMVB with ab initio MO packages to perform hybrid valence bond method calculations, such as VB-DFT, VBPCM, VBSM, etc. The parallel version of XMVB, based on the message-passing interface (MPI), is also available.[109] XMVB can be used as a stand-alone program that is freely available from the author (e-mail weiwu@xmu.edu.cn, Web site http://ctc.xmu.edu.cn/xmvb/). It has also been incorporated into GAMESS-US,[300] which also includes the BLW method.

TURTLE Software. TURTLE[110,111] is also designed to perform multistructure VB calculations and can execute calculations of the VBSCF, SCVB, BLW, or BOVB types. Currently, TURTLE involves analytical gradients to optimize the energies of individual VB structures or multistructure electronic states with respect to the nuclear coordinates.[301] A parallel version has been developed and implemented using the MPI for the sake of

making the software portable.[107] TURTLE is now implemented in the GAMESS-UK program.[302]

VB2000 Software. VB2000[112] is an ab initio VB package that can be used for performing nonorthogonal CI and multistructure VB with optimized orbitals, as well as SCVB, GVB, VBSCF, and BOVB. VB2000 can be used as a plug-in module for GAMESS-(US)[300] and Gaussian98/03[303] so that some of the functionalities of GAMESS and Gaussian can be used for calculating VB wave functions. GAMESS also provides an interface (option) for access of the VB2000 module.

CRUNCH Software. CRUNCH (Computational Resource for Understanding Chemistry) was written originally in Fortran by Gallup and recently translated into C.[304] This program can perform multiconfiguration VB calculations with fixed orbitals, plus a number of MO-based calculations such as RHF, ROHF, UHF (followed by MP2), orthogonal CI, and MCSCF.

SCVB Software. The SCVB method is now included in the MOLPRO software.[305]

AUTHOR INFORMATION

Corresponding Author

*E-mail: weiwu@xmu.edu.cn (W.W.); sason@yfaat.ch.huji.ac.il (S.S.); philippe.hiberty@u-psud.fr (P.C.H.). Phone: +86-5922182825 (W.W.); +972-26585909 (S.S.); +33-169156175 (P.C.H.). Fax: +86-5922184708 (W.W.); +972-26584680 (S.S.); +33-0169154447 (P.C.H.).

BIOGRAPHIES

Wei Wu received his B.Sc. (1983) and M.Sc. (1986) in physics and his Ph.D. (1990) in theoretical chemistry from Xiamen University with Qianer Zhang. From 1992 to 1994, he worked as a Postdoctoral Fellow with Roy McWeeny at the University of Pisa, and then he went back to Xiamen University as an Associate Professor. In 1995, he became Professor, and he is currently the director of the Institute of Theoretical and Computational Chemistry. He was appointed as a Changjiang Scholar of the Ministry of Education of China in 2004. From 1997 to 1999, he worked with Sason Shaik at the Hebrew University of Jerusalem. His research fields focus on the methodology developments in quantum chemistry, especially in ab initio valence bond theory and its implementation. He authored the XIAMEN and XMVB softwares. Since 1999, he has teamed with Sason Shaik and Philippe Hiberty in the Long VB March.

Peifeng Su was born in Longhai, China, in 1978. He received his B.Sc. in chemistry and his Ph.D. in theoretical chemistry from Xiamen University with Wei Wu. From 2008 to 2009, he worked as a Postdoctoral Fellow with Dr. Hui Li at the University of Nebraska—Lincoln. Then he became an Associate Professor at Xiamen University. His research fields focus on the methodology developments and application research in valence bond theory, intermolecular interactions, and solvation models.

Sason Shaik was born in Iraq and immigrated to Israel in 1951. He received his B.Sc. and M.Sc. from Bar-Ilan University and his Ph.D. from the University of Washington with Dr. Epiotis. From 1978 to 1979, he spent a postdoctoral year with Dr. Hoffmann at Cornell University. In 1980, he started as a Lecturer at Ben-Gurion University and became Professor in 1988. In 1992, he joined the Hebrew University, where he is currently the director of The Lise Meitner-Minerva Center for Computational Quantum Chemistry. Among his awards are the 2001 Israel Chemical Society Prize and the 2007 Schrödinger Medal. His research interests cover the range of bonding in small molecules to the structure and reactivity of metalloenzymes. He generally uses quantum chemistry, and in particular VB theory, to develop paradigms, which can pattern data and lead to the generation of new problems. He has been active in the articulation and improvement of VB theory and in building bridges between MO and VB theories since 1981. Since 1985, he has teamed with Philippe Hiberty and later also with Wei Wu in the Long VB March.

Philippe C. Hiberty studied theoretical chemistry at the University of Paris-Sud with W. J. Hehre, completed his Ph.D. under the supervision of L. Salem, and obtained a research position at the CNRS. In 1979, he started his postdoctoral research with J. I. Brauman at Stanford University and then with H. F. Schaefer III at Berkeley. He went back to Orsay to join the Laboratoire de Chimie Théorique, where he developed a research program based on valence bond theory. He became Directeur de Recherche in 1986, and in addition, he taught Quantum Chemistry at the Ecole Polytechnique in Palaiseau for 12 years. He received the Grand Prix Philippe A. Guyé from the French Academy of Sciences in 2002. His research interests are, among others, the improvement of ab initio valence bond methods and the application of quantum chemistry and valence bond theory to fundamental concepts of organic chemistry. He has been active in creating bridges between MO and VB theories, and improving the latter, since 1979. Since 1985, he has teamed with Sason Shaik and later also with Wei Wu in the Long VB March.

ACKNOWLEDGMENT

W.W. is supported by the National Natural Science Foundation of China (Grant 20873106) and the Ministry of Science and Technology (2011CB808504). S.S. is supported by Israel Science Foundation Grant ISF 53/09. P.C.H. is grateful to Profs. Y. Mo and J. P. Malrieu for helpful discussions.

LIST OF ABBREVIATIONS

aNR	approximate Newton−Raphson method
ARE	adiabatic resonance energy
B3LYP	a hybrid functional consisting of 20% Hartree−Fock and 80% Becke88 exchange combined with the Lee−Yang−Parr correlation functional
BDOs	bond-distorted orbitals
BLW	block-localized wave function method
BOVB	breathing-orbital valence bond method
BT	bonded tableau
BTUGA	bonded tableau unitary group approach
CASPT2	complete active space second-order perturbation theory
CASPT3	complete active space third-order perturbation theory
CASSCF	complete active space self-consistent field method
CCSD	coupled cluster method with single and double excitations
CCSD(T)	coupled cluster method with single and double excitations and a perturbative treatment of triple excitations
CDC	consistent diabatic configuration
CI	configuration interaction
CISD	configuration interaction with single and double excitations
D-BOVB	breathing-orbital valence bond method with delocalized inactive orbitals
DE	delocalization energy
DE-VB/MM	density-embedding VB/MM (see below for definition of VB/MM)
DFT	density functional theory
ECRE	extra cyclic resonance energy
EDA	energy decomposition analysis
EH-MOVB	effective-Hamiltonian molecular orbital valence bond method
EVB	empirical valence bond
FOs	fragment orbitals
GVB	generalized valence bond method
HAOs	hybrid atomic orbitals
HF	Hartree−Fock method
HLSP	Heitler−London−Slater−Pauling-type wave function
L-BOVB	breathing-orbital valence bond method with all orbitals strictly localized on their respective fragments
MCSCF	multiconfiguration self-consistent field method
MM	molecular mechanics
MOVB	molecular orbital valence bond method
MP2	Møller−Plesset perturbation method of the second order
MRCI	multireference configuration interaction
MRPT2	multireference second-order perturbation method
NBO	natural bond orbital
NICS	nucleus-independent chemical shift
NR	Newton−Raphson optimization method
OEO	overlap-enhanced orbital
P	product state
*P**	promoted excited state of the product
PCM	polarizable continuum model
PPD	paired-permanent-determinant approach
QM	quantum mechanics
R	reactant state
*R**	promoted excited state of the reactant
RE	resonance energy
RHF	restricted Hartree−Fock
SCF	self-consistent field
SCRF	self-consistent reaction field
SCVB	spin-coupled valence bond method
SD-BOVB	breathing-orbital valence bond method with delocalized inactive orbitals and splitting of doubly occupied orbitals into two singly occupied and spin-paired orbitals
SL-BOVB	breathing-orbital valence bond method with all orbitals strictly localized on their respective fragments and split doubly occupied orbitals (see SD-BOVB above)
SM*x*	a series of universal solvation models, $x = 1-8$
TB	through-bond interaction
TS	through-space interaction
VB/MM	a quantum mechanics/molecular mechanics method that combines the ab initio valence bond method with molecular mechanics

VBCI	valence bond configuration interaction method
VBCIPT	valence bond configuration interaction method with an approximated perturbation estimation for high and less important excited structures
VBCIS	valence bond configuration interaction method with single excitation
VBCISD	valence bond configuration interaction method with single and double excitation
VBDFT(s)	a semiempirical valence bond method that incorporates the density functional theory energy of the nonbonded reference state
VBPCM	valence bond polarizable continuum model method
VBPT2	valence bond second-order perturbation method
VBSCD	valence bond state correlation diagram
VBSCF	valence bond self-consistent field method
VBSM	valence bond solvation model method
VDC	variational diabatic configuration
VRE	vertical resonance energy
XC	exchange-correlation functionals
XMVB	an ab initio nonorthogonal valence bond program

REFERENCES

(1) Bobrowicz, F. W.; Goddard, W. A., III. In *Methods of Electronic Structure Theory*; Schaefer, H. F., Ed.; Springer: Berlin, Heidelberg, 1977; Vol. 4, p 79.

(2) Goddard, W. A., III; Dunning, T. H.; Hunt, W. J.; Hay, P. J. *Acc. Chem. Res.* **1973**, *6*, 368.

(3) Goddard, W. A., III. *Phys. Rev.* **1967**, *157*, 81.

(4) Goddard, W. A., III; Harding, L. B. *Annu. Rev. Phys. Chem.* **1978**, *29*, 363.

(5) Goddard, W. A., III. *Int. J. Quantum Chem.* **1969**, *4*, 593.

(6) Coulson, C. A.; Fischer, I. *Philos. Mag.* **1949**, *40*, 386.

(7) Carter, E. A.; Goddard, W. A., III. *J. Chem. Phys.* **1988**, *88*, 3132.

(8) Murphy, R. B.; Friesner, R. A.; Ringnalda, M., N; Goddard, W. A., III. *J. Chem. Phys.* **1994**, *101*, 2986.

(9) Murphy, R. B.; Messmer, R. P. *Chem. Phys. Lett.* **1991**, *183*, 443.

(10) Murphy, R. B.; Friesner, R. A. *Chem. Phys. Lett.* **1998**, *288*, 403.

(11) Murphy, R. B.; Pollard, W. T.; Friesner, R. A. *J. Chem. Phys.* **1997**, *106*, 5073.

(12) Robert, B. M.; Michael, D. B.; Richard, A. F.; Murco, N. R. *J. Chem. Phys.* **1995**, *103*, 1481.

(13) Hay, P. J.; Dunning, T. H.; Goddard, W. A., III. *J. Chem. Phys.* **1975**, *62*, 3912.

(14) Wadt, W. R.; Goddard, W. A., III. *J. Am. Chem. Soc.* **1975**, *97*, 3004.

(15) Walch, S. P.; Goddard, W. A., III. *J. Am. Chem. Soc.* **1975**, *97*, 5319.

(16) Voter, A. F.; Goddard, W. A., III. *Chem. Phys.* **1981**, *57*, 253.

(17) Voter, A. F.; Goddard, W. A., III. *J. Am. Chem. Soc.* **1986**, *108*, 2830.

(18) Voter, A. F.; Goddard, W. A., III. *J. Chem. Phys.* **1981**, *75*, 3638.

(19) Perry, J. K.; Ohanessian, G.; Goddard, W. A., III. *Organometallics* **1994**, *13*, 1870.

(20) Ohanessian, G.; Goddard, W. A., III. *Acc. Chem. Res.* **1990**, *23*, 386.

(21) Ohanessian, G.; Brusich, M. J.; Goddard, W. A., III. *J. Am. Chem. Soc.* **1990**, *112*, 7179.

(22) Perry, J. K.; Goddard, W. A., III; Ohanessian, G. *J. Chem. Phys.* **1992**, *97*, 7560.

(23) Gerratt, J. *Adv. At. Mol. Phys.* **1971**, *7*, 141.

(24) Cooper, D. L.; Gerratt, J.; Raimondi, M. *Chem. Rev.* **1991**, *91*, 929.

(25) Cooper, D. L.; Gerratt, J.; Raimondi, M. In *Advances in Chemical Physics*; Lawley, K. P., Ed.; John Wiley & Sons: New York, 1987; Vol. 69, p 319.

(26) Sironi, M.; Raimondi, M.; Martinazzo, R.; Gianturco, F. A. In *Valence Bond Theory*; Cooper, D. L., Ed.; Elsevier: Amsterdam, 2002; p 261.

(27) Cooper, D. L.; Gerratt, J.; Raimondi, M. In *Valence Bond Theory and Chemical Structure*; Klein, D. J., Trinajstic, N., Eds.; Elsevier: Amsterdam, 1990; p 287.

(28) Cooper, D. L.; Gerratt, J.; Raimondi, M. In *Advances in the Theory of Benzenoid Hydrocarbons*; Gutman, I., Cyvin, S. J., Eds.; Springer: Berlin, Heidelberg, 1990; Vol. 153, p 41.

(29) Raimondi, M.; Cooper, D. L. In *Correlation and Localization*; Springer: Berlin, Heidelberg, 1999; Vol. 203, p 165.

(30) Gerratt, J.; Cooper, D. L.; Karadakov, P. B.; Raimondi, M. *Chem. Soc. Rev.* **1997**, *26*, 87.

(31) Gerratt, J.; Cooper, D. L.; Karadakov, P. B.; Raimondi, M. *Spin-Coupled Theory*; John Wiley & Sons: New York, 1998.

(32) Cooper, D. L.; Gerratt, J.; Raimondi, M.; Sironi, M.; Thorsteinsson, T. *Theor. Chem. Acc.* **1993**, *85*, 261.

(33) Cooper, D. L.; Gerratt, J.; Raimondi, M. *Int. Rev. Phys. Chem.* **1988**, *7*, 59.

(34) Raimondi, M.; Sironi, M.; Gerratt, J.; Cooper, D. L. *Int. J. Quantum Chem.* **1996**, *60*, 225.

(35) da Silva, E. C.; Gerratt, J.; Cooper, D. L.; Raimondi, M. *J. Chem. Phys.* **1994**, *101*, 3866.

(36) Wright, S. C.; Cooper, D. L.; Gerratt, J.; Raimondi, M. *J. Phys. Chem.* **1992**, *96*, 7943.

(37) Karadakov, P. B.; Gerratt, J.; Cooper, D. L.; Raimondi, M. *J. Phys. Chem.* **1995**, *99*, 10186.

(38) Cooper, D. L.; Gerratt, J.; Raimondi, M. *Nature* **1986**, *323*, 699.

(39) Sironi, M.; Cooper, D. L.; Gerratt, J.; Raimondi, M. *J. Chem. Soc., Chem. Commun.* **1989**, 675.

(40) Karadakov, P. B. *J. Phys. Chem. A* **2008**, *112*, 12707.

(41) Karadakov, P. B. *J. Phys. Chem. A* **2008**, *112*, 7303.

(42) Josep, M. O.; Joseph, G.; David, L. C.; Peter, B. K.; Mario, R. *J. Chem. Phys.* **1997**, *106*, 3663.

(43) Karadakov, P. B.; Cooper, D. L.; Gerratt, J. *J. Am. Chem. Soc.* **1998**, *120*, 3975.

(44) Hill, J. G.; Cooper, D. L.; Karadakov, P. B. *J. Phys. Chem. A* **2008**, *112*, 12823.

(45) Karadakov, P. B.; Cooper, D. L.; Uhe, A. *Int. J. Quantum Chem.* **2009**, *109*, 1807.

(46) Blavins, J. J.; Cooper, D. L.; Karadakov, P. B. *J. Phys. Chem. A* **2004**, *108*, 194.

(47) Karadakov, P. B.; Hill, J. G.; Cooper, D. L. *Faraday Discuss.* **2007**, *135*, 285.

(48) Karadakov, P. B.; Cooper, D. L.; Gerratt, J. *Theor. Chem. Acc.* **1998**, *100*, 222.

(49) Blavins, J. J.; Karadakov, P. B.; Cooper, D. L. *J. Org. Chem.* **2001**, *66*, 4285.

(50) Blavins, J. J.; Karadakov, P. B.; Cooper, D. L. *J. Phys. Chem. A* **2003**, *107*, 2548.

(51) Malrieu, J. P.; Maynau, D. *J. Am. Chem. Soc.* **1982**, *104*, 3021.

(52) Maynau, D.; Said, M.; Malrieu, J. P. *J. Am. Chem. Soc.* **1983**, *105*, 5244.

(53) Malrieu, J. P. In *Models of Theoretical Bonding*; Maksic, Z. B., Ed.; Springer: Berlin, Heidelberg, 1990; p 108.

(54) Malrieu, J. P. In *Valence Bond Theory and Chemical Structure*; Klein, D. J., Trinajstic, N., Eds.; Elsevier: Amsterdam, 1990; p 135.

(55) Klein, D. J. *Pure Appl. Chem.* **1983**, *55*, 299.

(56) Jiang, Y.; Li, S. In *Valence Bond Theory*; Cooper, D. L., Ed.; Elsevier: Amsterdam, 2002; p 565.

(57) Maynau, D.; Malrieu, J. P. *J. Am. Chem. Soc.* **1982**, *104*, 3029.

(58) Malrieu, J. P.; Maynau, D.; Daudey, J. P. *Phys. Rev. B* **1984**, *30*, 1817.

(59) Said, M.; Maynau, D.; Malrieu, J. P.; Garcia-Bach, M. A. *J. Am. Chem. Soc.* **1984**, *106*, 571.

(60) Said, M.; Maynau, D.; Malrieu, J. P. *J. Am. Chem. Soc.* **1984**, *106*, 580.

(61) Guihery, N.; Maynau, D.; Malrieu, J. P. *New J. Chem.* **1998**, *22*, 281.
(62) Sanchez-Marin, J.; Malrieu, J. P. *J. Phys. Chem.* **1985**, *89*, 978.
(63) Ghailane, R.; Malrieu, J. P.; Maynau, D. *J. Phys. Chem. A* **2001**, *105*, 3365.
(64) Miguel, B.; Guihéry, N.; Malrieu, J. P.; Wind, P. *Chem. Phys. Lett.* **1998**, *294*, 49.
(65) Bernardi, F.; Olivucci, M.; Robb, M. A. *J. Am. Chem. Soc.* **1992**, *114*, 1606.
(66) Bearpark, M. J.; Robb, M. A.; Bernardi, F.; Olivucci, M. *Chem. Phys. Lett.* **1994**, *217*, 513.
(67) Bearpark, M. J.; Bernardi, F.; Olivucci, M.; Robb, M. A. *J. Phys. Chem. A* **1997**, *101*, 8395.
(68) Treboux, G.; Maynau, D.; Malrieu, J. P. *J. Phys. Chem.* **1995**, *99*, 6417.
(69) Bearpark, M. J.; Smith, B. R.; Bernardi, F.; Olivucci, M.; Robb, M. A. In *Combined Quantum Mechanical and Molecular Mechanical Methods*; Gao, J., Thompson, M. A., Eds.; American Chemical Society: Washington, DC, 1998; Vol. 712, p 148.
(70) Bearpark, M. J.; Boggio-Pasqua, M. *Theor. Chem. Acc.* **2003**, *110*, 105.
(71) Bearpark, M. J.; Boggio-Pasqua, M.; Robb, M.; Ogliaro, F. *Theor. Chem. Acc.* **2006**, *116*, 670.
(72) Garavelli, M.; Ruggeri, F.; Ogliaro, F.; Bearpark, M. J.; Bernardi, F.; Olivucci, M.; Robb, M. A. *J. Comput. Chem.* **2003**, *24*, 1357.
(73) Katherine, F. H.; Andrei, M. T.; Michael, J. B.; Martial, B.-P.; Michael, A. R. *J. Chem. Phys.* **2007**, *127*, 134111.
(74) Clifford, S.; Bearpark, M. J.; Bernardi, F.; Olivucci, M.; Robb, M. A.; Smith, B. R. *J. Am. Chem. Soc.* **1996**, *118*, 7353.
(75) Bearpark, M. J.; Bernardi, F.; Clifford, S.; Olivucci, M.; Robb, M. A.; Smith, B. R.; Vreven, T. *J. Am. Chem. Soc.* **1996**, *118*, 169.
(76) Vanni, S.; Garavelli, M.; Robb, M. A. *Chem. Phys.* **2008**, *347*, 46.
(77) Moffitt, W. *Proc. R. Soc. London, Ser. A* **1953**, *218*, 486.
(78) Hiberty, P. C.; Leforestier, C. *J. Am. Chem. Soc.* **1978**, *100*, 2012.
(79) Karafiloglou, P.; Ohanessian, G. *J. Chem. Educ.* **1991**, *68*, 583.
(80) Bachler, V.; Schaffner, K. *Chem.—Eur. J.* **2000**, *6*, 959.
(81) Bachler, V. *J. Comput. Chem.* **2004**, *25*, 343.
(82) Karafiloglou, P.; Malrieu, J. P. *Chem. Phys.* **1986**, *104*, 383.
(83) Trinquier, G.; Malrieu, J. P.; Garcia-Cuesta, I. *J. Am. Chem. Soc.* **1991**, *113*, 6465.
(84) Trinquier, G.; Malrieu, J. P. *J. Am. Chem. Soc.* **1991**, *113*, 8634.
(85) Cooper, D. L.; Karadakov, P. B.; Thorsteinsson, T. In *Valence Bond Theory*; Cooper, D. L., Ed.; Elsevier: Amsterdam, 2002; p 41.
(86) Cooper, D. L.; Thorsteinsson, T.; Gerratt, J. In *Advances in Quantum Chemistry*; Löwden, P.-O., Ed.; Academic Press: New York, 1998; Vol. 32, p 51.
(87) Thorsteinsson, T.; Cooper, D. L. In *Quantum Systems in Chemistry and Physics. Vol. 1: Basic Problems and Model Systems*; Hernández-Laguna, A., Maruani, J., McWeeny, R., Wilson, S., Eds.; Kluwer: Dordrecht, The Netherlands, 2000; p 303.
(88) Ruedenberg, K.; Schmidt, M. W.; Gilbert, M. M. *Chem. Phys.* **1982**, *71*, 51.
(89) Chen, H.; Ikeda-Saito, M.; Shaik, S. *J. Am. Chem. Soc.* **2008**, *130*, 14778.
(90) Roos, B. O.; Veryazov, V.; Conradie, J.; Taylor, P. R.; Ghosh, A. *J. Phys. Chem. B* **2008**, *112*, 14099.
(91) Radoń, M.; Broclawik, E.; Pierloot, K. *J. Phys. Chem. B* **2010**, *114*, 1518.
(92) Nakayama, K.; Nakano, H.; Hirao, K. *Int. J. Quantum Chem.* **1998**, *66*, 157.
(93) Kimihiko, H.; Haruyuki, N.; Kenichi, N.; Michel, D. *J. Chem. Phys.* **1996**, *105*, 9227.
(94) van Lenthe, J. H.; Balint-Kurti, G. G. *J. Chem. Phys.* **1983**, *78*, 5699.
(95) van Lenthe, J. H.; Balint-Kurti, G. G. *Chem. Phys. Lett.* **1980**, *76*, 138.
(96) Prosser, F.; Hagstrom, S. *Int. J. Quantum Chem.* **1968**, *2*, 89.
(97) Verbeek, J.; Van Lenthe, J. H. *Int. J. Quantum Chem.* **1991**, *40*, 201.
(98) Li, X.; Zhang, Q. *Int. J. Quantum Chem.* **1989**, *36*, 599.
(99) McWeeny, R. *Int. J. Quantum Chem.* **1988**, *34*, 25.
(100) Li, J.; Wu, W. *Theor. Chem. Acc.* **1994**, *89*, 105.
(101) Li, J. *Theor. Chem. Acc.* **1996**, *93*, 35.
(102) Li, J.; Pauncz, R. *Int. J. Quantum Chem.* **1997**, *62*, 245.
(103) Li, J. *J. Math. Chem.* **1995**, *17*, 295.
(104) Dijkstra, F.; Van Lenthe, J. H. *Int. J. Quantum Chem.* **1998**, *67*, 77.
(105) Dijkstra, F.; van Lenthe, J. H. *Chem. Phys. Lett.* **1999**, *310*, 553.
(106) van Lenthe, J. H.; Faas, S.; Snijders, J. G. *Chem. Phys. Lett.* **2000**, *328*, 107.
(107) Dijkstra, F.; van Lenthe, J. H. *J. Comput. Chem.* **2001**, *22*, 665.
(108) Song, L.; Mo, Y.; Zhang, Q.; Wu, W. *XMVB: An ab Initio Non-orthogonal Valence Bond Program*; Xiamen University: Xiamen, China, 2003.
(109) Song, L.; Mo, Y.; Zhang, Q.; Wu, W. *J. Comput. Chem.* **2005**, *26*, 514.
(110) van Lenthe, J. H.; Dijkstra, F.; Havenith, R. W. A. In *Theoretical and Computational Chemistry. Vol. 10: Valence Bond Theory*; Cooper, D. L., Ed.; Elsevier: Amsterdam, 2002; Vol. 10, p 79.
(111) Verbeek, J.; Langenberg, J. H.; Byrman, C. P.; Dijkstra, F.; van Lenthe, J. H., Theoretical Chemistry Group, Utrecht University, Utrecht, The Netherlands.
(112) Li, J.; Duke, B.; McWeeny, R., SciNet Technologies, San Diego, CA, 2005.
(113) Hiberty, P. C.; Shaik, S. *Theor. Chem. Acc.* **2002**, *108*, 255.
(114) Hiberty, P. C.; Humbel, S.; Byrman, C. P.; van Lenthe, J. H. *J. Chem. Phys.* **1994**, *101*, 5969.
(115) Hiberty, P. C.; Flament, J. P.; Noizet, E. *Chem. Phys. Lett.* **1992**, *189*, 259.
(116) Song, L.; Wu, W.; Zhang, Q.; Shaik, S. *J. Comput. Chem.* **2004**, *25*, 472.
(117) Wu, W.; Song, L.; Cao, Z.; Zhang, Q.; Shaik, S. *J. Phys. Chem. A* **2002**, *106*, 2721.
(118) Chen, Z.; Song, J.; Shaik, S.; Hiberty, P. C.; Wu, W. *J. Phys. Chem. A* **2009**, *113*, 11560.
(119) Tomasi, J.; Mennucci, B.; Cammi, R. *Chem. Rev.* **2005**, *105*, 2999.
(120) Tomasi, J.; Persico, M. *Chem. Rev.* **1994**, *94*, 2027.
(121) Cramer, C. J.; Truhlar, D. G. *Chem. Rev.* **1999**, *99*, 2161.
(122) Shurki, A.; Crown, H. A. *J. Phys. Chem. B* **2005**, *109*, 23638.
(123) Mo, Y.; Song, L.; Wu, W.; Zhang, Q. *J. Am. Chem. Soc.* **2004**, *126*, 3974.
(124) Mo, Y. *J. Chem. Phys.* **2003**, *119*, 1300.
(125) Mo, Y.; Gao, J. *J. Phys. Chem. A* **2000**, *104*, 3012.
(126) Mo, Y.; Zhang, Y.; Gao, J. *J. Am. Chem. Soc.* **1999**, *121*, 5737.
(127) Mo, Y.; Peyerimhoff, S. D. *J. Chem. Phys.* **1998**, *109*, 1687.
(128) Kollmar, H. *J. Am. Chem. Soc.* **1979**, *101*, 4832.
(129) Kitaura, K.; Morokuma, K. *Int. J. Quantum Chem.* **1976**, *10*, 325.
(130) Ziegler, T.; Rauk, A. *Theor. Chem. Acc.* **1977**, *46*, 1.
(131) Bickelhaupt, F. M.; Baerends, E. J. In *Reviews in Computational Chemistry*; Kenny, B., Lipkowitz, D. B. B., Eds.; Wiley-VCH: New York, 2000; Vol. 15, p 1.
(132) Hirao, H. *Chem. Phys. Lett.* **2007**, *443*, 141.
(133) Su, P.; Li, H. *J. Chem. Phys.* **2009**, *131*, 014102.
(134) Pauncz, R. *Spin Eigenfunctions*; Plenum Press: New York, 1979.
(135) Rumer, G. *Göttinger Nachr.* **1932**, 377.
(136) Massimo, S.; Ermanno, G.; Ida, V. *J. Chem. Phys.* **1968**, *48*, 1579.
(137) Chirgwin, B. H.; Coulson, C. A. *Proc. R. Soc. London, Ser. A* **1950**, *201*, 196.
(138) Löwdin, P.-O. *Ark. Mat., Astron. Fys.* **1947**, *A35*, 9.
(139) Gallup, G. A.; Norbeck, J. M. *Chem. Phys. Lett.* **1973**, *21*, 495.
(140) Verbeek, J.; Van Lenthe, J. H. *J. Mol. Struct.: THEOCHEM* **1991**, *229*, 115.
(141) Van Lenthe, J. H.; Verbeek, J.; Pulay, P. *Mol. Phys.* **1991**, *73*, 1159.

(142) Su, P.; Wu, J.; Gu, J.; Wu, W.; Shaik, S.; Hiberty, P. C. *J. Chem. Theory Comput.* **2011**, *7*, 121.
(143) Su, P.; Song, L.; Wu, W.; Hiberty, P. C.; Shaik, S. *J. Comput. Chem.* **2007**, *28*, 185.
(144) Mo, Y.; Lin, Z.; Wu, W.; Zhang, Q. *J. Phys. Chem.* **1996**, *100*, 11569.
(145) Song, L.; Wu, W.; Hiberty, P. C.; Danovich, D.; Shaik, S. *Chem.—Eur. J.* **2003**, *9*, 4540.
(146) Hiberty, P. C.; Humbel, S.; Archirel, P. *J. Phys. Chem.* **1994**, *98*, 11697.
(147) Maitre, P.; Lefour, J. M.; Ohanessian, G.; Hiberty, P. C. *J. Phys. Chem.* **1990**, *94*, 4082.
(148) Gallup, G. A.; Vance, R. L.; Collins, J. R.; Norbeck, J. M. In *Advances in Quantum Chemistry*; Löwden, P.-O., Ed.; Academic Press: New York, 1982; Vol. 16, p 229.
(149) Hollauer, E.; Nascimento, M. A. C. *Chem. Phys. Lett.* **1991**, *184*, 470.
(150) Wu, W.; McWeeny, R. *J. Chem. Phys.* **1994**, *101*, 4826.
(151) Clarke, N. J.; Raimondi, M.; Sironi, M.; Gerratt, J.; Cooper, D. L. *Theor. Chem. Acc.* **1998**, *99*, 8.
(152) Martinazzo, R.; Famulari, A.; Raimondi, M.; Bodo, E.; Gianturco, F. A. *J. Chem. Phys.* **2001**, *115*, 2917.
(153) Cooper, D. L.; Clarke, N. J.; Stancil, P. C.; Zygelman, B. *Advances in Quantum Chemistry*; Academic Press: New York, 2001; Vol. 40, p 37.
(154) Gu, J.; Lin, Y.; Ma, B.; Wu, W.; Shaik, S. *J. Chem. Theory Comput.* **2008**, *4*, 2101.
(155) Su, P.; Wu, W.; Shaik, S.; Hiberty, P. C. *ChemPhysChem* **2008**, *9*, 1442.
(156) Murphy, R. B.; Messmer, R. P. *J. Chem. Phys.* **1992**, *97*, 4170.
(157) Dunietz, B. D.; Friesner, R. A. *J. Chem. Phys.* **2001**, *115*, 11052.
(158) Sejpal, M.; Messmer, R. P. *J. Chem. Phys.* **2001**, *114*, 4796.
(159) Sejpal, M.; Messmer, R. P. *Chem. Phys.* **2001**, *270*, 237.
(160) Miertus, S.; Scrocco, E.; Tomasi, J. *Chem. Phys.* **1981**, *55*, 117.
(161) Miertus, S.; Tomasi, J. *Chem. Phys.* **1982**, *65*, 239.
(162) Cossi, M.; Barone, V.; Cammi, R.; Tomasi, J. *Chem. Phys. Lett.* **1996**, *255*, 327.
(163) Cossi, M.; Barone, V.; Robb, M. A. *J. Chem. Phys.* **1999**, *111*, 5295.
(164) Cossi, M.; Barone, V. *J. Chem. Phys.* **2000**, *112*, 2427.
(165) Mennucci, B.; Cances, E.; Tomasi, J. *J. Phys. Chem. B* **1997**, *101*, 10506.
(166) Cances, E.; Mennucci, B.; Tomasi, J. *J. Chem. Phys.* **1997**, *107*, 3032.
(167) Cancès, E.; Mennucci, B. *J. Math. Chem.* **1998**, *23*, 309.
(168) Song, L.; Wu, W.; Zhang, Q.; Shaik, S. *J. Phys. Chem. A* **2004**, *108*, 6017.
(169) Su, P.; Ying, F.; Wu, W.; Hiberty, P. C.; Shaik, S. *ChemPhysChem* **2007**, *8*, 2603.
(170) Su, P.; Song, L.; Wu, W.; Shaik, S.; Hiberty, P. C. *J. Phys. Chem. A* **2008**, *112*, 2988.
(171) Kelly, C. P.; Cramer, C. J.; Truhlar, D. G. *J. Chem. Theory Comput.* **2005**, *1*, 1133.
(172) Marenich, A. V.; Olson, R. M.; Kelly, C. P.; Cramer, C. J.; Truhlar, D. G. *J. Chem. Theory Comput.* **2007**, *3*, 2011.
(173) Su, P.; Wu, W.; Kelly, C. P.; Cramer, C. J.; Truhlar, D. G. *J. Phys. Chem. A* **2008**, *112*, 12761.
(174) Warshel, A.; Weiss, R. M. *J. Am. Chem. Soc.* **1980**, *102*, 6218.
(175) Aaqvist, J.; Warshel, A. *Chem. Rev.* **1993**, *93*, 2523.
(176) Sharir-Ivry, A.; Crown, H. A.; Wu, W.; Shurki, A. *J. Phys. Chem. A* **2008**, *112*, 2489.
(177) Mo, Y.; Gao, J. *J. Comput. Chem.* **2000**, *21*, 1458.
(178) Mo, Y.; Song, L.; Lin, Y. *J. Phys. Chem. A* **2007**, *111*, 8291.
(179) Mo, Y. *J. Chem. Phys.* **2007**, *126*, 224104.
(180) Shaik, S.; Danovich, D.; Silvi, B.; Lauvergnat, D., L.; Hiberty, P. C. *Chem.—Eur. J.* **2005**, *11*, 6358.
(181) Cao, Z.; Wu, W.; Zhang, Q. *Sci. China, B* **1997**, *40*, 548.
(182) Shaik, S. S. *J. Am. Chem. Soc.* **1981**, *103*, 3692.
(183) Shaik, S.; Hiberty, P. C. *A Chemist's Guide to Valence Bond Theory*; Wiley-Interscience: New York, 2008.
(184) Shaik, S.; Hiberty, P. C. In *Advances in Quantum Chemistry*; Löwdin, P.-O., Ed.; Academic Press: New York, 1995; Vol. 26, p 99.
(185) Pross, A. *Theoretical and Physical Principles of Organic Reactivity*; Wiley-Interscience: New York, 1995.
(186) Shaik, S.; Shurki, A. *Angew. Chem., Int. Ed.* **1999**, *38*, 586.
(187) Shaik, S.; Hiberty, P. C. In *Reviews in Computational Chemistry*; Kenny, B. Lipkowitz, R. L., Cundari, T. R., Eds.; Wiley-VCH: New York, 2004; Vol. 20, p 1.
(188) Song, L.; Gao, J. *J. Phys. Chem. A* **2008**, *112*, 12925.
(189) Shaik, S.; Wu, W.; Dong, K.; Song, L.; Hiberty, P. C. *J. Phys. Chem. A* **2001**, *105*, 8226.
(190) Su, P.; Song, L.; Wu, W.; Hiberty, P. C.; Shaik, S. *J. Am. Chem. Soc.* **2004**, *126*, 13539.
(191) Shaik, S.; Lai, W.; Chen, H.; Wang, Y. *Acc. Chem. Res.* **2010**, *43*, 1154.
(192) Shaik, S.; Kumar, D.; de Visser, S. P. *J. Am. Chem. Soc.* **2008**, *130*, 10128–10140; erratum p 14016.
(193) Song, L.; Wu, W.; Hiberty, P. C.; Shaik, S. *Chem.—Eur. J.* **2006**, *12*, 7458.
(194) These are vertical valence electron affinities, which are normally negative values; see, e.g.: Jordan, K. B.; Barrow, P. D. *Acc. Chem. Res.* **1978**, *11*, 341–348. One must be very careful not to simply calculate the R* state as a Rydberg state.
(195) Song, L.; Mo, Y.; Gao, J. *J. Chem. Theory Comput.* **2008**, *5*, 174.
(196) Shaik, S.; Schlegel, H. B.; Wolfe, S. *Theoretical Aspects of Physical Organic Chemistry: The SN2 Mechanism*; John Wiley & Sons: New York, 1992.
(197) Shaik, S. S. *Prog. Phys. Org. Chem.* **1985**, *15*, 195.
(198) Shaik, S. S. *J. Am. Chem. Soc.* **1984**, *106*, 1227.
(199) Sharir-Ivry, A.; Shurki, A. *J. Phys. Chem. A* **2008**, *112*, 13157.
(200) Muller, R. P.; Warshel, A. *J. Phys. Chem.* **1995**, *99*, 17516.
(201) Luo, Y.; Song, L. C.; Wu, W.; Danovich, D.; Shaik, S. *ChemPhysChem* **2004**, *5*, 515.
(202) Wu, W.; Luo, Y.; Song, L. C.; Shaik, S. *Phys. Chem. Chem. Phys.* **2001**, *3*, 5459.
(203) Wu, W.; Zhong, S. J.; Shaik, S. *Chem. Phys. Lett.* **1998**, *292*, 7.
(204) Wu, W.; Danovich, D.; Shurki, A.; Shaik, S. *J. Phys. Chem. A* **2000**, *104*, 8744.
(205) Wiberg, K. B.; Laidig, K. E. *J. Am. Chem. Soc.* **1987**, *109*, 5935.
(206) Wiberg, K. B.; Breneman, C. M. *J. Am. Chem. Soc.* **1992**, *114*, 831.
(207) Wiberg, K. B.; Rablen, P. R. *J. Am. Chem. Soc.* **1993**, *115*, 9234.
(208) Wiberg, K. B.; Rablen, P. R. *J. Am. Chem. Soc.* **1995**, *117*, 2201.
(209) Laidig, K. E.; Cameron, L. M. *J. Am. Chem. Soc.* **1996**, *118*, 1737.
(210) Yamada, S. *Angew. Chem., Int. Ed. Engl.* **1995**, *34*, 1113.
(211) Yamada, S. *J. Org. Chem.* **1996**, *61*, 941.
(212) Bennet, A. J.; Somayaji, V.; Brown, R. S.; Santarsiero, B. D. *J. Am. Chem. Soc.* **1991**, *113*, 7563.
(213) Lauvergnat, D.; Hiberty, P. C. *J. Am. Chem. Soc.* **1997**, *119*, 9478.
(214) Mo, Y.; Schleyer, P. v. R.; Wu, W.; Lin, M.; Zhang, Q.; Gao, J. *J. Phys. Chem. A* **2003**, *107*, 10011.
(215) Hoffmann, R.; Imamura, A.; Hehre, W. J. *J. Am. Chem. Soc.* **1968**, *90*, 1499.
(216) Winkler, M.; Sander, W. *J. Phys. Chem. A* **2001**, *105*, 10422.
(217) Wei, H.; Hrovat, D. A.; Mo, Y.; Hoffmann, R.; Borden, W. T. *J. Phys. Chem. A* **2009**, *113*, 10351.
(218) Ladner, R. C.; Goddard, W. A., III. *J. Chem. Phys.* **1969**, *51*, 1073.
(219) Hiberty, P. C.; Shaik, S. *J. Comput. Chem.* **2007**, *28*, 137.
(220) Brunck, T. K.; Weinhold, F. *J. Am. Chem. Soc.* **1979**, *101*, 1700.
(221) Weinhold, F.; Reed, A. E. *Isr. J. Chem.* **1991**, *31*, 277.
(222) Weinhold, F. *Angew. Chem., Int. Ed.* **2003**, *42*, 4188.
(223) Bickelhaupt, F. M.; Baerends, E. J. *Angew. Chem., Int. Ed.* **2003**, *42*, 4183.

(224) Mo, Y.; Wu, W.; Song, L.; Lin, M.; Zhang, Q.; Gao, J. *Angew. Chem., Int. Ed.* **2004**, *43*, 1986.
(225) Song, L.; Lin, Y.; Wu, W.; Zhang, Q.; Mo, Y. *J. Phys. Chem. A* **2005**, *109*, 2310.
(226) Mo, Y.; Gao, J. *Acc. Chem. Res.* **2007**, *40*, 113.
(227) Mo, Y.; Song, L.; Wu, W.; Cao, Z.; Zhang, Q. *J. Theor. Comput. Chem.* **2002**, *1*, 137.
(228) Saytzeff, A. M. *Justus Liebigs Ann. Chem.* **1875**, *179*, 296.
(229) Palleros, D. R. *Organic Chemistry*; John Wiley & Sons: New York, 2000; p 260.
(230) Ouellette, R. J. *Organic Chemistry*; Prentice-Hall: Upper Saddle River, NJ, 1996; p 326.
(231) Vollhardt, K. P. C.; Schore, N. E. *Organic Chemistry: Structure and Function*, 4th ed.; W. H. Freeman: New York, 2002.
(232) Streitwieser, A.; Heathcock, C. H.; Kosower, E. M. *Introduction to Organic Chemistry*, 4th ed.; MacMillan: New York, 1992.
(233) Braida, B.; Prana, V.; Hiberty, P. C. *Angew. Chem., Int. Ed.* **2009**, *48*, 5724.
(234) Tanaka, M.; Sekiguchi, A. *Angew. Chem., Int. Ed.* **2005**, *44*, 5821.
(235) Mo, Y. *Org. Lett.* **2006**, *8*, 535.
(236) Gayatri, G.; Soujanya, Y.; Fernández, I.; Frenking, G.; Sastry, G. N. *J. Phys. Chem. A* **2008**, *112*, 12919.
(237) Pauling, L.; Wheland, G. W. *J. Chem. Phys.* **1933**, *1*, 362.
(238) Cooper, D. L.; Gerratt, J.; Raimondi, M. In *Pauling's Legacy: Modern Modelling of the Chemical Bond*; Elsevier: Amsterdam, 1999; p 503.
(239) van Lenthe, J. H.; Havenith, R. W. A.; Dijkstra, F.; Jenneskens, L. W. *Chem. Phys. Lett.* **2002**, *361*, 203.
(240) Dijkstra, F.; Van Lenthe, J. H.; Havenith, R. W. A.; Jenneskens, L. W. *Int. J. Quantum Chem.* **2003**, *91*, 566.
(241) Zielinski, M.; Havenith, R. W. A.; Jenneskens, L.; van Lenthe, J. *Theor. Chem. Acc.* **2010**, *127*, 19.
(242) Mo, Y.; Hiberty, P. C.; Schleyer, P. v. R. *Theor. Chem. Acc.* **2010**, *127*, 27.
(243) Dijkstra, F.; Van Lenthe, J. H. *Int. J. Quantum Chem.* **1999**, *74*, 213.
(244) Havenith, R. W. A.; van Lenthe, J. H.; Dijkstra, F.; Jenneskens, L. W. *J. Phys. Chem. A* **2001**, *105*, 3838.
(245) Havenith, R. W. A.; Jiao, H.; Jenneskens, L. W.; van Lenthe, J. H.; Sarobe, M.; Schleyer, P. v. R.; Kataoka, M.; Necula, A.; Scott, L. T. *J. Am. Chem. Soc.* **2002**, *124*, 2363.
(246) Zielinski, M.; van Lenthe, J. H. *J. Phys. Chem. A* **2008**, *112*, 13197.
(247) Norbeck, J. M.; Gallup, G. A. *J. Am. Chem. Soc.* **1974**, *96*, 3386.
(248) Linares, M.; Humbel, S.; Braida, B. *J. Phys. Chem. A* **2008**, *112*, 13249.
(249) Shaik, S.; Shurki, A.; Danovich, D.; Hiberty, P. C. *Chem. Rev.* **2001**, *101*, 1501.
(250) Mo, Y.; Schleyer, P. v. R. *Chem.—Eur. J.* **2006**, *12*, 2009.
(251) Schaad, L. J.; Hess, B. A. *Chem. Rev.* **2001**, *101*, 1465.
(252) Schleyer, P. v. R.; Pühlhofer, F. *Org. Lett.* **2002**, *4*, 2873.
(253) Dewar, M. J. S.; McKee, M. L. *Pure Appl. Chem.* **1980**, *52*, 1431.
(254) Dewar, M. J. S. *J. Am. Chem. Soc.* **1984**, *106*, 669.
(255) Cremer, D.; Kraka, E. *J. Am. Chem. Soc.* **1985**, *107*, 3800.
(256) Cremer, D.; Gauss, J. *J. Am. Chem. Soc.* **1986**, *108*, 7467.
(257) Schleyer, P. v. R. In *Substituent Effects in Radical Chemistry*; Viehe, H. G., Janousek, Z., Merényi, R., Eds.; Springer: Dordrecht, The Netherlands, 1986; p 69.
(258) Wu, W.; Ma, B.; Wu, J. I.-C.; Schleyer, P. v. R.; Mo, Y. *Chem.—Eur. J.* **2009**, *15*, 9730.
(259) McDouall, J. J. W.; Robb, M. A. *Chem. Phys. Lett.* **1986**, *132*, 319.
(260) Malrieu, J. P.; Angeli, C.; Cimiraglia, R. *J. Chem. Educ.* **2008**, *85*, 150.
(261) Slater, J. C. *J. Chem. Phys.* **1951**, *19*, 220.
(262) Harcourt, R. D.; Hall, N. *J. Mol. Struct.: THEOCHEM* **1996**, *369*, 217.
(263) Harcourt, R. D.; Hall, N. *J. Mol. Struct.: THEOCHEM* **1995**, *342*, 59.
(264) Harcourt, R. D. *J. Chem. Soc., Faraday Trans.* **1991**, *87*, 1089.
(265) Harcourt, R. D. *J. Chem. Soc., Faraday Trans.* **1992**, *88*, 1119.
(266) Klapötke, T. M.; Harcourt, R. D.; Li, J. *Inorg. Chim. Acta* **2005**, *358*, 4131.
(267) Harcourt, R. D. *J. Mol. Struct.: THEOCHEM* **1990**, *206*, 253.
(268) Harcourt, R. D.; Klapötke, T. M. *Z. Naturforsch.* **2002**, *57b*, 983.
(269) Harcourt, R. D.; Klapötke, T. M. *Z. Naturforsch.* **2003**, *58b*, 121.
(270) DeBlase, A.; Licata, M.; Galbraith, J. M. *J. Phys. Chem. A* **2008**, *112*, 12806.
(271) Havenith, R. W. A.; van Lenthe, J. H.; van Walree, C. A.; Jenneskens, L. W. *J. Mol. Struct.: THEOCHEM* **2006**, *763*, 43.
(272) Havenith, R. W. A.; van Lenthe, J. H.; Jenneskens, L. W. *J. Org. Chem.* **2005**, *70*, 4484.
(273) Jung, Y.; Heine, T.; Schleyer, P. v. R.; Head-Gordon, M. *J. Am. Chem. Soc.* **2004**, *126*, 3132.
(274) Gerratt, J.; McNicholas, S. J.; Karadakov, P. B.; Sironi, M.; Raimondi, M.; Cooper, D. L. *J. Am. Chem. Soc.* **1996**, *118*, 6472.
(275) Thorsteinsson, T.; Cooper, D. L. *J. Math. Chem.* **1998**, *23*, 105.
(276) Harcourt, R. D.; Klapotke, T. M.; Schulz, A.; Wolynec, P. *J. Phys. Chem. A* **1998**, *102*, 1850.
(277) Skrezenek, F. L.; Harcourt, R. D. *J. Am. Chem. Soc.* **1984**, *106*, 3934.
(278) Harcourt, R. D.; Skrezenek, F. L. *J. Mol. Struct.: THEOCHEM* **1987**, *151*, 203.
(279) Klapötke, T. M.; Li, J.; Harcourt, R. D. *J. Phys. Chem. A* **2004**, *108*, 6527.
(280) Skrezenek, F. L.; Harcourt, R. D. *Theor. Chem. Acc.* **1985**, *67*, 271.
(281) Skrezenek, F. L.; Harcourt, R. D. *Theor. Chem. Acc.* **1986**, *70*, 237.
(282) Havenith, R. W. A.; van Lenthe, J. H. *Chem. Phys. Lett.* **2004**, *385*, 198.
(283) Löwdin, P.-O. *Phys. Rev.* **1955**, *97*, 1474.
(284) Prosser, F.; Hagstrom, S. *J. Chem. Phys.* **1968**, *48*, 4807.
(285) Miller, J.; Friedman, R. H.; Hurst, R. P.; Matsen, F. A. *J. Chem. Phys.* **1957**, *27*, 1385.
(286) Raimondi, M.; Simonetta, M.; Tantardini, G. F. *J. Chem. Phys.* **1972**, *56*, 5091.
(287) Balint-Kurti, G. G.; Karplus, M. *J. Chem. Phys.* **1969**, *50*, 478.
(288) Matsen, F. A. *Advances in Quantum Chemistry*; Academic Press: New York, 1964; Vol. 1, p 59.
(289) Amos, A. T.; Hall, G. G. *Proc. R. Soc. London, Ser. A* **1961**, *263*, 483.
(290) Archbold, J. W. *Algebra*; Pitman Publishing: London, 1961.
(291) Levy, B.; Berthier, G. *Int. J. Quantum Chem.* **1968**, *2*, 307.
(292) McWeeny, R. *Methods of Molecular Quantum Mechanics*; Academic Press: London, 1989.
(293) Zhang, Q.; Li, X. *J. Mol. Struct.* **1989**, *198*, 413.
(294) Wu, W.; Zhang, Q. *J. Phys. A* **1992**, *25*, 3737.
(295) Wu, W.; Wu, A.; Mo, Y.; Lin, M.; Zhang, Q. *Int. J. Quantum Chem.* **1998**, *67*, 287.
(296) Li, J.; McWeeny, R. *Int. J. Quantum Chem.* **2002**, *89*, 208.
(297) Song, L.; Song, J.; Mo, Y.; Wu, W. *J. Comput. Chem.* **2009**, *30*, 399.
(298) Elian, M.; Hoffmann, R. *Inorg. Chem.* **1975**, *14*, 1058.
(299) Shaik, S. *New J. Chem.* **2007**, *31*, 2015.
(300) Schmidt, M. W.; Baldridge, K. K.; Boatz, J. A.; Elbert, S. T.; Gordon, M. S.; Jensen, J. H.; Koseki, S.; Matsunaga, N.; Nguyen, K. A.; Su, S.; Windus, T. L.; Dupuis, M.; Montgomery, J. A., Jr. *J. Comput. Chem.* **1993**, *14*, 1347−1363. See the Web site of GAMESS: http://www.msg.ameslab.gov/GAMESS/GAMESS.html.
(301) Dijkstra, F.; van Lenthe, J. H. *J. Chem. Phys.* **2000**, *113*, 2100.
(302) GAMESS-UK is a package of ab initio programs written by M. F. Guest, J. H. van Lenthe, J. Kendrick, K. Schöffel, P. Sherwood, and

R. J. Harrison, with contributions from R. D. Amos, R. J. Buenker, M. Dupuis, N. C. Handy, I. H. Hillier, P. J. Knowles, V. Bonacic-Koutecky, W. von Niessen, V. R. Saunders, and A. Stone. The package is derived from the original GAMESS code due to M. Dupuis, D. Spangler, and J. Wendoloski: *NRCC Software Catalog*; University of California: Berkeley, CA, 1980; Vol. 1, Program No. QG01 (GAMESS). See: Guest, M. F.; Bush, I. J.; van Dam, H. J. J.; Sherwood, P.; Thomas, J. M. H.; van Lenthe, J. H.; Havenith, R. W. A.; Kendrick, J. *Mol. Phys.* **2005**, *103*, 719. For the latest version, see the Web site http://www.cfs.dl.ac.uk/gamess-uk/index.shtml.

(303) Frisch, M. J.; Trucks, G. W.; Schlegel, H. B.; Scuseria, G. E.; Robb, M. A.; Cheeseman, J. R.; Montgomery, J. A., Jr.; Vreven, T.; Kudin, K. N.; Burant, J. C.; Millam, J. M.; Iyengar, S. S.; Tomasi, J.; Barone, V.; Mennucci, B.; Cossi, M.; Scalmani, G.; Rega, N.; Petersson, G. A.; Nakatsuji, H.; Hada, M.; Ehara, M.; Toyota, K.; Fukuda, R.; Hasegawa, J.; Ishida, M.; Nakajima, T.; Honda, Y.; Kitao, O.; Nakai, H.; Klene, M.; Li, X.; Knox, J. E.; Hratchian, H. P.; Cross, J. B.; Bakken, V.; Adamo, C.; Jaramillo, J.; Gomperts, R.; Stratmann, R. E.; Yazyev, O.; Austin, A. J.; Cammi, R.; Pomelli, C.; Ochterski, J. W.; Ayala, P. Y.; Morokuma, K.; Voth, G. A.; Salvador, P.; Dannenberg, J. J.; Zakrzewski, V. G.; Dapprich, S.; Daniels, A. D.; Strain, M. C.; Farkas, O.; Malick, D. K.; Rabuck, A. D.; Raghavachari, K.; Foresman, J. B.; Ortiz, J. V.; Cui, Q.; Baboul, A. G.; Clifford, S.; Cioslowski, J.; Stefanov, B. B.; Liu, G.; Liashenko, A.; Piskorz, P.; Komaromi, I.; Martin, R. L.; Fox, D. J.; Keith, T.; Al-Laham, M. A.; Peng, C. Y.; Nanayakkara, A.; Challacombe, M.; Gill, P. M. W.; Johnson, B.; Chen, W.; Wong, M. W.; Gonzalez, C.; Pople, J. A. *Gaussian 03*, revision C.02; Gaussian, Inc.: Wallingford, CT, 2004.

(304) Gallup, G. A. *Valence Bond Methods*; Cambridge University Press: Cambridge, U.K., 2002.

(305) MOLPRO is a package of ab initio programs written by H.-J. Werner, P. J. Knowles, M. Schütz, R. Lindh, P. Celani, T. Korona, G. Rauhut, F. R. Manby, R. D. Amos, A. Bernhardsson, A. Berning, D. L. Cooper, M. J. O. Deegan, A. J. Dobbyn, F. Eckert, C. Hampel, G. Hetzer, A. W. Lloyd, S. J. McNicholas, W. Meyer, M. E. Mura, A. Nicklass, P. Palmieri, R. Pitzer, U. Schumann, H. Stoll, A. J. Stone, R. Tarroni, and T. Thorsteinsson. See the Web site http://www.molpro.net/.